THE RECRUITMENT AND DYNAMICS OF TRANSCRIPTION FACTORS AT THE HSP70 LOCI IN LIVING CELLS

A Dissertation

Presented to the Faculty of the Graduate School

of Cornell University

in Partial Fulfillment of the Requirements for the Degree of

Doctor of Philosophy

by

Katie Leigh Zobeck

January 2011

THE RECRUITMENT AND DYNAMICS OF TRANSCRIPTION FACTORS AT THE HSP70 LOCI IN LIVING CELLS

Katie Leigh Zobeck, Ph.D.

Cornell University 2011

Chromatin Immunoprecipitation (ChIP) provides snapshots of the localization of transcription factors on chromatin in cell populations. However, through the development of fluorescent proteins and subsequent live cell imaging techniques, it has become possible to address protein localization and dynamics in single living cells. Furthermore, the application of these techniques to the naturally amplified *Drosophila* polytene chromosomes allows the resolution of specific chromosomal loci within the natural three-dimensional state of living nuclei. Therefore, we applied live cell imaging methods to address the recruitment, dynamics and retention at the inducible *Hsp70* loci in individual *Drosophila* salivary gland nuclei for (1) a number of transcription factors, including HSF, Pol II, P-TEFb, Spt6, and Topo I; (2) H2B and Poly ADP Ribose (PAR) Polymerase (PARP); and (3) a previously uncharacterized *Drosophila* ortholog of SET1, dSet1.

We observed that the recruitment of the master regulator, HSF, is first detected within 20 seconds of gene activation, and that the timing of its recruitment resolves from RNA polymerase II and P-TEFb, and these factors resolve from Spt6 and Topo I. Remarkably, the recruitment of each factor is highly synchronous between different cells. Fluorescence Recovery after Photobleaching (FRAP) analyses show that the entry and exit of multiple factors are progressively constrained upon gene activation, suggesting the gradual formation of a transcription compartment at the *Hsp70* loci. Using live cell imaging methods and perfusion of PJ34, a specific inhibitor of PARP catalytic activity, we were

able to show that the maintenance of the transcription compartment and subsequent retention of transcription factors is dependent on the activity of PARP, which is indicative of the role of PAR in the transcription compartment. Furthermore, we observed the retention of H2B and PARP at the *Hsp70* loci before and after HS, even though mean fluorescence intensity of these factors decreases after activation. Finally, we applied these live cell imaging methods to characterize dSet1. In yeast, SET1 is responsible for the trimethylation of Histone H3 Lysine 4 (H3K4me3) a histone mark that is required for active elongation. Therefore, we addressed the timing of recruitment and dynamics of dSet1 at the *Hsp70* loci and observed recruitment of dSet1 occurs slightly before Pol II, indicating that H3K4me3 occurs before elongation of Pol II at the *Hsp70* loci. Together these live cell imaging assays provide an important assay which can be used to distinguish possible mechanisms for the role of transcription factors, histones, PARP and dSet1 in transcription activity.

BIOGRAPHICAL SKETCH

Katie L. Zobeck was born at Blodgett Hospital in Grand Rapids, Michigan on October 9, 1981, the second of three daughters born to David and Bonita Zobeck. She grew up in Jenison, MI a small suburb of Grand Rapids, where she attended Jenison Christian Elementary School followed by Jenison Public Junior and Senior High School.

Immediately following high school, Katie was admitted to Michigan State University, where she graduated four years later with a degree in Microbiology with a specialization in Genomics and Genetics. While at Michigan State, Katie worked as an Undergraduate Researcher in the Lab of Dr. Zachary Burton, where she studied the mechanism of Pol II translocation during elongation.

In 2004, Katie was admitted to the Biochemistry, Molecular and Cell Biology Graduate Program in the department of Molecular Biology and Genetics at Cornell University. There she joined the research lab of John T. Lis and completed her Ph.D., with this thesis, in 2011.

To my family and friends.

ACKNOWLEDGEMENTS

This work would not have been possible with out the contributions, scientifically and otherwise, of numerous people. First, I would like to thank my advisor, Dr. John T. Lis for his support, encouragement and advice. His enthusiasm for the project kept me moving forward. I would like to thank the other members of my Ph.D. committee, Drs. Daniel A. Barbash and Jeffrey W. Roberts, for their support and direction during committee meetings.

Many other faculty members in the Department of Molecular Biology and Genetics, Department of Applied Engineering and Department of Biomedical Engineering provided advice and support for this project. I am deeply thankful for the discussions and technical support from Drs. Watt W. Webb and Warren R. Zipfel, and I would also like to acknowledge the guidance received from Drs. Eric E. Alani and Mariana Wolfner on many occasions.

I am deeply grateful to Dr. Jie Yao, a former student from the Webb lab for developing the method of multiphoton imaging of living *Drosophila* salivary glands. With out his pioneering research, I would not have had the opportunity to embark on this research. I must also specifically thank Dr. Martin S. Buckley from the Lis Lab for his assistance and collaboration on the live cell imaging recruitment project and Dr. Behfar Ardehali from the Lis Lab for the dSet1 imaging project. I would like to thank the other members of the Lis lab, past and present for their helpful discussion and advice on this project, including: Aarti Sevilimedu Veeravalli, Abbie Saunders, Abdullah Ozer, Ali Adem Bahar, Amanda Manfredo, Colin Waters, Hans Salamanca, Hoojoon Kwak, Irene Min, Iris Jonkers, Janis Werner, Joshua Waterfall, Karen Adelman, Katherine Kieckhafer, Katy Munson, Leighton Core, Mei Hui Liu, Mike Geurtin, Nick Fuda, Rebekka Sprouse, Steve Mauro, Steven Petesch, Xiaoching Zhao, and Zhouyu Ni.

I would like to thank the people who have supported my research by maintaining and training me on the numerous microscopes. First, I would like to acknowledge the generosity of Drs. Nina Allen and Scott Olyench for allowing Martin and I to use the brand new Zeiss Cell Observer SD at the David H. Murdock Research Institute in Kanapolis, North Carolina. I would like to thank Drs. Rebecca Williams, Jesse McMullen and Warren Zipfel for keeping the Zeiss LSM 510 Meta up and running long enough for me to finish my studies.

Surviving grad school and finishing this thesis would not have been possible, except for the support and encouragement from my friends and family. The years I spent in Ithaca are filled with wonderful memories because of you. Thank you for being there for me, even if it is was only a phone call when we needed each other.

Finally, I would like to thank my loving husband, Tudor Marian. He has helped my research in many ways, from massaging my shoulders after a hard days work at the microscope to writing MatLab programs to facilitate my data analysis. Thank you for spending the time to teach me how to write scripts, thank you for writing the MatLab programs over and over again because I was unable to tell you exactly what I needed, and thank you for loving me.

TABLE OF CONTENTS

LIST OF FIGURES

LIST OF TABLES

LIST OF ABBREVIATIONS

°C	Degrees Celsius
Å	Angström
AD	Activation Domain
ADP	Adenosine Di-Phosphate
AR	Androgen Receptor
ARNT	Aryl Hydrocarbon Receptor Nuclear Translocator
Ash1	Absent, Small, or Homeotic discs 1
ATP	Adenosine Tri-Phosphate
bp	base pairs
BRD4	Bromodomain-containing protein 4
BREu	TFIIB Recognition Element, upstream
BRG	Brahma-Related Gene
BRM	Brahma
CCD	Charge Coupled Device
CBP	CREB Binding Protein
Cdk9	Cyclin Dependent Kinase 9
ChIP	Chromatin Immunoprecipitation
CRM	Confocal Reflection Microscopy
CTD	C-Terminal Domain
CycT	Cyclin T
DCE	Downstream Core Element
DBD	DNA Binding Domain
DIC	Differential Interference Contrast microscopy
DNA	Deoxyribonucleic Acid
DPE	Downstream Promoter Element

DRB	5,6-dichloro-1-beta-D-ribofuranosylbenzimidazole
dSet1	*Drosophila* ortholog of the SET domain containing protein 1
DSIF	DRB Sensitivity Inducing Factor
eGFP	enhanced Green Fluorescent Protein
ER	Estrogen Receptor
FACT	Facilitates Chromatin Transcription
F. I.	Fluorescence Intensity
Fkh	Forkhead
FRAP	Fluorescence Recovery After Photobleaching
FRET	Fluorescence/Förster Resonance Energy Transfer
FP	Fluorescent Protein
GFP	Green Fluorescent Protein
GR	Glucocorticoid Receptor
H1	Histone 1
H2A	Histone 2A
H2B	Histone 2B
H3	Histone 3
H3K4	Histone H3 Lysine 4
H3K4me3	Histone H3 Lysine 4 trimethylation
H4	Histone 4
HEXIM	Hexamethylene BisAcetamide Inducible Protein
Hif1	Hypoxia-Inducible Factor 1
HS	Heat Shock
HSE	HSF Binding Element
HSF	Heat Shock Factor
Hsp70	Heat shock protein 70

Inr	Initiator
Iws1	Interacts with Spt6 1
kb/min	kilobases per minute
KD	Knock Down
KDa	kiloDalton
k_{off}	Dissociation rate constant, or “off rate”
k_{on}	Association rate constant, or “on rate”
LacI	Lac Inhibitor (Lac Repressor)
LacO	Lac Operator
LSCM	Laser Scanning Confocal Microscopy
mg	milligram
mM	milliMolar
μm	micrometer
MMTV	Mouse Mammary Tumor Virus
MTE	Motif Ten Element
MPM	Multi-Photon Microscopy
mRFP	monomeric Red Flourescent Protein
mRNA	messenger RNA
NA	Numerical Aperture
NAD^+	Nicotinamide Adenine Dinucleotide
NELF	Negative Elongation Factor
NHS	Non-Heat Shock
NTD	N-Terminal Domain
p53	protein 53 kDa
PA	Photoactivation
PAF53	Polymerase Activating Factor 53 kDa

paGFP	photoactivatable Green Flourescent Protein
PAR	Poly(ADP)-Ribose
PARP	Poly(ADP)-Ribose Polymerase
PARG	Poly(ADP)-Ribose Glycohydrolase
PCR	Polymerase Chain Reaction
PIC	Pre-Initiation Complex
PGR-β	Progesterone Receptor β
PMT	PhotoMultiplier Tube
Pol II	RNA Polymerase II
poly(A)	Poly Adenosine Monophosphates
P-TEFb	Positive Transcription Elongation Factor b
RAR	Retinoic Acid Receptor
RAS	Rat Sarcoma
RAT1	Ribonucleic Acid Trafficking 1
rDNA	ribosomal DNA
RNA	Ribonucleic Acid
RNAi	RNA interference
ROI	Region of Interest
Rpb3	RNA polymerase beta subunit 3
SAGA	Spt-Ada-Gcn5-Acetyltransferase
SDCM	Spinning Disk Confocal Microscopy
SEM	Standard Error of the Mean
SET1	SET domain containing protein 1
SF2/ASF	Splicing Factor 2 / Alternative Splicing Factor
Sgs3	Salivary gland secretion 3
snRNA	Small Nuclear RNA

Spt6	Suppressor of Ty 6
Src-1	Steroid Receptor Coactivator 1
SWI/SNF	SWItch/Sucrose NonFermentable
$\tau_{1/2}$	Half Time of Maximal Recovery
TAF_I	Transcription Activating Factor of RNA polymerase I
TATA box	DNA recognition element with DNA sequence TATAAA
TBP	TATA Binding Protien
TFII	Transcription Factor for RNA polymerase II
THR	Thyroid Hormone Receptor
Topo I	Topoisomerase I
TRA1	Transformer 1
Trr7	Trithorax-related 7
Trx6	Trithorax 6
TSS	Transcription Start Site
UAS	Upstream Activator Sequence
UBF	Upstream Binding Factor
YSPTSPS	Tyrosine Serine Proline Threonine Serine Proline Serine
XCPE1	X Core Promoter Element 1
XRN2	5'-3' exoribonuclease 2

CHAPTER 1

INTRODUCTION

Regulation of gene expression is critical for the proper development and survival of an organism. Therefore, cells have evolved intricate mechanisms to regulate the timing, location, and levels of expression for a gene product at multiple stages of gene regulation, including transcription, RNA splicing, RNA export, translation, and post-translational modification. In many cases, gene expression is regulated at a number of these stages, providing redundancy in the control of gene expression. However, occasionally, these regulatory steps are bypassed causing developmental defects, formation of cancer, and cell death.

Expression of the Heat Shock Protein 70 (Hsp70) is no exception. Hsp70 is a molecular chaperone that is expressed in response to heat shock (HS) and other cellular stresses and functions to allow the refolding of proteins that are denatured in such conditions [81]. In *Drosophila*, Hsp70 is not required for survival under normal growth conditions, however, when stressed by a severe HS (39°C) *Hsp70* knock out flies are unable to survive the HS [69]. On the other hand, over-expression of Hsp70 leads to tumorigenicity of mouse fibrosarcoma cells [91], and in a number of human cancers, the over-expression of Hsp70 appears to be caused by the mis-regulation of transcription [29]. Interestingly, a knockout of the master regulator of the HS response, Heat Shock Factor (HSF) 1, protects mice from forming RAS or p53 dependent tumors [43].

These links to cancer and development make the *Hsp70* genes an excellent clinical target for the study of transcriptional regulation, however, additional features of *Hsp70* make it an excellent biological model system, as well. First, the *Hsp70* genes are rapidly and robustly activated, with a $>$100 fold increase in expression upon stimulation in less than 3 minutes [66, 156]. These properties are beneficial for quantitative and mech-

anistic studies. Furthermore, a number of novel regulatory mechanisms discovered at these genes, including RNA polymerase II (Pol II) pausing at the 5' end of the gene, are conserved between different genes and species [76].

In the introduction, I will describe mechanisms, techniques, and results pertinent to the understanding of this thesis. In section 1.1, I will describe the regulation of transcription generally and as it occurs at the *Drosophila Hsp70* gene and identify key factors that are involved its regulation. Then, as most of the current understanding of the regulation of *Hsp70* and other genes stems from *in vivo* and *in vitro* experiments, which take "snap-shots" of the process and can not address the dynamics of the interactions occurring during transcription regulation, section 1.2 will describe optical methods used to address the dynamics of transcription factors and will summarize current studies using these techniques to identify the dynamics of the transcription factors. Finally, in section 1.3, I will give a brief overview of the contents of this thesis.

1.1 Regulation of Gene Expression

1.1.1 General Mechanisms of Transcriptional Regulation

Transcriptional regulation of gene expression occurs at multiple stages in the transcription cycle, including activation, initiation, elongation and termination. The first stage, transcription activation, is regulated through both binding and activity of transcription activators at the promoter of the gene. There are a number of mechanisms to regulate the activity of these genes by activators, which can include: (1) the temporal and spatial regulation of an activator, which occurs through the regulation of its transcription or localization, as is the case with the dorsal-ventral patterning in Drosophila embryos [146]; (2) the binding of the activator to the binding elements; (3) post-transcriptional modifications and ligand-induced conformational changes; and (4) the association of

repressors.

Positioning of a nucleosome over the activator-binding element can inhibit the binding of most activators to their binding elements [160]. Many transcription activators, therefore, recruit SWI/SNF and histone acetyl transferases (HATs) in order to maintain an open chromatin conformation [151]. However binding site accessibly is not the only way binding can be inhibited. HSF, for example, can be maintained in a conformation that prevents DNA binding. Upon HS, HSF changes conformation and dissociates from inhibiting factors, allowing trimerization and binding of the recognition elements [144].

Furthermore, conformational changes and post-transcriptional modifications can play multiple roles in the regulation of activation. First, as with HSF a conformation change is required in order to bind the recognition elements [144], however, some activators, such as the Retinoic Acid Receptor (RAR) can bind the recognition elements before activation by the addition of ligand. When no ligand is present it recruits co-repressors, but upon introduction of the ligand it now recruits co-activators [133]. As with RAR, the binding of repressors negatively regulates gene expression. In fact, repressors can inhibit the activation of both basal and inducible genes [89]. Together the activators and repressors interact in order to provide a cell type specific regulation of the entire genome.

The next regulated stage of transcription is initiation, the process of positioning Pol II at the transcription start site (TSS) in order to begin transcription. As with activators, a positioned nucleosome over the TSS can prevent initiation [128]. However, sequence specific characteristics can also influence the strength of initiation and positioning of transcription initiation, they include promoter elements such as TATA box, upstream Transcription Factor II (TFII) B recognition element (BREu), Initiator (Inr), motif ten element (MTE), downstream promoter element (DPE), downstream core ele-

ment (DCE), and X core promoter element 1 (XCPE1) [95]. These features can be found together, in various combinations, or completely absent from core-promoter sequences. When present these features focus the site of initiation, but when absent initiation can still occur in dispersed manner [95].

Protein factors also affect the regulation of initiation. At TATA box regulated genes, initiation requires the pre-assembly of the pre-initiation complex (PIC), consisting of TATA binding protein (TBP), TFIID, TFIIA and TFIIB, which is then followed by the recruitment of Pol II, TFIIF, TFIIE and TFIIH [212]. All of these factors except TFIIA are essential for PIC formation at TATA box regulated genes [212]. TFIIB, TFIIE, TFIIF, TFIIH and Pol II are encoded by single copy genes, but TBP, TFIID and TFIIA have either parologs or variant proteins that can influence the regulation of transcription initiation, either by recognizing different core-promoter sequences (TBP) or interacting with different activator/co-activator complexes (TFIID or TFIIA) [6].

For a number of genes, initiation is thought to be a major rate-limiting step. Recent global studies, however, are identifying a large number of genes that are rate-limited at the step of proximal Pol II pausing [39, 100, 149]. Paused Pol II is a transcriptionally engaged and competent Pol II, which is inhibited from elongating by the association of Negative Elongation Factor (NELF) and DRB Sensitivity Inducing Factor (DSIF) at +30 – +50 bases from the TSS [184, 64, 116]. In the paused state, the C-Terminal Domain (CTD) of Rpb1, Pol II's largest subunit, is phosphorylated at Serine 5 and the RNA transcript is capped [174]. The release of Pol II from the pause occurs with the recruitment of Positive Transcription Elongation Factor b (P-TEFb), which phosphorylates DSIF, NELF, and Serine 2 of the Pol II CTD [184].

Gene directed studies identified that a number of *Drosophila* developmental genes containing a paused Pol II are synchronously activated, while developmental genes lack-

ing the paused Pol II are stochastically activated over 20 minutes [23], suggesting that genes that need to be rapidly activated are regulated via pausing. In fact, global studies in *Drosophila* have supported this hypothesis by showing that paused Pol II genes are enriched for developmental and stimulus response genes [149], which need to respond rapidly.

Regulation of elongation occurs with a change in the factors associated with Pol II. Most of the general transcription factors have dissociated from the elongation complex after the initial bases were synthesized [179], and remain associated with the promoter region as members of a re-initiation scaffold [241]. Additionally, transcription factors responsible for efficient elongation are recruited, including chromatin remodelers, histone chaperones and topoisomerases [131, 184]. If Pol II arrests during elongation, it is ubiquitylated and degraded [184].

The final stage in which transcription can be regulated is termination, where the transcribing Pol II detaches from the DNA. Termination regulation is an important step, because early termination may form incomplete and unstable transcripts, which are rapidly degraded, and late termination may lead to the inhibition of another gene [170]. The specific mechanism of termination is not yet known, however two models exist, which may not be mutually exclusive. One model is the torpedo model, where after Pol II transcribes the poly(A) sites and the nascent RNA is cleaved, a 5' to 3' exonuclease, Rat1 (yeast) or Xrn2 (humans), chews up the RNA, eventually catching up to Pol II [129]. When this happens, Pol II releases from the DNA. The second model is the allosteric model. In this model, Pol II undergoes a conformational change after transcribing the poly(A) site, which then allows it to dissociates from the DNA [184].

In all of these steps, regulation occurs through post-translational modifications affecting protein activity or binding or the recruitment proteins to activated genes. P-

TEFb, is an excellent example for these multiple methods of regulation. First, the P-TEFb complex is sequestered in a transcriptionally inactive complex consisting of HEXIM and 7SK snRNA [238]. 7SK snRNA causes a conformational change in HEXIM, which allows it to bind the Cyclin T (CycT), a subunit of P-TEFb, and repress the kinase activity of Cyclin Dependent Kinase 9 (Cdk9), another subunit of P-TEFb [119]. Recruitment of P-TEFb to activated genes occurs through an interaction with Brd4, which detects Histone H4 acetylation marks [50]. Interestingly, when P-TEFb inhibition is perturbed, either through the degradation of the 7SK snRNA or the knockout of HEXIM, developmental and embryonic defects linked to excess transcription occur [14, 49, 163]. Additionally, the kinase activity of Cdk9 is required for phosphorylating a number of transcription factors (as mentioned above), as well as phosphorylating the Pol II CTD, which provides a platform for binding of numerous transcription factors involved in transcription elongation, splicing and polyadenylation [184].

P-TEFb is not the only regulated and regulatory protein associated with the transcription elongation. A number of other transcription factors also appear to have secondary activities relating to transcription regulation. For example, in addition to its role in relieving topological stress, Topo I also phosphorylates the splicing factor SF2/ASF [180]. In turn, phosphorylation of SF2/ASF leads to the inhibition of Topo I mediated DNA relaxation [3]. Additionally, histones are post-transcriptionally modified through acetylation and methylation of their histone tails. These histones are differentially modified depending on the transcriptional activity of the region, and can provide a specific signal for the binding of transcription factors to active chromatin, including Brd4 (mentioned above) [50, 88, 105].

1.1.2 Transcription of the *Drosophila Hsp70* genes

Upon HS, the transcription of HS protein encoding genes is rapidly activated, including the *Hsp70* genes. This process is known as the HS response and was first described in 1962, when it was observed that heat induced the formation of a new set of "puffs" on the chromosomes of *Drosophila* salivary glands [228]. However, it was not until 1973 that the cytological response was correlated with the expression of a new set of protein encoding genes, which were regulated at the level of transcription [121]. The HS response is not restricted to *Drosophila*, and has been detected in all organisms, including bacteria, yeast and humans [121, 228]. In each of these cases, HS rapidly and robustly induces the transcription of HS genes and can be detected by an increase in the mRNA levels of these genes, or in *Drosophila*, by the appearance of transcriptionally active "puffs" on the polytene chromosomes [228, 121].

The inducible, rapid and robust activation makes the HS genes an attractive model system for studying transcription. Because of this, there is a lot known about the regulation of transcription for most of the HS genes, especially *Hsp70*. *Drosophila Hsp70* is regulated by a promoter that contains 4 trimeric HSF binding elements (HSEs) located between -50 and -263 [233, 197]. The two most proximal sites are essential for *Hsp70* activation. Interspersed and overlapping the HSEs are a number of GAGA factor binding sites, which are responsible for maintain the promoter in an open chromatin conformation before gene activation [221]. The first nucleosome in the body of the gene is positioned at +330 [164].

During non-heat shock (NHS), initiation of transcription occurs and is regulated by the TBP binding to the sequence TATAAA (TATA box) and TFIID to the Inr [115, 171, 229]. After initiation Pol II transcribes a short distance before becoming paused around two major positions +22 and +30 [174]. At +22 position, the RNA is partially capped,

while at +30 it is completely capped [174]. Activation of transcription and escape from the pause occurs after activation by a HS of 25°C to 37°C, through the recruitment of the activator, HSF, co-activators and the CTD kinase, P-TEFb [184]. Even after activation and escape from the pause, the +22 and +30 paused sites are prominent [174], and biochemical measurements estimate that Pol II escapes from the pause at a rate of one polymerase every 10 minutes, during NHS and every 4 seconds after HS [125].

After escaping the pause, transcription elongation is aided by the recruitment a number of elongation factors including the nucleosome remodeler, Suppressor of Ty 6 (Spt6) and the DNA topoisomerase, Topo I [4, 61]. Finally, after transcribing 2400 bases, Pol II transcribes the poly(A) site, which is then cleaved and polyadenylated, one of the steps to making mature RNA. Pol II, however, does not terminate at this site. Instead, termination of the *Hsp70* genes occur 200-230 nucleotides downstream of the poly(A) site. The termination position appears to be condition-specific, as an increase in HS duration leads to termination 450 nucleotides downstream of the poly(A) site [19].

Our lab has previously carried out a kinetic analysis of factors involved in *Hsp70* transcription using Chromatin Immunoprecipitation (ChIP) of *Drosophila* Kc cells and immunostaining of *Drosophila* polytene chromosomes [22, 185]. These studies helped determine the timing and localization specific transcription factors are recruited to the *Hsp70* gene. Some of the factors studied were HSF, P-TEFb, Spt6, and Pol II [22, 185]. A simplistic kinetic model of transcription activation, based on these kinetic studies, is presented in Figure 1.1.

During NHS conditions, HSF shows minimal binding to the HSEs and Pol II is transcriptionally engaged but paused at the 5' end of the gene (Figure 1.1A) [181]. Even though it is not shown, Pol II is known to interact with negative elongation factors NELF and DSIF while paused [230], and the initiation complex is thought to remain associ-

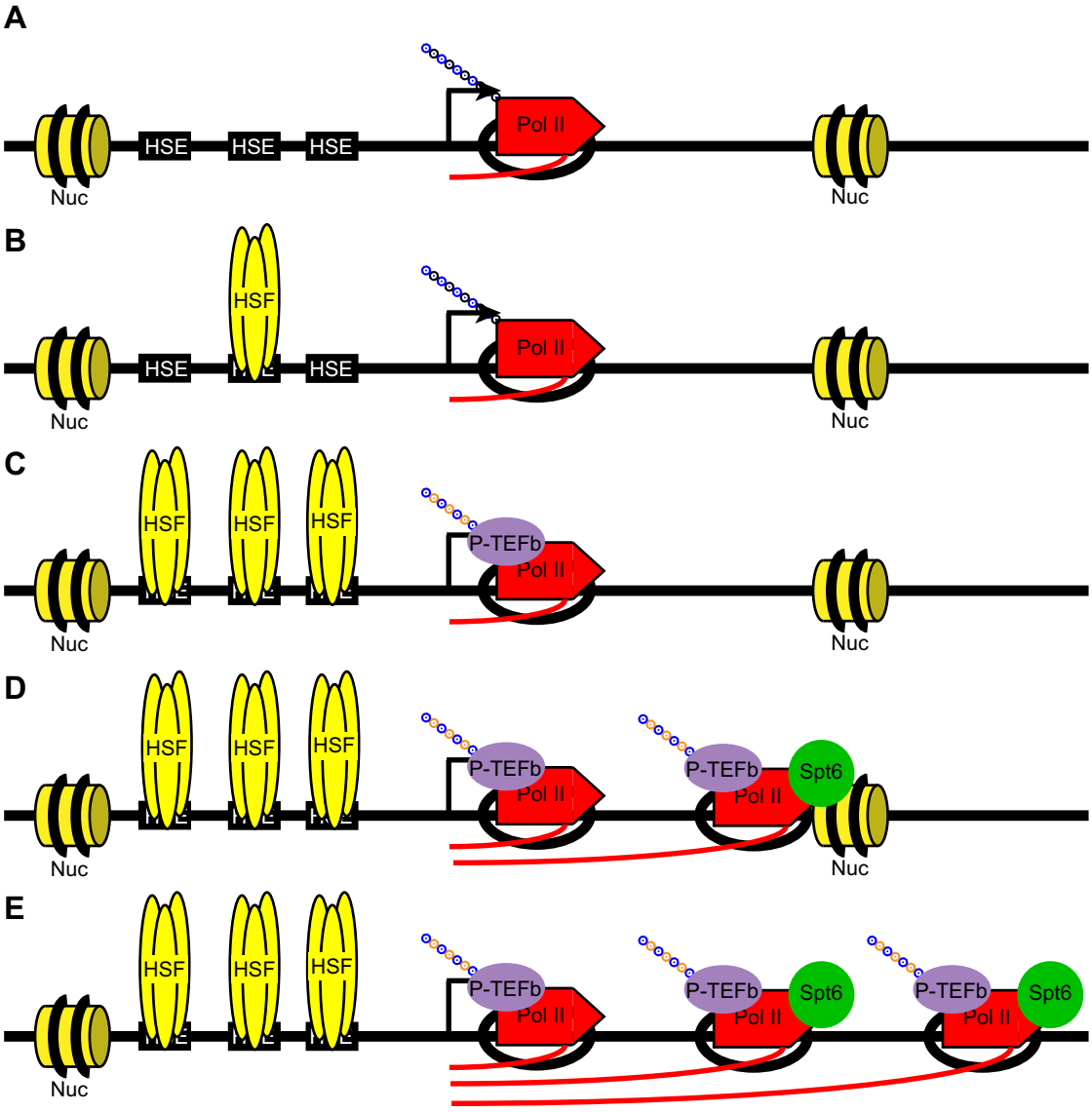

Figure 1.1: The Recruitment and Localization of Transcription Factors on the *Hsp70* gene upon HS

Localization of transcription factors to the *Hsp70* gene after (A) NHS, (B) 5 seconds HS, (C) 75 seconds HS, (D) 150 seconds HS, and (E) 5 minutes HS. Circles on the tail of Pol II (red pentagon) represent the phosphorylation status of the CTD with black unphosphorylated Serine 2, orange phosphorylated Serine 2, and blue representing phosphorylated Serine 5. Yellow oval represents HSF; purple oval, P-TEFb; green circle, Spt6; and the yellow cylinder represents the nucleosomes. The arrow depict the TSS. Summarized from Boehm *et al.*, 2003 [22] and Saunders *et al.*, 2003 [185], not to scale.

ated [115]. After a very short amount of HS (5 seconds), HSF begins to be recruited to the HSEs (Figure 1.1B, although no other changes in protein association are observed [22, 185]. After 75 seconds of HS (Figure 1.1C), the initial recruitment of Pol II and P-TEFb is observed in the kinetic ChIP studies [22, 185]. The recruitment of P-TEFb and subsequent phosphorylation of the Pol II CTD, DSIF and NELF allows Pol II to escape from the pause and begin active transcription [33, 163]. This also the time HSF level reaches maximum enrichment at the promoter of the gene. Slightly later, 150 seconds after HS, Pol II and P-TEFb are spreading into the gene. This is also the time that elongation factors, required for traversing nucleosomes, are recruited to the gene. Thus, we see the increase in Spt6 binding by ChIP near the first nucleosome [22, 185]. By 5 minutes after HS (Figure 1.1E), it appears that Pol II, P-TEFb and Spt6 have all reached maximal levels along the body of the gene, as measured by ChIP [22, 185].

A number of other transcription factors have also been localized to the *Hsp70* loci before or after HS activation. These factors are important for regulating transcription activation, efficiency and fidelity and include chromatin remodelers [184], RNA processing factors [131], and topoisomerases [218]. In this subsection, I will focus on describing the role and regulation of the transcription factors that are of interest to this thesis.

HSF

HSF is the activator that mediates the HS response. *Drosophila* HSF is 691 amino acids long and contains an N-terminal DNA Binding Domain (DBD) with an adjacent trimerization domain consisting of two hydrophobic repeats. At the C-terminus, there is another hydrophobic repeat and a transactivation domain [124, 225]. These two regions are connected together by a long flexible region, which may be involved in repressing

the transactivation domain [225].

During NHS, HSF is present as a monomer and in a transcriptionally inactive form, it consists of the C-terminal hydrophobic repeat folding back and interacting with the N-terminal hydrophobic repeats [172]. HSF can also be be sequestered by Hsp70 [234]. Then, upon HS, Hsp70 dissociates from HSF, and a conformational change in HSF allows trimerization to occur [228]. Trimerization increases the affinity of HSF to the heat shock elements (HSEs) [228], and binding of HSF to the HSEs is required for the activation of the HS response [93]. However binding of HSF to the HSEs is not sufficient for HS activation, as salicylate treatment of *Drosophila* cells leads to the recruitment of HSF to the HSEs but no subsequent recruitment of Pol II [223]. Therefore, the activation ability of *Drosophila* HSF is likely due to a post-translation modification and may be due to the differential phosphorylation of HSF, rather than the overall increase in phosphorylation as observed in yeast and humans [62].

Pol II

Pol II is the polymerase that transcribes protein-encoding genes in eukaryotes. It is a complex consisting of 12 subunits with a total molecular weight of over 500 kiloDaltons (kDa) and is highly conserved from yeast to humans. The initial high-resolution structures of Pol II were determined in yeast using a 10-subunit core polymerase that lacked the Rpb4/Rpb7 module [40, 41, 68]. Subsequent structures, including either the Rpb4/Rpb7 module or different transcription factors, have been solved, elucidating the mechanisms and identifying the structural basis for transcription [11, 21].

The overall structure of Pol II resembles a crab claw, with the active site, composed of Rpb1 and Rpb2, located near the center of the molecule. The DNA gains access to the

active site by way of a cleft. The downstream edge of the transcription bubble is at +4 from the active site, while the upstream portion of the transcription bubble is maintained by a fork loop within Rpb1 as well as a few other structures. RNA synthesis occurs at +1 in a process requiring two Mg^{++} ions, and the DNA/RNA hybrid persists for about 8 bases. At the active site, the DNA is forced to bend 90° because of a dense protein wall positioned beyond the active site [68].

The surface of Pol II is extensive and allows for many possible binding sites between Pol II and other factors for regulation. But the Rpb1 subunit also contains a large unstructured C-terminal domain (CTD), which can bind a number of proteins. The CTD consists of heptapeptide repeats of Tyrosine Serine Proline Threonine Serine Proline Serine (YSPTSPS), which can be differentially phosphorylated on Serine 2, by P-TEFb or Serine 5, by TFIIH [169, 184]. The different phosphorylation states promote binding of factors that regulate transcription. The two phosphorylation states of the CTD are Serine 5 and both Serine 2 and Serine 5, although other combinations exist [166]. These phosphorylation states occur at different stages of transcription with Serine 5 phosphorylation occurring mainly during initiation, but the phosphorylation mark can remain through transcription of the gene [166]. Serine 2 phosphorylation occurs during elongation and in the case of the *Drosophila Hsp70* genes is required for Pol II to escape the pause [154]. Proteins that bind the CTD are sensitive to the phosphorylation status. For example, the unphosphorylated CTD can interact with subunits of the co-activator Mediator, while the phosphorylated CTD is unable to associate with it [138]. Capping enzyme binds the Serine 5 phosphorylated CTD, and in mammals its enzymatic activity is inhibited by phosphorylation at Serine 2 [104, 83]. Finally, a number of elongation factors associate with the Serine 2 and Serine 5 phosphorylated CTD including Poly(ADP)-Ribose Polymerase (PARP), Spt6, and Topo I [31, 167, 239].

P-TEFb

Activation of the *Hsp70* gene requires recruitment of P-TEFb, which is composed of two subunits: Cdk9 and CycT [127]. Via Cdk9, P-TEFb phosphorylates Serine 2 of the Pol II CTD [169], and when the kinase activity of P-TEFb is inhibited, phosphorylated Serine 2 levels decrease [155]. Interestingly, inhibition of P-TEFb kinase activity by flavopiridol results in the time dependent clearing of Pol II from the body of the gene with no significant decrease in levels of paused Pol II [154]. This result suggests that P-TEFb activity is required for escape from the pause, but the kinase activity is not required to keep elongation progressing.

As previously mentioned, the recruitment of P-TEFb occurs after HSF recruitment [22], and using a temperature-sensitive mutant HSF strain, hsf_4, it was possible to show that P-TEFb recruitment is also dependent on HSF [93]. However, a study using a polymeric HSE line has determined that HSF recruitment is not sufficient to recruit P-TEFb [127]. Still the precise method by which P-TEFb is recruited to the *Hsp70* loci is unknown, but it can be speculated based on observations from yeast, that is through the recruitment of P-TEFb to Mediator via the interaction of Brd4 [71].

Spt6

As mentioned above, Spt6 is also recruited to *Hsp70* [4, 185]. Spt6 is a 170 kDa protein the consists of an acidic N-terminal end and a C-terminal regions contains an SH2 domain and a CSZ domain, consisting of two helix-hairpin-helix motifs YqgF-homologous domain that have RNase like features [56]. It interacts directly with the Serine 2 phosphorylated Pol II CTD [239] and at the *Drosophila Hsp70* genes it associates with the nucleosome containing portion by migrates along the gene with Pol II, positively reg-

ulating transcription [185]. At some genes, however, Spt6 is present at the promoter region, where it instead of aiding transcription it inhibits transcription, possibly through the positioning of histones on these promoters [56].

Spt6 is an H3/H4 histone chaperone [25] and with FACT (Facilitates Chromatin Transcription, an H2A/H2B histone chaperone, disassembles and reassembles nucleosomes during transcription [157]. Disassembly of nucleosomes is important to allow Pol II to transcribe through these nucleosomes efficiently, while reassembly of nucleosomes is important for the prevention of cryptic initiation along the gene [97, 226]. In fact, Spt6 enhances the rate of Pol II *in vivo*, with a knockdown of Spt6 reducing that rate of Pol II elongation at *Hsp70* from $\sim$1.1 kilobases per minute (kb/min) to $\sim$0.5 kb/min [9].

The histone chaperone activity of Spt6 is not the only role Spt6 plays at active genes. Recent studies have linked Spt6 to RNA 3' end formation, processing and export, by physically associating with Iws1 and the components of the exosome complex [5, 110, 96, 239], although its involvement in these activities are not yet fully understood [239].

Topo I

Topo I is a Type 1B topoisomerase, which regulates the topological state of DNA by relaxing both positive and negative supercoils generated during transcription and chromatin remodeling [54, 213, 219]. *In vitro* experiments using a chromatin template show that elongation by Pol II requires Topo I activity [143]. Additionally, it is required for transcription along chromatin templates *in vivo*, with inhibition becoming apparent with longer transcripts ($>$200 nucleotides) [143].

Topo I interacts with the coding region of *Hsp70* upon activation, but not with the

non-transcribed regions upstream or downstream of the gene [67]. Using camptotecin, a drug that stabilizes the Topo I:DNA covalent complex, it was possible to map the sites of DNA cleavage. This shows that there are no sites of DNA cleavage on *Hsp70* before activation, however, after activation, there are an increase in the number of DNA cleavage sites distributed along the coding region of the *Hsp70* [109]. Furthermore, immunostaining of *Drosophila* polytene chromosomes show that colocalization between Topo I and transcriptionally active regions of the chromosome occurs on a global scale [193]. Interestingly, this association with transcriptionally active sites is independent of the DBD and catalytic activity and solely requires N-terminal domain (NTD) of Topo I [193]. Further experiments have shown that this is due to a direct interaction between Topo I and the Serine 2 and Serine 5 phosophorylated CTD [31].

Histones

In vivo, DNA is packaged as chromatin, which must be unwrapped in order for transcription to occur. The major component of chromatin, the nucleosome consists of an H3/H4 tetramer and two H2A/H2B dimers wrapped around 147 base pairs (bp) of DNA. At physiological condition, Pol II cannot transcribe through nucleosomes, therefore it has evolved to recruit histone chaperones (i.e. Spt6 and FACT) and ATP-dependent chromatin remodelers to either reposition the nucleosome or displace it from the DNA.

Post-translation modifications on the N-terminal tails of the histones can influence the outcome of transcriptional regulation. With certain methylation and/or acetylation marks representative of active chromatin (including H3K4me3, H3K24me1, H3K9ac and H4K20me1) and other methylation mark representative of inactive condensed chromatin (including H3K9me3 and H3K27me3) [88, 105]. Histone variants can also be used as marks of transcriptional activity with H3.3 deposited during transcrip-

tion [189, 224] and H2A.Z present at inactive promoters [75]. At the *Hsp70* gene, activation leads to the rapid loss of H3 and replacement with the histone variant H3.3 [189].

One ongoing question is whether activation leads to the dissociation of histone from the activated genes. *In vivo* crosslinking experiments have shown variable results depending on the domain assayed. If the globular domains of H2A/H2B are used, then a significant loss of histones is observed [150]. If however, the histone tails were used there is no corresponding loss [150]. Recent studies, however, have shown that there is a rapid nucleosome loss at *Hsp70* following activation and corresponding loss of H3 [164], showing that nucleosomes are no longer directly associating with the DNA.

PARP

PARP catalyzes the formation of Poly(ADP)-Ribose (PAR) polymers from NAD^+ onto target proteins, including Histones, Pol II, Spt6 and Topo I and various other proteins [44, 108]. Like other covalent modifications, PARylation is reversible through the endo- and exo-glycosylase activity of PAR glycohydrolase (PARG), and *in vivo*, the steady state levels of PAR are maintained by the opposing activities of these two enzymes, PARP and PARG [46, 100].

PARP is involved in the regulation of a number of nuclear processes including DNA repair, cell death and transcription, however its activity in transcription is of interest here. PARP acts to stimulate transcription through the displacement of H1 on nucleosomes [107] as well as modifying nucleosomes and co-activators [44]. However, it is not solely involved in activation as there are known cases where PARPs activity in fact represses transcription [141, 211].

In *Drosophila* it is required for *Hsp70* puff formation, with the inhibition of PARP

activity leading to decreased puff size and reduced Hsp70 protein levels upon HS [215]. Using a Green Fluorescent Protein-tagged to PARP, Tulin and Sprading [215] showed that it is present at transcriptionally active puffs, as well as being broadly distributed along the chromosome. They also showed that the product of PARPs catalytic activity, PAR, accumulates at active puffs, including the *Hsp70* loci, showing that PARP is functional at these sites [215]. Interestingly, PARP activity is also important for early steps in transcription, as the rapid wave of H3 loss does not occur when PARP is inhibited [164].

SET1

H3K4 trimethylation (H3K4me3) has been shown to be a major mark of chromatin at the 5'-end of transcriptionally active genes in yeast and metazoans [15, 183, 188]. In budding yeast this methylation is carried out by SET domain containing protein 1 (SET1) [183], however a homolog of SET1 has not yet been identified in *Drosophila*. Instead, in *Drosophila*, *in vitro* and *in vivo* studies have attributed H3K4 methylation to three different methyltransferases: Trithorax (Trx6), Trithorax-related (Trr7) and the absent, small, or homeotic discs 1 (Ash1) [18, 28]. To date, the widely held consensus is that these factors are responsible for deposition of histone H3K4me3 mark in *Drosophila* [55, 118]. However, with the exception of the aforementioned studies where a limited number of genes were examined in vivo, no compelling evidence exists to show these enzymes are responsible for writing the H3K4 trimethylation mark at the global level. In this thesis, I will discuss optical methods used to characterize CG40351 a recently identified *Drosophila* ortholog of SET1.

1.2 Live Cell Imaging of Nuclear Proteins

The advent of GFP and its spectral derivatives has allowed the visualization of proteins in living cells and more specifically within cellular compartments, including the nucleus. In 1994, Nobel laureate, M. Chalfie was the first to express GFP in living organisms, which has provided proof-of-principle results for the use of GFP in living cells [32]. Then, in 1997, T. Misteli and D. Spector used a GFP-fusion protein, GFP-SF2/ASF to study mRNA splicing in the nucleus [139]. Since then, live cell imaging has been used to identify the localization of nuclear proteins and has been adapted to address the dynamics of proteins and processes, including RNA transcription.

GFP was cloned from the jellyfish *Aequorea victoria* [32]. It has a major excitation peak at 395 nm and a minor excitation peak at 475 nm, with peak emission occurring at 509 nm [42]. Interest in the biophysical properties and optimization of GFP has led to the generation of entire collection of variants proteins, which will be referred to in mass as fluorescent proteins (FPs). These FPs have single excitation and emission peaks spanning the visible light spectrum and beyond, creating a rainbow of fluorescence. But new "colors" are not the only improvements for FPs. The GFP chromophore has been manipulated leading to the development of photoactivatable, photoswichable and photoconvertable FPs [37, 79, 194].

Over time, FPs have become a universal method to address protein localization and dynamics *in vivo*, because they are amenable to fusions with protiens and a number of the optical properties of FPs (listed in [37]) make it possible study using optical techniques. This section will describe optical methods to address protein localization, interactions and dynamics (Subsection 1.2.1) within the nucleus and will review the insights obtained from these methods on transcription and its regulation (Subsection 1.2.2).

1.2.1 Imaging Technologies

Multi-channel and/or Time-lapse Microscopy

Multi-channel microscopy provides the ability to either simultaneously or sequentially excite two different FPs in order to determine whether these proteins localize to similar regions. However, resolution of two points in multi-channel microscopy is limited by the defraction of light, $\sim$200 nm, which means two co-localizing proteins may not be directly interacting. Therefore multi-channel microscopy does not identify direct protein–protein interactions, but it still can be used to determine if two proteins are found in similar domains or structures. Time-lapse microscopy, on the other hand, involves the acquisition of numerous images over the course of time and can be most helpful in determining the general localization of proteins and how they change over time. Together these techniques can be used to determine differences in protein movement within the nucleus and as we use in this study, whether two proteins are recruited to specific chromosomal loci at the same time.

Fluorescence / Förster Resonance Energy Transfer

Currently, direct protein–protein interactions can only be detected, in living cells, using Fluoresence / Förster Resonance Energy Transfer (FRET). The theory for FRET was first described in 1948 by T. Förster [152], however its application to biological problems blossomed with the application of FPs [190]. FRET measures the transfer of energy from one fluorophore to another, and can identify the direct interaction between two proteins located less than 60 $\AA$ away from each other. FRET can be observed by two methods. First, in intensity FRET there is an observed decrease in fluorescence of the "donor" molecule and an increase in the "acceptor" molecule. The second method,

lifetime FRET, measures the lifetime of fluorescence for the "donor" molecule, which in the presence of a FRET interaction decreases.

Fluorescence Recovery After Photobleaching

The previous methods are used to study the localization and direct interactions between proteins, however to address the kinetics of interactions in living cells it requires fluorescence recovery after photobleaching (FRAP). This method was developed, before FPs, as a method to study the diffusion of lipids in the cell membrane [57], but has rapidly been applied to FPs in the cell and nucleus in order to measure the diffusion constants of the tagged proteins as well as the kinetics of a binding interaction. FRAP is based the physical property of most FPs which causes an irreversible loss of fluorescence upon exposure to high intensity excitation light [210]. Because these bleached molecules can not re-activate, any recovery in fluorescence is due to the movement of fluorescent molecules into the bleached area.

FRAP is accomplished by bleaching a region of interest (ROI) with high intensity excitation light and then the fluorescence intensity is monitored over time. The fluorescence recovery profile can identify a number of features. First, the intensity where the recovery plateaus, can identify the fraction of "mobile" versus "immobile" molecules. Second, the time it takes to reach half of the maximum recovery ($\tau_{1/2}$) can be used to determine the relative mobility of the "mobile" fraction [202]. Additionally, non-linear curve fitting can be used to determine the rate of diffusion and/or the kinetics of specific interactions occurring in the focal volume. Different equations, listed in Sprague *et al.*, 2004 [203] can differentiate a situation where the molecule does not bind to the chromatin or other nuclear binding site and is freely diffusing in the nucleus (pure-diffusion dominant model), a binding reaction occurs that is faster than diffusion rate (effective

diffusion model), or if the binding reaction is much slower than diffusion rate (reaction dominant model) [203]. In the context of the nucleus this can identify either the diffusion coefficient of the protein, or determine the on and off rates (k_{on} and k_{off}) of binding DNA. I will refer to the different types of associations as freely diffusable, transiently associating or stable for situations where the $\tau_{1/2}$ is equal to the estimated diffusion coefficient, or $>$ the diffusion coefficient by recovery is still observed, or no recovery is observed.

The specific ROI bleached can effect the interpretation of the FRAP profiles. In most of the nuclear FRAP experiments, the ROI contains both nucleoplasm and chromatin, which makes it essential to consider both diffusion and binding contributions of the FP-tagged protein. However, recently, researchers have begun to address the dynamics of transcription factors at specific genetic loci using either tandem arrays or naturally amplified polytene chromosomes [16, 45, 142, 206, 236]. By specifically bleaching the site chromatin where the transcription factor binds, the effect of diffusion can be minimized.

Finally, variations on FRAP exist including the photoactivation (PA) of a photoactivatable GFP (paGFP) and a number different photobleaching methods, discussed in Houtsmuller, 2005 [86]. PA has become a new method to study protein mobility [123]. Initially, paGFP does not fluoresce until it is activated using 405 nm light. After activation, the rate of fluorescence loss from the site of activation is monitored. PA provides complementary experimental results as FRAP, but unlike FRAP, PA can only provide information for k_{off}.

1.2.2 Insights into the Dynamics and Interactions of Transcription Factors *in vivo*

Historically, studies to determine the mechanism of chromatin dependent transcription and its regulation have focused on biochemical techniques using *in vitro* systems not designed to measure protein dynamics. This has led to the view that transcription and its regulation is composed of numerous stable interactions [217]. Live cell imaging studies using FP-tagged transcription factors, however, have revealed that this previous static view of transcriptional regulation is inaccurate. In fact, as Table 1.1 illustrates, most of the factors involved in transcription and its regulation are dynamically associated with the chromatin and/or freely diffusing through the nucleoplasm. Additionally, live cell imaging has identified direct interactions that occur during these processes.

Transcriptional Activators and Coactivators

As Table 1.1 illustrates, most of the factors addressed using FRAP are transcription activators and coactivators. Activators are essential for the proper regulation of gene expression, and are used to determine what genes are expressed at specific times. Activators typically consist of at least two regulatory domains, a sequence specific DBD and an AD [13]. The DBD serves as a method to tether the protein to appropriate sites. This allows the AD to recruit Pol II through interactions with co-activators and basal transcription factors.

Inducible activators require the addition of a ligand (or activation signal) to activate transcription. Some ligand inducible activators, including Progesterone Receptor β (PGR-β), Androgen Receptor (AR), Estrogen Receptor (ER), and Glucocorticoid Receptor (GR), increase the stability of their interaction with chromatin in the presence of an activation signal (Table 1.1) [103, 133, 137]. Before the addition of a ligand,

Table 1.1: List of Nuclear Proteins and their Dynamics as Measured by FRAP
The dynamics of transcription factors involved in multiple aspects of transcription regulation were compared from multiple FRAP experiments. These experiments photobleached a variety of regions, under a number of different conditions.
[1] Regions photobleached are listed as follows: cytoplasm, half nucleus, nucleoplasm and nucleolus are random regions bleached, which provide a general, non-gene specific measurement of protein dynamics; HIV-1 TS, LacER array, LacO cassette, and the MMTV array are tandem arrays of specific genes or binding sites and are used to detect protein dynamics at specific loci in diploid cells; dev loci and *Hsp70* loci are specific chromosomal loci, which were bleached in polytene chromosomes, proving the dynamics of proteins in a naturally amplified system.
[2] Conditions used for the FRAP experiments indicate additional experimental conditions that influence the dynamics of transcription factors. These conditions include specific drug treatments, temperature, protein knockdowns or mutations. Unlisted conditions are done at standard conditions for the cell type. Specific details can be founding in the corresponding references.
[3] Species are listed as follows: *Dm, Drosophila melanogaster*; *Hs, Homo sapiens*; *Ma, Mesocricetus auratus* (Chinese hamster); *Mm, Mus musculas*; *Sc, Saccharomyces cerivisiae*; *Sd, Sus domestica* (Pig).
[‡] $\tau_{1/2}$ values and/or % recoveries were estimated from FRAP curves, or from charts presented in referenced paper because they either did not directly report these values or they used a different definition of $\tau_{1/2}$.

Transcription Activators & Co-Activators						
Protein	$\tau_{1/2}$ (s)	Recovery (%)	Region[1]	Condition[2]	Species[3]	Ref
Ace1	0.08 ‡	95 ‡	nucleoplasm		*Sc*	[99]
	0.05 ‡	100 ‡	nucleoplasm		*Sc*	[204]
	0.05 ‡	95 ‡	nucleoplasm	ΔDBD	*Sc*	[99]
AhR	5 ‡	100 ‡	half nucleus		*Mm*	[165]
AR	0.2	95 ‡	MMTV array		*Mm*	[103]
	5.5 ‡	100‡	nucleoplasm	+ ligand	*Hs*	[58]
	5.0	85 ‡	MMTV array	TST	*Mm*	[103]
ARNT	4 ‡	100 ‡	half nucleus		*Mm*	[165]
	31	100	nucleoplasm	+ hypoxia	*Hs*	[227]
BRD4	4 ‡	100 ‡	half nucleus		*Ma*	[165]
CBP	4.2 ± 1.1	100	LacER Array	+ E_2 20 min	*Ma*	[206]
C/EBP	7 ‡	100 ‡	half nucleus		*Ma*	[165]
ER	1.6 ± 0.3	86	nucleoplasm		*Hs*	[133]
	0.8 ± 0.2	100	nucleoplasm		*Hs*	[207]
	5.8 ± 0.4	66	nucleoplasm	+ E_2	*Hs*	[133]
	5.9 ± 0.2	100	nucleoplasm	+ E_2	*Hs*	[207]
	6.9 ± 0.7	68	nucleoplasm	+ E_2 + SRC	*Hs*	[133]
FBP	37.8 ‡	100 ‡	half nucleus		*Ma*	[165]
Fos	10 ‡	100 ‡	half nucleus		*Ma*	[165]
GR	0.43 ± 0.04	100 ‡	nucleoplasm		*Mm*	[137]
	0.4 ‡	75 ‡	nucleoplasm		*Mm*	[146]
	1.36 ± 0.15	100 ‡	nucleoplasm	+ Dex	*Mm*	[137]
	1.6 ± 0.09	100 ‡	MMTV Array	+ Dex	*Mm*	[137]
	1.53 ± 0.08	60 ‡	nucleoplasm	+ cortisol	*Hs*	[111]
	0.83 ± 0.12	100 ‡	MMTV Array	+ corticosterone	*Mm*	[137]
	1.46	75 ‡	nucleoplasm	+ cortisone	*Hs*	[186]
	∼ 2 ‡	100 ‡	MMTV Array	+ ligand	*Mm*	[136]

Table 1.1: (continued)

Transcription Activators & Co-Activators, continued						
Protein	$\tau_{1/2}$ (s)	Recovery (%)	Region[1]	Condition[2]	Species[3]	Ref
GRIP1	2.5 ‡	100	MMTV Array	+ Dex	*Mm*	[16]
HIF-1α	65	100	nucleoplasm	+ hypoxia	*Hs*	[227]
HoxB7	9.3 ‡	100 ‡	nucleoplasm		*Hs*	[58]
HSF	15	100 ‡	dev loci	NHS	*Dm*	[236]
	>6 min	30 ‡	*Hsp70* loci	HS	*Dm*	[236]
Jun	10 ‡	100 ‡	half nucleus		*Ma*	[165]
Klf4	13 ‡	100 ‡	nucleoplasm		*Hs*	[58]
Mad	4 ‡	100 ‡	half nucleus		*Ma*	[165]
Max	5 ‡	100 ‡	half nucleus		*Ma*	[165]
	0.2 ‡	80 ‡	nucleoplasm		*Mm*	[146]
Med6	8 ‡	80 ‡	nucleoplasm	SAP1 AD	*Mm*	[12]
	13 ‡	40 ‡	nucleoplasm	NET AD	*Mm*	[12]
Myc	6 ‡	100 ‡	half nucleus		*Ma*	[165]
NF1	4 ‡	100 ‡	half nucleus		*Ma*	[165]
NF-κB (p65)	0.8 ‡	100	nucleoplasm		*Mm*	[208]
	2.5 ‡	100 ‡	nucleoplasm		*Cs*	[187]
p53	0.7 ‡	80 ‡	nucleoplasm		*Hs*	[82]
	0.4 ‡	80 ‡	nucleoplasm		*Mm*	[146]
Pax6	36.4 ± 0.1	90 ‡	nucleoplasm		*Hs*	[58]
Pc	.2 ‡	75 ‡	nucleoplasm		*Dm*	[60]
	60 ‡	70 ‡	dev loci		*Dm*	[60]
PGRβ	0.6	100 ‡	nucleoplasm		*Mm*	[175]
	3.7	100 ‡	MMTV array	+ R5020	*Mm*	[175]
	4	100 ‡	nucleoplasm	+ R5020	*Mm*	[175]
RAR	1.9 ± 0.2	82	nucleoplasm		*Hs*	[133]
	2.3 ± 0.4	82	nucleoplasm	+ RA	*Hs*	[133]
Sp1	13 ‡	100 ‡	nucleoplasm		*Hs*	[58]
SPBP	24 ‡	90 ‡	nucleoplasm		*Hs*	[58]

Table 1.1: (continued)

Transcription Activators & Co-Activators, continued						
Protein	$\tau_{1/2}$ (s)	Recovery (%)	Region[1]	Condition[2]	Species[3]	Ref
SRC-1	2.1 ± 0.8	100	LacER Array		*Ma*	[206]
	~ 2	100	nucleoplasm		*Sc*	[207]
	7.5 ± 1.2	100	LacER Array	+ E_2 20min	*Ma*	[206]
	9.8 ± 2.9	100	nucleoplasm	+ E_2 20min	*Sc*	[207]
	30.2 ± 15.2	100	LacER Array	+ E_2 2hrs	*Ma*	[206]
Tat	40 ‡	80 ‡	HIV-1 TS		*Hs*	[142]
THR	1.8 ± 0.3	88	nucleoplasm		*Hs*	[133]
	1.8 ± 0.2	86	nucleoplasm	+ T_3	*Hs*	[133]
XBP	4 ‡	100 ‡	half nucleus		*Ma*	[165]
RNA Pol II and Transcription Factors						
Brd4	.75 ‡	90 ‡	nucleoplasm	G1	*Mm*	[51]
Cdk9	35 ‡	80 ‡	HIV-1 TS		*Hs*	[142]
CycT	30	75 ‡	*Hsp70* loci	HS 10min	*Dm*	[244]
Mot1	0.05 ‡	100 ‡	nucleoplasm		*Sc*	[204]
Nup98	1.16	~ 95 ‡	nucleoplasm		*Hs*	[72]
	11.8	75	Nuclear Bodies		*Hs*	[72]
	5 ‡	20	Nuclear Bodies	+ DRB	*Hs*	[72]
Pol II	83 ± 27	100	dev loci		*Dm*	[235]
	45 ‡	91 ‡	*Hsp70* loci	HS 15min	*Dm*	[235]
	81	78 ‡	*Hsp70* loci	HS+Spt6 KD	*Dm*	[9]
	167 ‡	75 ‡	HIV-1 TS		*Hs*	[24]
	72 ‡	100	MMTV Array	+ Dex	*Mm*	[16]
	32 ‡	90 ‡	LacO cassette		*Hs*	[45]
	125 ‡	100	nucleus		*Ma*	[102]
Spt6	40	60	*Hsp70* loci	HS 10min	*Dm*	[244]
TAF1	0.1 ‡	90 ‡	nucleoplasm		*Hs*	[47]
	0.1 ‡	100 ‡	nucleoplasm		*Sc*	[204]

Table 1.1: (continued)

RNA Pol II and Transcription Factors, continued						
Protein	$\tau_{1/2}$ (s)	Recovery (%)	Region[1]	Condition[2]	Species[3]	Ref
TAF5	0.1 ‡	90 ‡	nucleoplasm		*Hs*	[47]
TAF10	0.25	100	cytoplasm		*Hs*	[201]
	3	100	nucleoplasm	+ TAF8	*Hs*	[201]
TBP	0.1 ‡	66 ‡	nucleoplasm		*Hs*	[47]
	0.28 ‡	74 ‡	nucleoplasm		*Sc*	[204]
	∼60	100	nucleoplasm		*Hs*	[34]
	0.05 ‡	90 ‡	nucleoplasm	TBP V71R	*Sc*	[204]
	0.1 ‡	44 ‡	nucleoplasm	ΔMot1	*Sc*	[204]
	0.1 ‡	44 ‡	nucleoplasm	siBTAF1	*Hs*	[47]
TFIIB	0.05 ‡	100 ‡	nucleoplasm		*Sc*	[204]
TFIIH	3.5 ‡	100 ‡	nucleoplasm		*Hs*	[58]
	0.1 ‡	100 ‡	nucleoplasm		*Sc*	[204]
	0.23 ‡	90 ‡	nucleoplasm	ΔMot1	*Sc*	[204]
RNA Pol I and Transcription Factors						
UBF1	3 ‡	95 ‡	nucleolus		*Hs*	[53]
UBF2	3 ‡	95 ‡	nucleolus		*Hs*	[53]
TAF$_I$48	3 ‡	75 ‡	nucleolus		*Mm*	[53]
PAF53	5 ‡	75 ‡	nucleolus		*Hs*	[53]
RPA194	5-10 ‡	90 ‡	nucleolus		*Hs*	[53]
RPA40	5 ‡	75 ‡	nucleolus		*Mm,Hs*	[53]
RPA43	5-10 ‡	80 ‡	nucleolus		*Mm,Hs*	[53]
RPA16	10 ‡	75 ‡	nucleolus		*Mm,Hs*	[53]
Histones and Chaperones						
ASF/SF2	18.7 ± 3.1	100	nucleoplasm		*Hs,Mm*	[111]
BRG1	8 ‡	100 ‡	nucleoplasm		*Ma*	[165]
	0.9 ‡	100 ‡	MMTV array		*Mm*	[94]
	3.2 ‡	90 ‡	MMTV array	+ Dex	*Mm*	[94]

Table 1.1: (continued)

Histones and Chaperones, continued						
Protein	$\tau_{1/2}$ (s)	Recovery (%)	Region[1]	Condition[2]	Species[3]	Ref
BRM	.7 ‡	100 ‡	MMTV array		*Mm*	[94]
	1.6 ‡	90 ‡	MMTV array	+ Dex	*Mm*	[94]
HMGB1	2 ‡	100 ‡	nucleoplasm		*Ma, Hs*	[165]
HMGN1	15 ‡	100 ‡	nucleoplasm		*Ma, Hs*	[165]
H1	18.7 ± 5.7	94	nucleoplasm		*Hs*	[117]
	40 ‡	90 ‡	euchromatin		*Mm*	[140]
	24 ‡	54 ‡	euchromatin		*Dm*	[168]
	0.49 ± 0.11	100	nucleoplasm	ΔCTD	*Hs*	[117]
	40.4 ± 20.8	93	nucleoplasm	+ DRB	*Hs*	[117]
H2AX	hours ‡	<5	nucleoplasm		*Hs,Ma*	[198]
H2B	hours ‡	45	nucleoplasm		*Hs*	[101]
H3	hours ‡	80	nucleoplasm		*Hs*	[101]
H4	hours ‡	80	nucleoplasm		*Hs*	[101]
HP1 β	8 ‡	100 ‡	nucleoplasm		*Ma*	[165]
PARG	3 ‡	80 ‡	euchromatin		*Dm*	[168]
PARP	10 ‡	80 ‡	euchromatin		*Dm*	[168]
PCAF	4 ‡	100 ‡	nucleoplasm		*Mm*	[165]
Topo I	3 ‡	100	nucleoplasm		*Hs*	[35]
	29 ‡	83	nucleoplasm	+ CPT	*Hs*	[35]
	10	80 ‡	*Hsp70* loci	HS 10min	*Dm*	[244]
	5 ‡	100	nucleolus		*Hs*	[35]
	19 ‡	83	nucleolus	+ CPT	*Hs*	[35]
Topo II α	4 ‡	100	nucleoplasm		*Hs*	[36]
	8 ‡	100	nucleolus		*Hs*	[36]
Topo II β	4.5 ‡	93 ‡	nucleoplasm		*Hs*	[36]
	12 ‡	90 ‡	nucleolus		*Hs*	[36]

the observed $\tau_{1/2}$ is roughly equivalent to the expected $\tau_{1/2}$ for diffusion of a protein of a similar size (in the nucleus and at tandem arrays). After the addition of a ligand, however, the $\tau_{1/2}$ increases at least 2 fold, suggesting that a binding event occurs. Notably, the binding of these factors is still transient, with some people suggesting that the activator complex turns over after every round of transcription initiation [122].

Activation of HSF by HS also causes an increase in the stability of binding of HSF to DNA as compared to NHS. In contrast to the other activators, HSF remains stably associated with binding sites after activation ($\tau_{1/2} > 6$ minutes), even if these sites do not lead to productive activation [236]. HSF also shows unique behavior before activation with its association with the locus, which suggests a binding interaction rather than free diffusion. This may be due to the affinity of the transcription factor to specific sites during NHS.

Not all activators show an increase in stability when activated. Before activation, the $\tau_{1/2}$ of both RAR and THR are is greater than expected for diffusion [133, 202], suggesting that they might already be associated with the chromatin. This is supported by the biology and function of these receptors as both can recruit co-repressors in the absence of ligand [133]. Thus the addition of a ligand has a different effect on RAR and THR than with the other activators; instead of stabilizing the DBD and its interaction with chromatin, the ligand allows it to recruit co-activators instead of co-repressors.

Co-activators also transiently bind to chromatin or transcription complexes, such that their $\tau_{1/2}$ is much greater than expected for diffusion. In the case of SRC-1 and CBP, binding of the activator to regulatory sites leads to an increase in the $\tau_{1/2}$ at specific binding sites. This result shows that transcription activation complexes are highly dynamic both at the level of activator–DNA binding and at protein–protein interactions occurring within the complex [207].

Other live cell imaging studies of activator and/or co-activator interactions have been performed. Bhaumik *et al.* [20] used FRET to identify a direct interaction between the Tra1 subunit of SAGA and the activator Gal4 in yeast. This result begins to define the specific interactions that are required for the transduction of the activation signal to activation of transcription. More recently, direct interactions between activator complexes have been identified, such as in the heterodimeric activator complex Hif1 (composed of Hif-1α and ARNT), which has an increased frequency of interaction during hypoxia [227].

RNA Pol II and Transcription Factors

The dynamics of transcription regulation in living cells is not limited to the study of activators and co-activators, as Table 1.1 illustrates. In fact, the dynamics of a number of transcription factors involved in transcription initiation (basal transcription factors) have been studied in both human and yeast cells [34, 47, 204], as have the dynamics of Pol II [9, 24, 235] and a select few elongation factors. In this thesis, I have expanded the selection of transcription factors studied in this method to include the CycT subunit of P-TEFb, Spt6, and Topo I (a chromatin associating factor that is required for efficient transcription elongation in the context of chromatin).

The basal transcription factors, including the TAFs, TBP, TFIIB, and TFIIH are highly dynamic in living cells; however, the $\tau_{1/2}$ for each of these factors is longer than the expected $\tau_{1/2}$ for diffusion [47, 202, 204]. For the yeast experiments, it was also shown that a DNA binding deficient form of Ace1 (Ace1ΔDBD-GFP), which is a similar size as these factors, recovers faster than the basal transcription factors [204]. Together these observations concerning the rate of recovery indicate that basal transcription factors, like activators, transiently associate with the DNA. Contradictory results for TBP,

suggesting a much more stable interaction were observed in human cells when TBP was transiently over expressed [34], however when expressed at a normal level the dynamics of TBP in human cells were similar to the observed result in yeast [47]. It is important to note that all of these studies photobleached a region of the nucleoplasm, not specific gene loci. Therefore, it is possible that the actual binding interaction at specific gene loci is more stable than estimated with these studies.

In contrast to the other transcription factors and activators, Pol II is a processive enzyme, remaining bound to the chromatin as it translocates along the DNA. The average rate of elongation for Pol II is $\sim$3.8 kb/min, but rate estimates range from 1.1 kb/min to 6 kb/min [8]. For the *Drosophila Hsp70* genes, the rate of RNA synthesis was estimated to be 1.2 kb/min [156]. FRAP results in *Drosophila* salivary glands are consistent with this estimate. For the *Hsp70* loci, where $\tau_{1/2} = 45$ seconds and the gene length is $\sim$2.5 kb, the rate of elongation is estimated to be $\sim$1.5 kb/min [235]. Live cell imaging estimates of elongation rate range from 1.2 kb/min to 4.3 kb/min.

Transcription of rDNA occurs by RNA polymerase I (Pol I), and sites of rDNA transcription are relegated to a nuclear substructure, known as the nucleolus. Like transcription by Pol II, Pol I requires the aid of multiple transcription factors to properly initiate and elongate. Dundr *et al.* [53] addressed the dynamics of these factors in the nucleolus using FRAP in living cells. The dynamics of the Pol I transcription factors, UBF1, UBF2, TAF$_I$48, and PAF53, have similar dynamics as Pol II transcription factors with $\tau_{1/2}$ = 3 seconds, suggesting a transient binding interaction with the ribosomal genes. Unlike Pol II, however, the subunits of Pol I have a $\tau_{1/2}$ of 5-10 seconds (Table 1.1), which suggests a transient interaction with the nucleolus.

Notably, many Pol II and Pol I FRAP curves are biphasic. The faster phase likely represents diffusion and/or non-productive initiation and the slower phase productive

elongation. A number of studies have tried to model the biphasic (or even multi-state) FRAP curves in order to understand the regulation of elongation and have suggested rates of initiation and elongation [45, 102]. For Pol I, the elongation rate was measured to be 5.7 kb/min [53].

Histones and Chaperones

In vivo, Pol II must transcribe through chromatin, which consists of DNA wrapped around nucleosomes. To promote efficient elongation, the individual subunits of the nucleosomes, can be moved. Movement can occur through nucleosome remodelers, which reposition the nucleosome on the DNA, or by histone chaperones, which temporarily displace histones from the gene. Most live cell imaging studies have been restricted to measuring the global dynamics of histones, and have discriminated between inactive chromatin and transcriptionally active chromatin. Polytene localization of the core histone H2B shows that core histones are found at a higher concentration at condensed regions of the chromosome [113, 244]. Therefore all global/random FRAP measurements are mostly a result of the interaction with inactive chromatin.

Photobleaching the core histones identify that they have a very stable interaction, with $\tau_{1/2}$ values ranging in hours. However, the stability of H1, is much more dynamic with $\tau_{1/2}$ values similar to some of the more stable, but dynamic associations of transcription factors with the chromosomes. Importantly, the inhibition of transcription elongation by DRB does change the binding affinity between H1 and the DNA [117]. As previously noted, these observations may not represent the dynamic interactions that occur at active sites of transcription, but they are consistent with known behaviors of the histones.

Unlike the core histones, and similar to transcription factors, histone chaperones and other chromatin interacting proteins are transiently associated with DNA, with $\tau_{1/2}$ values representing a delayed recovery due to binding. Notably, when these factors are associated with sites of active transcription, as illustrated with BRG1 and BRM at the Mouse Mammary Tumor Virus (MMTV) array, and Topo I and Topo II in the nucleolus, there is a retardation of the dynamics, showing that their interaction is stabilized with active transcription.

1.2.3 Conclusion

In conclusion, live cell imaging has enlightened the field about the dynamic nature of transcription. In most cases, transcription activation leads to the stabilization of transcription factors at specific loci. Nevertheless, even though these interactions are stabilized, they remain dynamic. There are exceptions. HSF stably associates with specific loci after HS ($\tau_{1/2}$ >6 minutes) and some factors already transiently associate with the chromatin before activation. However, using FRAP it has become clear that one can no longer assume complexes are stably bound and reused over the course of activation.

Interestingly, our lab has recently identified a progressive change in the fluorescence recovery (from 100% to 0% recovery) of Pol II at the *Hsp70* loci during activation [235]. This behavior is believed to be due to the formation of a transcription compartment. Such acompartment may permit cells to keep a local high concentration of transcription factors around a gene in order to promote efficient and continued transcription activation and elongation.

1.3 Organization of Thesis

This thesis describes projects that focus on the *in vivo* regulation of transcription, through the use of live cell imaging.

In **Chapter 2**, we describe the methods used in this thesis from expressing FP-tagged transcription factors in salivary glands to advantages and disadvantages of different microscope systems. We also describe the specific protocols and analyses used in this thesis.

Chapter 3 focuses on the recruitment and dynamics of transcription factors at the *Hsp70* loci in living cells, including HSF, Pol II, P-TEFb, Spt6 and Topo I. These factors are involved in multiple stages of transcription from activation to elongation. Due to their diverse functions in transcription, they also will provide different examples of behaviors for the extremely varied regulation of transcription. This study provides key insights into the regulation of gene activation through the description of three features: (1) the temporally distinct recruitment of transcription factors to the *Hsp70* loci, (2) the synchronous recruitment of these factors to the *Hsp70* loci and (3) the general "compartmentalization" of transcription factors at the *Hsp70* loci.

Chapter 4 addresses the structure of the transcription compartment. Interestingly, we observe that PARP catalytic activity is involved in the progressive retention of Pol II and other transcription factors. Furthermore, we address the localization of H2B and PARP at the *Hsp70* loci after activation, and observe that total levels of these factors do not decrease after activation.

In **Chapter 5**, we address the dynamics and localization of a newly identified homolog of Set1 at the *Hsp70* loci.

In the final chapter, **Chapter 6**, we offer an integrated view of transcription regulation in living cells as these studies have revealed. However, this thesis also provides the foundation for a number of mechanistic questions, which I will discuss and suggest as possible future directions.

Appendix A describes, in detail, the generation of transgenic FP-tagged fluorescent lines. And lists my contributions to the overall collection, which have not been used in this thesis.

CHAPTER 2

MATERIALS AND METHODS[1]

2.1 Expression of FP-tagged Transcription Factors in the *Drosophila* Salivary Glands

We have assembled a growing collection of *Drosophila* transcription factors involved in *Hsp70* gene activation that are tagged with various FPs. Individual fly stocks were either generated in house or acquired from large screens. The in-house transcription factors transgenically express a FP-tagged transcription factor; while the acquired fly stocks contain an endogenously tagged eGFP tagged transcription factor. For the former method, we generated a number of transgenic constructs that can be expressed in a tissue specific manner using the *Drosophila* UAS Gal4 inducible system [52]. Transcription factors were tagged either on the N- or C- terminus using the Gateway compatible *Drosophila* injection vectors containing the appropriate FP. Before cloning, we searched available yeast and *Drosophila* databases (`yeastgenome.org` and `flybase.org`) as well as the published literature to determine whether the candidate transcription factors (or their homologs) have been successfully tagged with GFP or another large affinity tag. Based on these data mining results, we created individual cloning schemes for each of the transcription factors (described in detail in Appendix A). In addition to these transgenic fly stocks, we acquired stocks from large screens, including FlyTrap [145]. In the FlyTrap screen, random insertions of an artificial exon encoding GFP were identified and mapped to specific sites. Some insertions occurred in the introns of transcription-factor-encoding genes [145].

For the recruitment assays, we began from the homozygous stocks listed in Table 2.1

[1] Parts of this chapter are published in Yao *et al.* 2008 [237] and Zobeck *et al.* 2010 [244]

Table 2.1: Genotypes of Homozygous Parental *Drosophila* Lines

Line	Genotype
FP-tagged Transcription Factors	
mRFP-CycT	w^{1118}; UAS-mRFP-CycT
mRFP-H2B	w^{1118}; + / +; UAS-mRFP-H2B
eGFP-HSF	w^{1118}; + / +; UAS-eGFP-HSF Sgs3-Gal4
PARP-eGFP	w^{1118}; + / +; UAS-PARP-eGFP
eGFP-Pol II	w^{1118}; UAS-eGFP-Rpb3 C147-Gal4
mRFP-Pol II	w^{1118}; + / +; UAS-mRFP-Rpb3 C729-Gal4
eGFP-Set1	w^{1118}; UAS-eGFP-Set1
eGFP-Spt6	w^{1118} eGFP-Spt6
eGFP-Topo I	w^{1118} eGFP-Topo I
Gal4 Driver lines	
Fkh-Gal4	w^{1118}; Fkh-Gal4; + / +
C729-Gal4	w^{1118}; + / +; C729-Gal4

and crossed an FP-tagged transcription factor with a homozygous line containing the complementary FP-tagged Pol II. The chromosome containing the FP-tagged Pol II was homologously recombined with a Gal4 driver [236]. Thus, using the homologously recombined Pol II construct ensures that both Pol II, and the transcription factor will be expressed in the salivary glands. HSF was previously recombined with the Sgs3-Gal4 driver line [236], and was not imaged directly with Pol II because the over expression of HSF using either Fkh-Gal4, C729-Gal4 or C147-Gal4 causes salivary gland defects and Pol lI is not expressed at sufficient levels when expressed with the Sgs3-Gal4. The final crosses used for the recruitment assay are listed in Table 2.2.

For the FRAP assays, we began from the homozygous stocks listed in Table 2.1. eGFP-Topo I and eGFP-Spt6 are expressed using their endogenous promoters and therefore are expressed in the salivary glands independently from the expression of the Gal4 driver. The other constructs required expression of a salivary gland driver in order to be properly expressed. For eGFP-Pol II we used the homologously recombined construct listed in Table 2.1. To express P-TEFb, we used the Fkh-Gal4 line, while to express

eGFP-Set1 we used the C729-Gal4 line. The genotypes for all the FRAP crosses are listed in Table 2.3.

2.2 *Drosophila* Salivary Gland Tissue Preparation

As *Drosophila* larvae undergo development, they begin to crawl out of the muck (early), wander along the culture tube wall (wandering) and then stop, evert their anterior spiracles and start puparization (late). Early and wandering stages of 3^{rd} instar larvae have well-defined salivary gland cell structures and appear slightly opaque under transmission microscopy. The nuclei are of spherical shape with diameters $\sim$25–35 μm, with early 3^{rd} instar larvae having smaller nuclei. Late 3^{rd} instar larva, however, show distinct morphology from the early stages: the cells layers are separated from the center and the glands, which are filled with glue, appear more "transparent" than earlier developmental stages. Normally, polytene cells within one salivary gland are identical in shape and show the same level of polytene endoreplication, and the polytene nucleus closest to the coverslip surface is usually at least 30 μm deep in the tissue

All of these stages can theoretically be used for live cell imaging methods, however the wandering 3^{rd} instar larva is preferred for a number of reasons. First, the dis-

Table 2.2: Genotypes of *Drosophila* Constructs used in Recruitment Analyses

Line	Genotype
CycT $\times$ Pol II	w^{1118}; UAS-eGFP-Rpb3 C147-Gal4 / UAS-mRFP-CycT; + / +
H2B $\times$ Pol II	w^{1118}; UAS-eGFP-Rpb3 C147-Gal4 / +; UAS-mRFP-H2B / +
HSF $\times$ H2B	w^{1118}; + / +; UAS-eGFP-HSF Sgs3-Gal4 / UAS-mRFP-H2B
PARP $\times$ Pol II	w^{1118}; + / +; UAS-PARP-eGFP / UAS-mRFP-Rpb3 C729-Gal4
Set1 $\times$ Pol II	w^{1118}; UAS-eGFP-Set1 / +; UAS-mRFP-Rpb3 C729-Gal4 / +
Spt6 $\times$ Pol II	w^{1118} eGFP-Spt6; + / +; UAS-mRFP-Rpb3 C729-Gal4 / +
Topo I $\times$ Pol II	w^{1118} eGFP-Topo I; + / +; UAS-mRFP-Rpb3 C729-Gal4 / +

Table 2.3: Drosophila Constructs used in FRAP

Line	Genotype
CycT	w^{1118}; UAS-mRFP-CycT/ Fkh-Gal4; + / +
Pol II	w^{1118}; UAS-eGFP-Rpb3 C147-Gal4
Set1	w^{1118}; UAS-eGFP-Set1 / +; C729-Gal4 / +
Spt6	w^{1118} eGFP-Spt6
Topo I	w^{1118} eGFP-Topo I

tinct separated morphology of late 3^{rd} instar larva is more fragile than the well-defined cell structures of early and wandering stages. Late 3^{rd} instar larva also have induced ecdysone puffs 74E & 74F making the identification of the *Hsp70* loci *in vivo* difficult. Second, the nuclei of early 3^{rd} instar larva have undergone fewer endoreplications and are therefore smaller than the wandering 3^{rd} instar larva.

Therefore, *Drosophila* salivary glands from wandering 3^{rd} instar larva were dissected as previously described [237]. Briefly, larvae are cultured in 5:1 Grace's Medium diluted with sterile water. Then, the dissected salivary glands are transferred with medium to either a Bioptechs FCCS3 Closed Chamber System with a 0.2 mm spacer, or a MatTek glass-bottom culture dish (P35G-1.0-14-C) with a glass coverslip placed on top to reduce evaporation and movement of the glands. The dissected salivary gland tissues are then examined with transmission light where tissues damaged during dissection are identified and excluded from imaging.

When salivary glands are maintained at room temperature, the genes involved in salivary gland development are expressed, but the *Hsp70* genes are inactive. A heat shock of the tissue at 36.5°C leads to a turndown in the developmental gene expression and activation of *Hsp70* gene transcription. It has previously been shown that transcription remains active for at least 1 hour after HS in similar conditions [235], while salivary glands remain viable and responsive to HS for at least 2 hours after dissection [237].

2.3 Live Cell Imaging of *Drosophila* Salivary Glands

2.3.1 Microscopy Techniques to Image Polytene Chromosomes

The structure and function of *Drosophila* polytene chromosomes have been studied microscopically using various techniques, from optical microscopy to electron microscopy [26, 192]. Dr. Sedat and colleagues developed a method with which to image the organization of the polytene chromosomes in the nucleus, using Hoechst dye and widefield deconvolution microscopy to optically section and image different focal planes of the nucleus [135, 1, 84, 85]. However, individual gene loci can be difficult to identify with the image quality provided by widefield deconvolution methods (Figure 2.2), and studying the dynamics of transcription regulation at individual genes in polytene nucleus is best accomplished with optical sectioning techniques that have high effective resolution in relatively thick tissues.

The most widely used optical sectioning microscopy is Laser Scanning Confocal Microscopy (LSCM) [38]. In this method, a focused laser is moved in a raster-scan fashion to acquire a 2D image one pixel at a time. With each pixel, the laser excites fluorescent molecules at the focal plane and above and below it. The fluorescence emission, however, is only collected for the focal plane by using a tiny pinhole that allows the in-focus fluorescence to reach the photomultiplier tube (PMT) detector and blocks the "out-of-focus" fluorescence from reaching the detector. Figure 2.1A shows the light path of LSCM.

As a variation of LSCM, spinning disk confocal microscope (SDCM) provides a higher scanning rate at the sacrifice of a loss in penetration [38]. This is largely due to the simultaneous detection of the entire field of view using CCD array detection versus individual pixel detection using a PMT. In this system, the laser beam is expanded

Figure 2.1: Schematic of Imaging Light Pathways for LSCM, SDCM and MPM
(A) LSCM light path. Single photon excitation of eGFP occurs with 488 nm wavelengths (blue line). eGFP then fluoresces at 504 nm (green line) and is collected with a photomultiplier tube (PMT) after passing through pinhole reducing collection of "out-of-focus" fluorescence. (B) SDCM light path. The single photon fluorescence beam is expanded, and then focused through the two spinning disks. Emission fluorescence from only the focal volume can pass through the lower spinning disk providing confocality. The fluorescence is the reflected to a CCD array and the entire field of view is collected because the rate of spinning is faster than the exposure time. (C) MPM light path. Two-photons of 910 nm light (red line) are used to excite eGFP only at the focal volume. The emission is then reflected into a PMT filter with out passing through a pinhole.

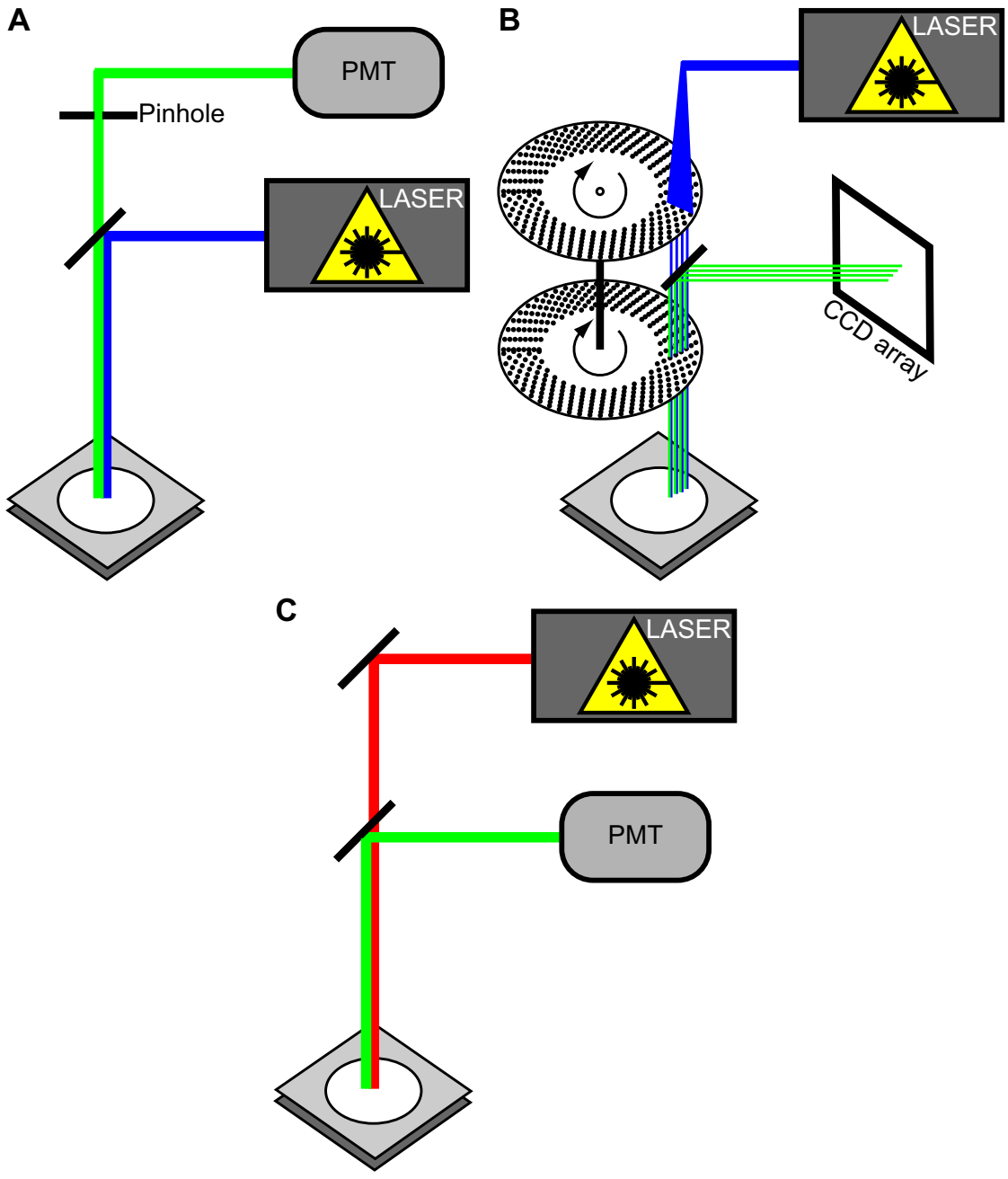
A
PMT
Pinhole
LASER
B
LASER
CCD array
C
LASER
PMT

to illuminate a large region of a spinning disk. In the Yokogawa CSU-X1 spinning disk unit, the first disk contains lenses to then focus the light through the pinholes on the second disk to the sample. Emission of eGFP is then reflected back through the second disk providing confocal sectioning by blocking "out-of-focus" fluorescence and is reflected onto a CCD array. The entire focal region is obtained in one image because the spinning rate is faster than the exposure time (Figure 2.1B).

The third method, Multiphoton Microscopy (MPM) has become widely used in biological and biomedical research [48, 243]. Two-photon excitation occurs only at the very proximal region to the focal point [48]. Therefore, the effective focal volume is intrinsically confined in both lateral and axial axes, eliminating the autofluorescence background, photobleaching, and photodamage from out-of-focus planes [243, 222]. The infrared laser used in MPM has deeper tissue penetration (as deep as 0.5 mm) and less scattering [243, 222, 70]. In MPM, no pinhole is needed to reject out-of-focus fluorescence as in LSCM, which greatly enhances the image signal. A schematic of the light path is show in Figure 2.1C.

We have tested a variety of widefield deconvolution, LSCM, SDCM, and MPM systems in imaging polytene nuclei in salivary gland tissue. Shown in Figure 2.2, images with satisfactory quality have been achieved with the LSCM systems (i.e., Zeiss LSM 510), SDCM systems (i.e. Zeiss Cell Observer SD) and MPM systems on salivary gland tissues expressing eGFP-tagged Pol II, however, widefield microscopy suffers from an excess of "out-of-focus" fluorescence. For mRFP, however, we were unable to excite it with two-photon excitation using the MaiTai laser. Therefore, we used confocal microscopy for imaging mRFP.

Each of these systems has advantages and disadvantages, which make a specific system better in certain cases. In this thesis, I have used each of these microscopy

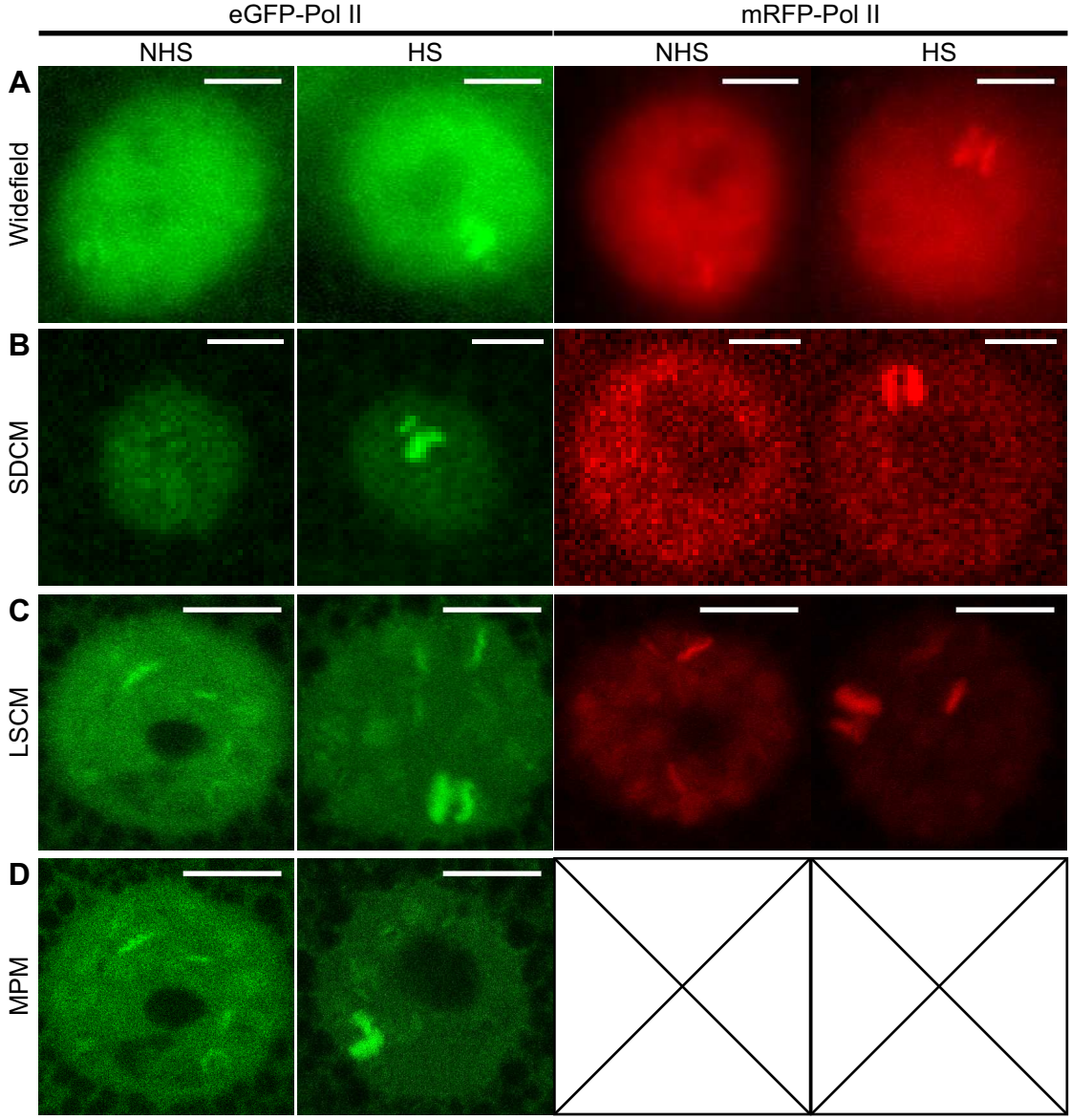

Figure 2.2: Comparison of Widefield, SDCM, LSCM and MPM imaging of polytene nuclei

(A-D) Representative images of Pol II-eGFP (left panels) and Pol II-mRFP (right panels) during NHS (first and third panel) and after HS (second and forth panel), NHS images are random focal planes, while HS images identify the *Hsp70* loci. Microscopy methods are (A) widefield microscope, (B) SDCM, (C) LSCM and (D) MPM. Note that we were unable to excite Pol II-mRFP using MPM. Scale bars = 10 μm.

systems as necessary.

2.3.2 Identification of Specific Chromosomal Loci

Although the visualization of individual banding pattern by DNA stain or by GFP-tagged transcription factors is aesthetically pleasing, the identification and mapping of these endogenous gene loci in a 3D-organized polytene nucleus is a significant challenge. In this thesis, we use both an "online" and "offline" method to identify specific loci.

For FRAP, it is necessary to identify specific loci "online", while acquiring data. We have found that the accumulation of Pol II at endogenous heat shock gene *Hsp70* loci 87A & 87C gives a distinctive doublet pattern throughout a polytene nucleus during HS, which can be identified in real time. This pattern can be confirmed to be *Hsp70* gene loci by two criteria: (1) the doublet is not visible before HS and only appears after HS; (2) the doublet is distinctive and the only pair throughout the entire nuclear section series. We have used this method for studying Pol II dynamics in living cells [235]. However, in cases where it is difficult to specifically identify specific loci, it is possible to insert multiple LacO repeats near the loci, which bind tightly to the LacI repressor [178]. Then, using a FP-tagged LacI, it is possible to locate the loci. This system has been used in *Drosophila* [216] and can be used to mark endogenous genes, including the *Hsp70* loci.

For the recruitment assays, however, we were unable to identify the *Hsp70* loci in real-time. Therefore, we collected a 4D series consisting of the entire nucleus at numerous time points after HS. After all data points were collected it was possible to extrapolate backward to identify the *Hsp70* loci before the presence of the distinctive *Hsp70* doublet.

2.3.3 Kinetic Analysis of Transcription Factor Recruitment to the *Hsp70* loci

In Chapters 3 and 5, we address rates and timing of transcription factor recruitment to the *Hsp70* loci, by co-expressing FP-tagged transcription factors with the complementary FP-tagged Pol II and imaging over the course of activation. It was also used to address the retention or loss of H2B and PARP from the *Hsp70* loci, as described in Chapter 4. For these experiments, a number of *Drosophila* lines expressing an eGFP-tagged protein and a mRFP-tagged protein were required. Table 2.2 lists the specific *Drosophila* lines used in these experiments. Specific methods, protocols, and analyses used for these experiments are listed below.

Image Acquisition with Spinning Disk Confocal Microscopy

For optimal temporal resolution of the recruitment of transcription factors to the *Hsp70* loci, we used a Carl Zeiss Cell Observer Spinning Disk system with the Yokogawa CSU-X1 spinning disk unit and a Hamamatsu C9100-13 EMCCD camera. Using this microscope we were able to obtain confocal 3D stacks with 2-channels with time intervals of 10–30 seconds.

To acquire both a NHS and HS z-stacks we used two identical Plan-Apochromat 40x/1.3 Oil Iris objectives. One objective was maintained at room temperature and one was heated on the microscope to 36°C using a Bioptechs Objective Heater. A 40 μm pre-activation z-stack, with 1 μm sections, was taken using the room temperature objective in both channels alternating channels every slice. Then the 36°C objective was moved into position. HS times were started the moment the immersion medium contacted the coverslip and due to the large heat capacity of the lens this contact causes a nearly instantaneous HS [235]. Then, an xyzt series with 40 z-sections was obtained after

readjusting the focal position. Time intervals were between 10-30 seconds and the time series lasted 20 minutes. Images were taken at a resolution of 512x512 pixels, using 16-bit color depth.

Image Acquisition with Laser Scanning Confocal Microscopy

A Carl Zeiss LSM510 META on an upright confocal/multi-photon microscope system was used for the kinetic analysis of Set1 recruitment to the *Hsp70* loci (see Chapter 5). In this case, we used identical C-Apochromat 61x, 1.2 NA, water immersion objectives at room temperature and 37°C, heated in the same manner as above. We used a scan zoom (1x) to image an individual nucleus from each salivary gland. A 35 μm pre-activation z-stack, with 1 μm sections was taken in both channels alternate channels every slice, then as with the SDCM method, the pre-heated objective was moved into position. Time intervals were around 150 seconds and the time series lasted 20 minutes. Images were taken at a resolution of 512x512 pixels, using 12-bit color depth.

Data Analysis

We used ImageJ v1.42 [173] to process our data before analysis. The ImageJ plugin MultiStackReg was used to align the images that over time drifted in x, y and z (we corrected for one channel and applied these corrections to the second channel). The images were then corrected for photobleaching using a small nuclear region and the sections containing the *Hsp70* loci were identified. T. Marian (personal correspondence) wrote a MatLab program for the analysis. This program measures the number and intensity of pixels above a threshold for a defined region of interest, in our case the *Hsp70* loci. For total intensity plots we used a threshold of 0; for mean intensity plots we calculated a

threshold such that all pixels in the 20 minutes HS time point were identified.

Non-linear curve fitting to estimate the rate of recruitment was done using gnuplot v4.2 (http://www.gnuplot.info/) using the exponential equation $f(t) = A(1 - e^{-k(t-t_0)})$, where A equals the plateau, k equals the rate of recruitment, t_0 equals the time recruitment begins. For the time differential plots, the parameters defined by non-linear curve fitting were used and the exponential equation solved for t, in order to calculate the time it takes for a factor to reach a specific fluorescence intensity. The time to reach the same fluorescence intensity for Pol II was subtracted from the transcription factor.

2.3.4 Fluorescence Recovery After Photobleaching Analysis of Transcription Factors at the *Hsp70* Loci and Developmental Loci

In Chapters 3, 4, and 5, we address the dynamics of the FP-tagged transcription factors with the *Hsp70* loci or developmental loci (Chapter 5 only). The *Drosophila* lines used are listed in Table 2.3, with the specifics on the experimental setup listed below.

Photobleaching with Multiphoton Microscopy and LSCM

Using the Carl Zeiss LSM510 META with a C-Apochromat 61x, 1.2 NA, water immersion objective, we were able to image and photobleach specific focal planes over time. We used a circular ROI limited to the dimensions of the *Hsp70* loci. To photobleach eGFP using MPM, we used 15-20 mW of laser power at 910 nm from a Mai Tai laser (Spectrum Physics) measured after the objective lens. For MPM photobleaching of mRFP photobleaching we used the same laser set to 800 nm with 40-50 mW at the sample. These settings photobleached the samples to 40-60% initial intensity. Images were corrected in the same manner as for the Recruitment Analysis (Subsection 2.3.3),

and a small nuclear section was monitored for acquisition photobleaching. We also used single photon excitation to photobleach eGFP, in this case we used a 488 nm laser and bleached the samples between 40-60% of the initial intensity.

Fluorescence Recovery After Photobleaching Analysis

We used ImageJ v1.42 [173] to process our data. To correct for any drift in x and y over time, we used the MultiStackReg plugin. Then, the images were corrected for photobleaching occurring over the course of imaging by measuring the fluorescence at a small nuclear region. In addition, the mean fluorescence intensity of the *Hsp70* loci was measured and corrected for photobleaching. FRAP curves were double normalized so that pre-bleach images equals one, and first image after the bleach equals 0. The $\tau_{1/2}$ was calculated for the "mobile" fraction using the time it takes to reach 50% of the level of the plateau. Recovery rates were obtained by fitting the FRAP data to $f(t) = A \times (1 - C_{eq} \times e^{-k_{off} \times t})$ [203].

2.3.5 Perfusion

Using a Bioptechs Micro-Perfusion Pump in conjunction with the Bioptechs FCCS3 imaging chamber, we were able to perfuse fresh media or drugs over the sample to asess their effect on the dynamics of the transcription factors at specific time points after HS. Using a 0.031-inch diameter "pump" tubing, we were able to perfuse media across the chamber at a rate of $\sim$350 μl/minute (manufacturers data) and have experimentally observed that the media reaches the center of the FCCS3 chamber in 95 seconds (Figure 2.3).

To confirm the effects seen with perfusion are specific to the drug treatment we re-

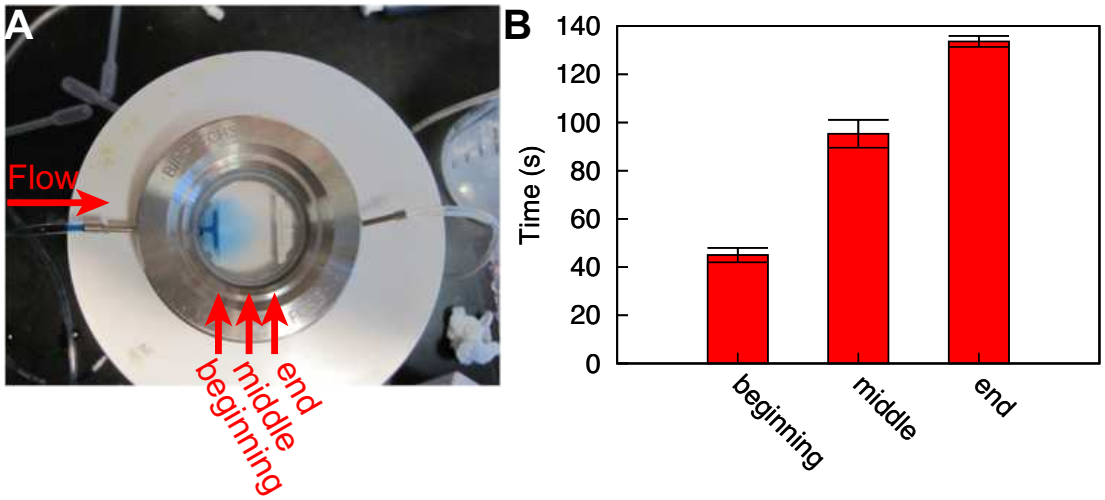

Figure 2.3: Timing for Media to Cross the FCCS3 Imaging Chamber after Perfusion

(A) Image of FCCS3 Imaging Chamber with the Micro-Perfusion Pump setup to perfuse Blue Dextran through the chamber. Beginning, Middle and End positions are marked. (B) Length of Perfusion required to reach appropriate position of chamber. n=3 and error bars represent the standard error of the mean (SEM).

ceived, all experiments were complemented with media only and no perfusion controls. Notably, using a larger diameter "pump" tubing (0.064 inch) causes detrimental effects on the localization and dynamics of different transcription factors, but the 0.031-inch tubing does not cause these problems.

In chapter 4, we perfuse 3 μM PJ34 diluted with 5:1 Grace's Media or 5:1 Graces Media only into the FCCS3 chamber occurred as depicted in Figure 4.5. Briefly, we used the Carl Zeiss LSM510 META, as was used for all FRAP experiments (see above), with a pre-heated C-Apochromat 61x, 1.2 NA, water immersion objective. We instantaneously heat shocked the glands in the chamber for 35 minutes and then begin perfusing PJ34 or media over the sample for 5 minutes. 40 minutes after HS, we stop perfusion, identify the *Hsp70* loci, photobleach the samples to 40-60% initial intensity, and monitor fluorescence recovery for 5 minutes.

2.4 Chromatin Immunoprecipitation (ChIP) on *Drosophila* Salivary Glands

2.4.1 Formation of Formaldehyde Cross-linked Salivary Gland Extract for ChIP

The previously published salivary gland ChIP protocol was modified from the established cell culture ChIP protocol from the Lis lab [185] to adjust for the use of *Drosophila* salivary glands as starting material [235]. Further modifications were made to this protocol in order provide a greater amount of chromatin to be isolated.

In our modified procedure, we dissected 15-20 salivary glands per IP in 5:1 Grace's Media with water, isolating glands from an eGFP-tagged Pol II expression line, w^{1118}; UAS-eGFP-Rpb3 C147-Gal4. We instantaneously HS the glands by adding an equal

amount of 48°C media to the glands and HS in a 37°C water bath for the indicated amount of time. HS material was subsequently cooled to room temperature using ice-cold media before adding paraformeldehyde to a final concentration of 1% for 2 minutes. The fixation was quenched by the addition of Glycine to a final concentration of 0.125M for 3 minutes. Glands were then incubated for 10 minutes in 1x Sonication Buffer (0.5% SDS, 20 mM Tris, 2 mM EDTA, 0.5 mM EGTA, 0.5 mM PMSF, 1x Roche Complete Protease Inhibitor) before sonicating using the Bioruptor (Diagenode) to produce fragments of 100-200 bases and then froze with liquid nitrogen.

2.4.2 ChIP

The ChIP step occurred as previously published [185, 235] with a few modifications. Briefly, formaldehyde crosslinked salivary gland extract was diluted 1:40 with IP buffer (0.5% Triton X-100, 2 mM EDTA, 20 mM Tris, 150 mM NaCl, 10% Glycerol) and then pre-cleared with 30 μl of 50% Protein-A agaroses beads / IP for 1-2 hours at 4°C with rotation. Pre-cleared extract from 18 salivary glands were then incubated at 4°C with rotation overnight using 4 μl Rpb3 [154], 4 μl Spt6 [9], 2 μl CycT [22], or 0 μl antibody as appropriate, and subsequently incubated with 100 μl of 50% Protein-A agarose beads / IP for 2 hours with rotation at 4°C.

Immunoprecipitated complexes were washed 1x with Low Salt Wash (0.1% SDS, 1% TritonX-100, 2 mM EDTA, 20 mM Tris, 150 mM NaCl), 3x with High Salt Wash (0.1% SDS, 1% TritonX-100, 2 mM EDTA, 20 mM Tris, 500 mM NaCl), 1x with LiCl Wash (1 mM EDTA, 10 mM Tris, 0.25 M LiCl, 1% NP40, 1% NaDeoxycholate), and 2x with TE. Washes were for 3–5 minutes on rotating mixer at room temperature followed by a 1 minute spin at 1000 rpm. Chromatin was eluted from the beads with freshly prepared elution buffer (1% SDS and 0.1 M $NaHCO_3$) by incubating at room

Table 2.4: Primers used for Real-Time PCR
Regions represent the position along the *Hsp70* gene in relation to the transcription start site (+ 1). The 87C primer set is positioned within the chromosomal puff 87C at a site that is devoid of all transcription.

Region	Primer	Sequence
– 154	*Hsp70* – 200 F	5'-TGCCAGAAAGAAAACTCGAGAAA
	Hsp70 – 108 R	5'-GACAGAGTGAGAGAGCAATAGTACAGAGA
+ 10	*Hsp70* – 48 F	5'-AAAAGAGCGCCGGAGTATAA
	Hsp70 + 68 R	5'-CAGCTGCGCTTGTTTATTTG
+ 96	*Hsp70* + 56 F	5'-ACAAGCGCAGCTGAACAAGCTA
	Hsp70 + 137 R	5'-ACTTGGTTGTTGGTTACTTT
+ 378	*Hsp70* + 334 F	5'-CACCACGCCGTCCTACGT
	Hsp70 + 423 R	5'-GGTTCATGGCCACCTGGTT
+ 1702	*Hsp70* + 1649 F	5'-GGGTGTGCCCCAGATAGAAG
	Hsp70 + 1754 R	5'-TGTCGTTCTTGATCGTGATGTTC
+ 2210	*Hsp70* + 2155 F	5'-GGTCGACTAAGGCCAAAGAGTCTA
	Hsp70 + 2266 R	5'-TCGATCGAAACATTCTTATCAGTCTCA
+ 4079	*Hsp70* + 4035 F	5'-GGAAACTGCCTCCAACAACTG
	Hsp70 + 4124 R	5'-AGACGCACGAGACCAATCTGTA
87C	87C–Bkgd–2F	5'-CAGGGATTTCTCAGCCATA
	87C–Bkgd–2R	5'-CCGGGGAGAAGTAAAGGACT

temperature with rotation for 30 minutes.

Protein::DNA crosslinks were removed by heating the samples at 65°C for at least 4 hours and then proteins were digested with Proteinase K. DNA was first cleaned up with 1 phenol/chloroform extraction and then precipitated with EtOH and pelleted by spinning at 14,000 $\times$ g for 20 minutes. Pellets were washed and allowed to dry before re-suspending in 100 μl H_2O. The input control was treated in the same manner as the ChIP samples beginning with the crosslink removal step through to the resuspension, except the input was resuspended to a final concentration of 10%.

2.4.3 Quantitative Real-Time PCR Analysis

Specific genomic regions bound to the immunoprecipitated proteins were analyzed using real time PCR with the primers listed in Table 2.4. Real-time PCR was described by Ni *et al.* [154] and was performed as described with a few modifications. Briefly, we used SYBR green PCR mix (0.8% glycerol, 6 mM Tris (pH 8), 25 mM KCl, 2.5 mM $MgCl_2$, 75 mM trehalose, 0.1% Tween, 0.1 mg of nonacetylated ultrapure bovine serum albumin/ml, 0.067x SYBR green I (Cambrex), 0.1 mM deoxynucleoside triphosphates, 50 U of Taq DNA polymerase/ml) on a Light Cycler® 480 (Roche). A standard curve was generated by serial diluting input samples in order to quantify the IP samples; all values were obtained in the linear range of amplification. Values reported are reported as the % input with the no-antibody sample subtracted. Error bars represent the standard error of the mean (SEM).

CHAPTER 3

RECRUITMENT AND DYNAMICS OF TRANSCRIPTION FACTORS[1]

3.1 Introduction

A variety of cellular signals trigger the recruitment of transcription factors to specific target genes, allowing for a myriad of biochemical processes that are required for high levels of transcription. Our knowledge of these processes has been guided mainly by biochemical techniques, including ChIP, that assay when, where, and to what levels transcription factors are associated with specific regions of the DNA. These spatial and temporal resolution assays have provided important constraints for models of transcription mechanisms *in vivo* [59, 184]. However, most of these studies are restricted to assaying static images of chromatin-protein interactions in a population of cells. Recent advances in live-cell imaging technology, however, allow for the real time imaging of transcription factors at specific loci in single cells, providing new insights into gene regulation [77].

Drosophila salivary glands offer a unique platform to carry out live-cell imaging studies of transcription [126]. Salivary gland nuclei contain polytene chromosomes, comprised of thousands of aligned DNA strands showing packing similar to interphase diploid nuclei [17]. This natural amplification allows for the imaging of the localization and dynamics of transcription factors at specific native loci in single cells [235, 236, 237].

HS results in decondensation of transcriptionally activated chromatin at the *Hsp70* loci that are visualized as a discrete pair of puffs on polytene chromosomes [177]. These two cytological loci, 87A and 87C, are 3-dimensional structures that contain 2 and 4

[1] Parts of this chapter are published in Zobeck *et al.* 2010 [244]

copies of *Hsp70*, respectively, as well as intervening DNA and a large spectrum of nuclear proteins. Studies of the distribution of specific proteins before and after HS have provided key insights into their function at the *Hsp70* loci [63, 65, 184]. Importantly, many of the proteins identified as involved in *Hsp70* gene regulation have corresponding roles at other genes and in a variety of organisms, indicating their functions during transcription are evolutionarily conserved [184].

HS induction leads to the recruitment of the transcription activator, HSF, which trimerizes and binds to the regulatory regions of HS genes [73, 124, 162]. Both fixed cell analyses [220] and more recent live cell imaging have shown that HSF-eGFP resides in the nucleoplasm and is recruited to many chromosomal sites, including the *Hsp70* loci upon HS [236]. FRAP of transcription activators has shown a dynamic associations with the chromatin [77]. In contrast, upon HS, HSF stably associates with active *Hsp70* loci to form a platform for programming many rounds of RNA Polymerase II (Pol II) transcription before dissociating from the locus [236].

Interestingly, even before HSF binds, Pol II is transcriptionally engaged but paused at the 5' end of the *Hsp70* gene. After HS, the paused Pol II escapes into active elongation and additional Pol II is recruited to the gene [181]. Live cell imaging studies of Pol II have provided insights into the molecular dynamics of a transcribing locus. Intriguingly, eGFP-Pol II reaches maximum fluorescence intensity at the *Hsp70* loci after its association with chromatin reaches saturation as measured by ChIP [235]. Additionally, FRAP assays show a dramatic change in the local dynamics of eGFP-Pol II at *Hsp70* loci after activation. During the early stages of HS (20 minute HS), eGFP-Pol II FRAP recovers completely over the course of 2 minutes, at a rate consistent with the elongation rate; however, after 40–60 minutes of HS, little or no recovery is observed, even though transcription continues [235]. Together these studies provide evidence for

the accumulation of Pol II at transcriptionally active loci followed by progressive retention and recycling of Pol II over the course of activation. The accumulation and progressive retention of Pol II at the *Hsp70* loci has been termed a transcription "compartment" and is postulated to provide a mechanism for the recycling of Pol II to allow continued rounds of transcription [235].

Transcriptional activation of the *Hsp70* genes by HS, results in the recruitment of numerous transcription factors including P-TEFb, Spt6 and Topo I [4, 67, 98, 127]. P-TEFb is a kinase responsible for phosphorylating the C-Terminal Domain (CTD) of Pol II to permit Pol II's escape into active elongation [132]. P-TEFb is composed of CycT and Cdk9 and localizes to the 5' end as well as the entire transcribed region of *Hsp70* after HS [22, 163]. Spt6 is a nucleosome chaperone [25], known to be recruited to the nucleosome-containing region of the gene upon activation and is notably absent from the 5' end of the gene, which is free of nucleosomes [154, 185]. Topo I is recruited to remove supercoils generated by transcription [219] and is strongly recruited to the *Hsp70* loci upon activation [61]. It has been identified as a hyperphosphorylated CTD interacting protein [31] and, like Spt6, associates with the nucleosome-containing region as opposed to the 5' end [67, 109]. Even though these factors bind to different regions of the *Hsp70* gene, ChIP studies done after different lengths of HS, show they are all rapidly recruited upon activation [22, 154]; however, these studies are not of sufficient temporal resolution to resolve their order of recruitment.

In this study, we examined the recruitment of the transcription activator (HSF), the RNA polymerase (Pol II) and the elongation factors P-TEFb, Spt6 and Topo I to the native *Hsp70* loci with unprecedented temporal resolution in living cells. Our studies resolve the recruitment timing of these factors, providing temporal information that sets limits for their functional roles, and identify a strikingly synchronous recruitment among

different cells of these factors upon activation. Then using FRAP, we test the possibility that these factors are progressively retained in a transcription "compartment" that forms over extended gene activation.

3.2 Results

3.2.1 Localization of Transcription Factors with Pol II at Active Transcription Loci in Living Cells

Activation of the *Hsp70* genes leads to the decondensation of the chromatin at the *Hsp70* loci (87A & 87C) and concomitant recruitment of Pol II to these sites. In both fixed chromosome spreads and intact living nuclei, these sites are the only doublet of Pol II "puffs" within HS nuclei and unambiguously identify the *Hsp70* loci [236, 92]. ChIP and immunostaining of polytene squashes have also shown that many transcription factors colocalize at the *Hsp70* loci after HS [126]. We selected key factors involved in different aspects of the transcription elongation; P-TEFb, Spt6, and Topo I, and examined their localization patterns and recruitment to the *Hsp70* loci in vivo. To do this, we generated *Drosophila* transgenic lines that express a fluorescent protein (FP, either eGFP or mRFP)-tagged transcription factor and the complementary fluorophore tagged on the Rpb3 subunit of Pol II, within third instar larval salivary glands. LSCM was used to identify their location before and after HS activation in living cells.

LSCM shows that FP-tagged P-TEFb, Spt6 and Topo I are primarily localized within the nucleus before and after HS. More specifically, we observed colocalization between all three factors and FP-tagged Pol II at developmentally regulated loci in NHS nuclei (Figure 3.1A–C and, G–I). After 20 minutes HS, the factors are depleted from the developmental loci and now colocalize with Pol II at the HS loci including the two *Hsp70* loci

(Figure 3.1D–F and J–L). These colocalization results concur with previous immunofluorescence studies on squashed polytene chromosome [4, 98, 127, 61] and confirm the recruitment of these factors to the *Hsp70* loci upon HS in living cells. Notably, these transcription factors are not detected at the *Hsp70* loci before HS (note the absence of signal for the *Hsp70* loci during NHS), unlike Pol II, which is present at these sites at low levels before HS. Additionally, consistent with what was seen previously in squashed polytene chromosomes [147, 61], we observe a strong recruitment of eGFP-Topo I to the nucleolus upon HS in living salivary glands.

3.2.2 Differences in the Timing and Rates of Recruitment among Transcription Factors

Figure 3.1 shows that mRFP-P-TEFb, eGFP-Spt6 and eGFP-Topo I are recruited to the *Hsp70* loci before 20 minutes HS. However, the precise timing and rate of this recruitment could differ, distinguishing between two possible mechanisms, whereby transcription factors are simultaneously corecruited upon activation or where they are recruited in ordered, temporally and kinetically distinct steps. To achieve sufficient temporal resolution, we used SDCM because it provides faster data acquisition than LSCM. 3D image stacks were collected in both green and red channels during NHS, using a 40$\times$ oil immersion objective maintained at room temperature. HS was activated by swapping in a matched objective heated to 36°C. The large heat capacity of the lens causes a nearly instantaneous HS [235] when the immersion medium contacts the cover slip ($t = 0$ sec). Then, after adjusting for any changes in the focal plane, we obtained a time series consisting of 2-channel 3D image stacks over a 20-minute period at time intervals of 20–30 seconds (Figure 3.2A and Chapter 2). As previously seen [235], activation of the *Hsp70* genes does not result in a relocation of the *Hsp70* loci.

Figure 3.1: Colocalization of P-TEFb, Spt6 and Topo I with Pol II at Developmental and *Hsp70* Loci in Living Polytene Nuclei.
(A–F) LSCM maximum intensity projections of polytene nuclei. (A & D) express mRFP-P-TEFb (pseudo-colored green, left panel) with eGFP-Pol II (pseudo-colored red, middle panel). (B & E) express eGFP-Spt6 (green, left panel) with mRFP-Pol II (red, middle panel). (C & F) express eGFP-Topo I (green, left panel) with mRFP-Pol II (red, middle panel). (A–C) images were acquired during NHS, while (D–F) images were taken of the same corresponding nuclei after 20 minutes HS. Images in left panel of (A–F) represent a green/red merge between the transcription factors (green) and Pol II (red).
(G–L) LSCM confocal optical sections, 1 μm thickness, of a the same nuclei as A–F. All images represent a green/red merge between the transcription factors (green) and Pol II (red). (G & J) express mRFP-P-TEFb with eGFP-Pol II. (H & K) express eGFP-Spt6 with mRFP-Pol II. (I & L) express eGFP-Topo I with mRFP-Pol II. (G–I) images were acquired during NHS, while (J–L) images were taken of the same corresponding nuclei after 20 minutes HS. Numbers on images represent distance from center in μm. Arrows point to position of the *Hsp70* loci. Scale bars equal 10 μm.

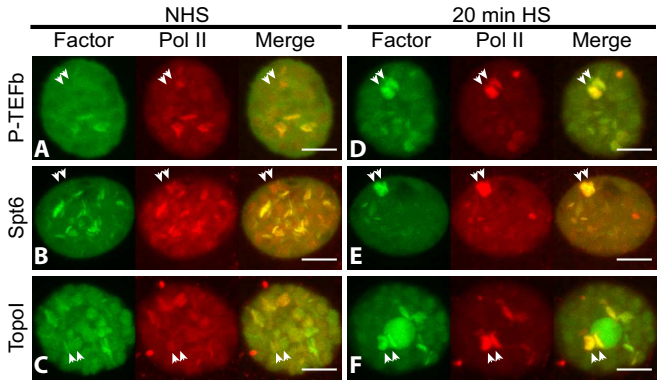
NHS
20 min HS
Factor
Pol II
Merge
Factor
Pol II
Merge
P-TEFb
Spt6
TopoI
A
B
C
D
E
F

Figure 3.1: (continued)

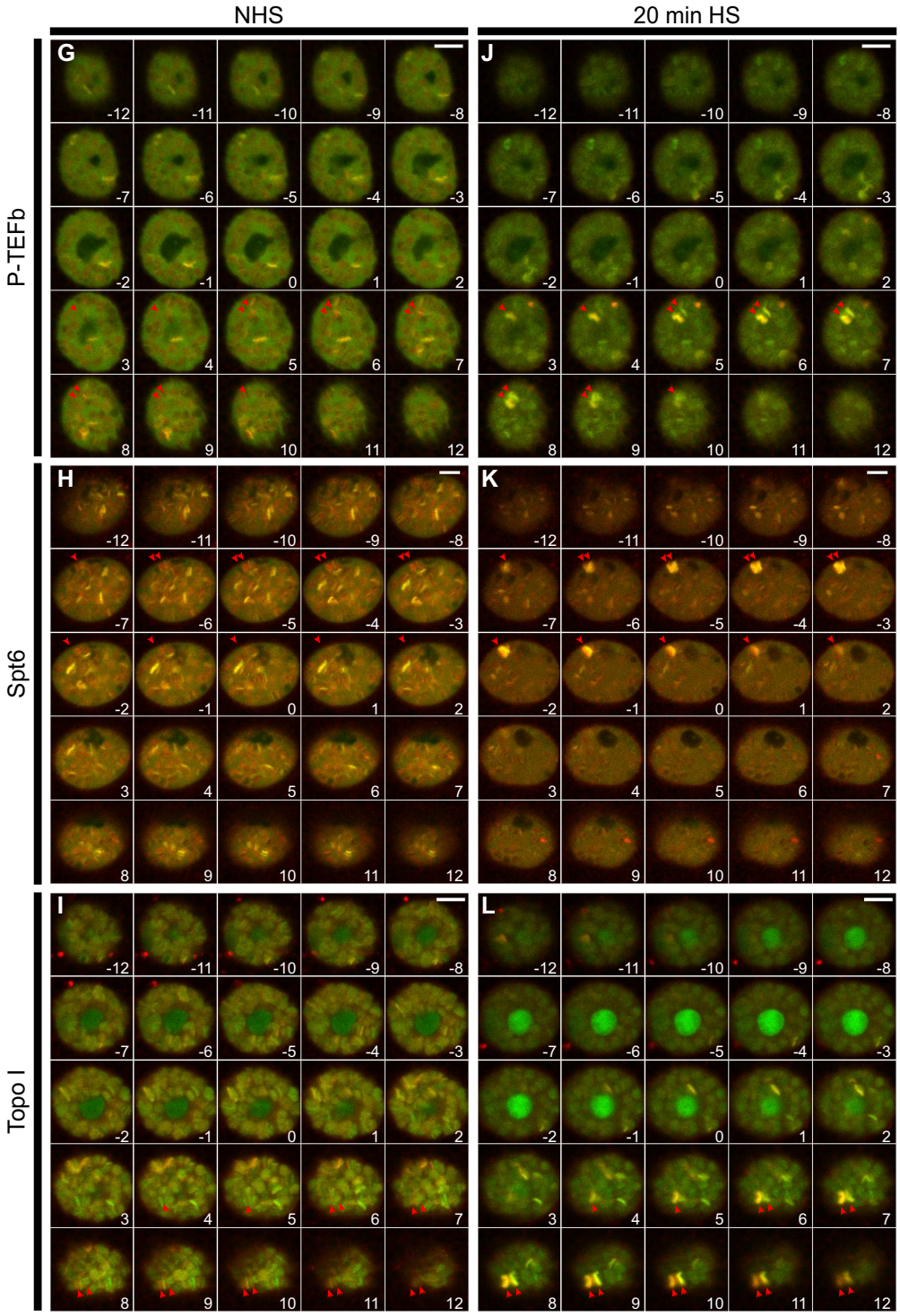

By imaging pairs of FP-tagged transcription factors, we are able to measure both the timing and rate of recruitment for both factors in the same nucleus. We measured the recruitment in the fly lines shown in Figure 3.1 as well as a line expressing HSF-eGFP, the activator of *Hsp70* transcription. The recruitment data for each factor was averaged using consecutive 10 seconds windows for both the mean intensity (Figure 3.2B) and the total intensity measurement (Figure 3.2C). Remarkably, the recruitment of HSF is detectable within 20 seconds after HS, while the recruitment of Pol II and the three other transcription factors occurs considerably later ($>$100 seconds after HS). Notably, HSF mean fluorescence intensity decreases $\sim$100 seconds after HS, while the HSF total fluorescence intensity plateaus at this time. Together with the observation that the *Hsp70* loci increase in volume with Pol II recruitment (Figure 3.3), these results suggest that the decrease in HSF mean intensity is due to chromatin decondensation, not its dissociation from the loci.

To quantify reproducible differences in the initial timing of recruitment, we fit paired data sets with exponential curves and calculated the difference in recruitment times (Δt) for the transcription factor and Pol II to reach the same normalized fluorescence intensity. Because HSF was not imaged with Pol II in the same cell, we used a random sample of Pol II curves to calculate the pair-wise differences in timing of recruitment. The time of initial recruitment, relative to Pol II, can be observed as the mean fluorescence intensities approach zero (Figure 3.2D-G). We report all measurements averaged over multiple samples along with the standard error of the mean. If the transcription factor is recruited faster than Pol II, the curve will slope to the left if it is recruited slower it will slope to the right. HSF is recruited 82 $\pm$ 5 seconds before Pol II. In contrast, P-TEFb is initially recruited around the same time as Pol II (1 $\pm$ 6 seconds after Pol II), and Spt6 and Topo I are recruited after Pol II (12 $\pm$ 4 and 22 $\pm$ 5 seconds after Pol II, respectively).

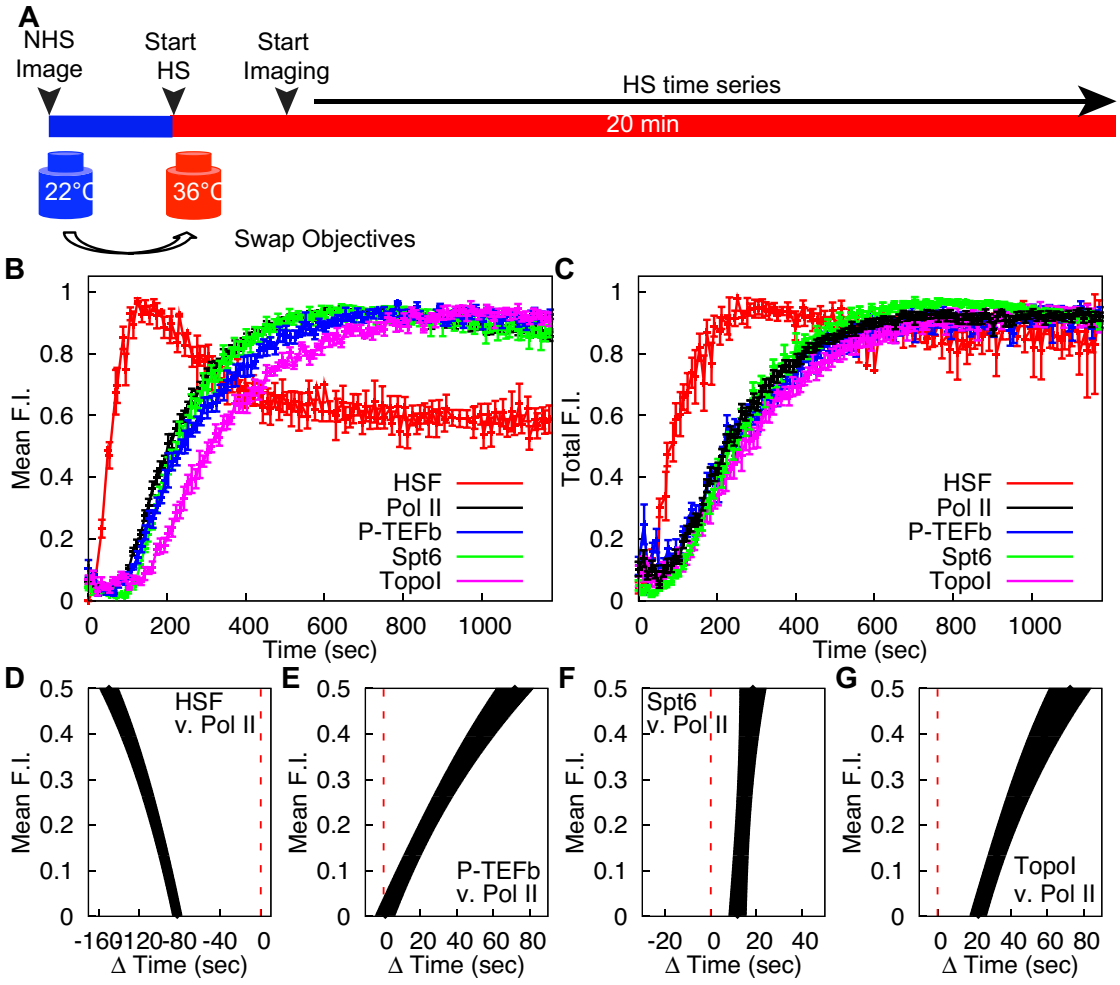

Figure 3.2: Recruitment Timing of Transcription Factors.
(A) SDCM was used to obtain 3D images of FP-tagged transcription factors with the complementary FP-tagged Pol II. First, *Drosophila* salivary glands were imaged using a room temperature objective, then an objective pre-heated to 36°C was swapped in, causing a nearly instantaneous HS. 3D time series were then obtained continuously over 20 minutes. (B-C) Normalized transcription factor fluorescence intensities were averaged using 10 second windows (B) using mean fluorescence intensities and (C) using total fluorescence intensities. HSF is plotted in red, Pol II in black, P-TEFb in blue, Spt6 in green, Topo I in purple (Number of samples (n) = 10, 32, 10, 12, and 10, respectively). (D-G) Reproducible differences in recruitment times relative to Pol II were calculated by fitting exponential curves to each set of recruitment data for each factor. (D) HSF ($n = 10$), (D) P-TEFb ($n = 10$), (E) Spt6 ($n = 12$), and (F) Topo I ($n = 10$). Times to reach a specific intensity were calculated and subtracted from the times for Pol II from the same nucleus. Because HSF was not imaged with Pol II, a random set of Pol II curves were used to calculate the paired differences. The red dotted line at $\Delta t = 0$ represents the time Pol II reaches the corresponding fluorescence intensity. Error bars represent SEM, where $n =$ the values previously noted.

Table 3.1: Recruitment Rates of Individual Transcription Factors.
P-value was calculated using the Student T Test, either using the Dependent t-test for paired samples (Paired) based on the rates of recruitment for Pol II and the transcription factor from the same cell, or with Independent two sample t-test for samples with equal variance (Equal Variance). $**$ Represent statistical difference with confidence greater than 95%.

	Rate (k) ($\times 10^{-3}$ FU·s^{-1})	P-value Paired	P-value Equal Variance	
HSF	12.6 ± 2.3	N/A	6.0×10^{-8}	$**$
Pol II	8.4 ± 0.8	N/A	1.0	
P-TEFb	5.1 ± 0.4	6.3×10^{-3}	2.7×10^{-2}	$**$
Spt6	7.1 ± 0.8	7.2×10^{-1}	3.5×10^{-1}	
Topo I	4.3 ± 0.4	8.9×10^{-4}	5.7×10^{-3}	$**$

The recruitment data also provide the rates of recruitment to the *Hsp70* loci (Table 3.1), as assessed by fitting the data to a single exponential curve. The rate of HSF recruitment is much faster than the rate for either Pol II or the three elongation factors, this was also observed in Figure 3.2D by the curve sloping to the left. Additionally, the rates of recruitment for P-TEFb and Topo I are significantly slower than Pol II (Figure 3.2E and G and Table 3.1). Spt6, however, has a rate that is indistinguishable from that of Pol II (Figure 3.2F and Table 3.1), suggesting a proportional recruitment of these two factors. These differences in timing and rates of recruitment for the different transcription factors demonstrate a sequential and independent recruitment of these factors to the *Hsp70* loci rather than a concerted co-recruitment of factors, supporting the view that each factor has its own mechanism and cue for recruitment.

3.2.3 Synchrony in the Recruitment of Transcription Factors to the *Hsp70* Loci

Boettiger *et al.* (2009) identified two patterns of developmental gene activation within *Drosophila* embryos: a stochastic activation of transcription, where the first detection of transcripts in different cells occurred over a range of 15–20 minutes, and a synchronous

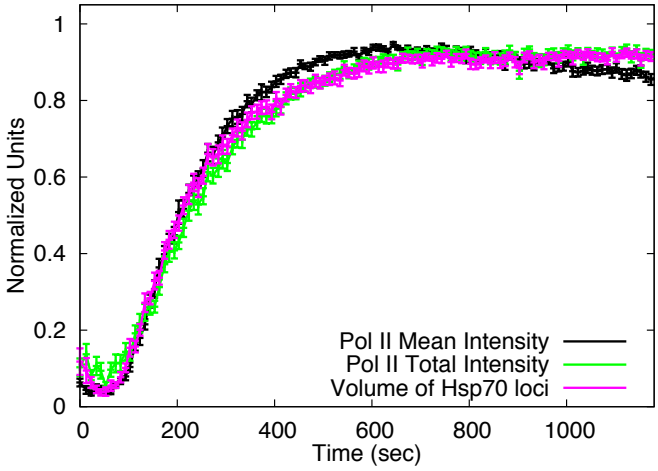

Figure 3.3: Plot of the Volume of the *Hsp70* Loci and Pol II Intensities after Activation.

Plot of normalized Pol II-eGFP fluorescence intensity or volume versus time comparing the timing of recruitment for the mean fluorescence intensity (measured using a changing volume), total fluorescence intensity (measured using a constant volume) and expansion of the *Hsp70* loci using the volume of the *Hsp70* loci from the mean fluorescence intensity volumes. Error bars represent the SEM, where $n = 32$

activation of transcription, where transcripts in cells are detected within a 3 minutes range. This synchronous activation is hypothesized to facilitate the homogeneous expression of genes vital for proper development. Similarly, the coordinated and rapid activation of HS genes may be required to survive HS [156]. Our time-lapse recruitment data provide a way to assess whether the recruitment of FP-tagged HSF, Pol II, P-TEFb, Spt6 and Topo I to the *Hsp70* loci occurs in a synchronous or stochastic manner in individual salivary gland nuclei. To assess the recruitment method, we compared the recruitment curves from nuclei within the same salivary gland as well as different salivary glands.

In all nuclei, even from different salivary glands, HSF is recruited to the *Hsp70* loci rapidly after HS and the initial recruitment is already observed by the first time point after HS (Figure 3.4A). Both the recruitment rates and times show little variation, reported here as standard errors, for nuclei in the same or from different glands, with the recruitment of HSF occurring 17 $\pm$ 1 second after HS. These data indicate rapid and highly synchronous recruitment. The recruitment times of Pol II following HS also show little variation, 103 $\pm$ 2 seconds (Figure 3.4B). Additionally, the recruitment times of the three transcription factors, P-TEFb, Spt6 and Topo I, are similarly restricted, 95 $\pm$ 3, 115 $\pm$ 2, and 132 $\pm$ 4 seconds, respectively (Figure 3.4C-E). Therefore, all five factors are recruited to the *Hsp70* loci in a synchronous manner.

3.2.4 Transcription Factors Progressively Retained in Transcription "compartment" over Time Course of HS

The FP-tagged transcription factors provide a means to examine their recruitment, as well as their dynamics of association with the *Hsp70* loci. For example, 10 minutes after HS FRAP of eGFP-Pol II shows a complete and linear recovery of fluorescence

Figure 3.4: Synchrony in the Recruitment of Transcription Factors to *Hsp70* loci Among Nuclei of the Same Gland or in Different Glands.
(A-E) Representative SDCM recruitment images, corresponding mean intensity recruitment plots, and corresponding total intensity recruitment plots for (A) mRFP-HSF, (B) Pol II (mRFP and eGFP), (C) mRFP-P-TEFb, (D) eGFP-Spt6 and (E) eGFP-Topo I. The 1^{st} image for each factor is the NHS image, 2^{nd} image is the time point before recruitment, while the rest of the images are spaced to depict the recruitment kinetics of the factors (note: HSF is recruited by the first time point after HS). Scale bars are 10 μm. Top plot in each panel shows the normalized mean fluorescence intensities of factors' recruitment in nuclei of the same gland (indicated by lines of same color) and nuclei from different glands (indicated by different color lines) over the time course of a 20 minutes HS. The bottom plot, shows the normalized total fluorescence using a constant volume. Each graph represents recruitment data from three or more glands containing 2 or more nuclei from each gland. Red arrows mark the location of the *Hsp70* loci.

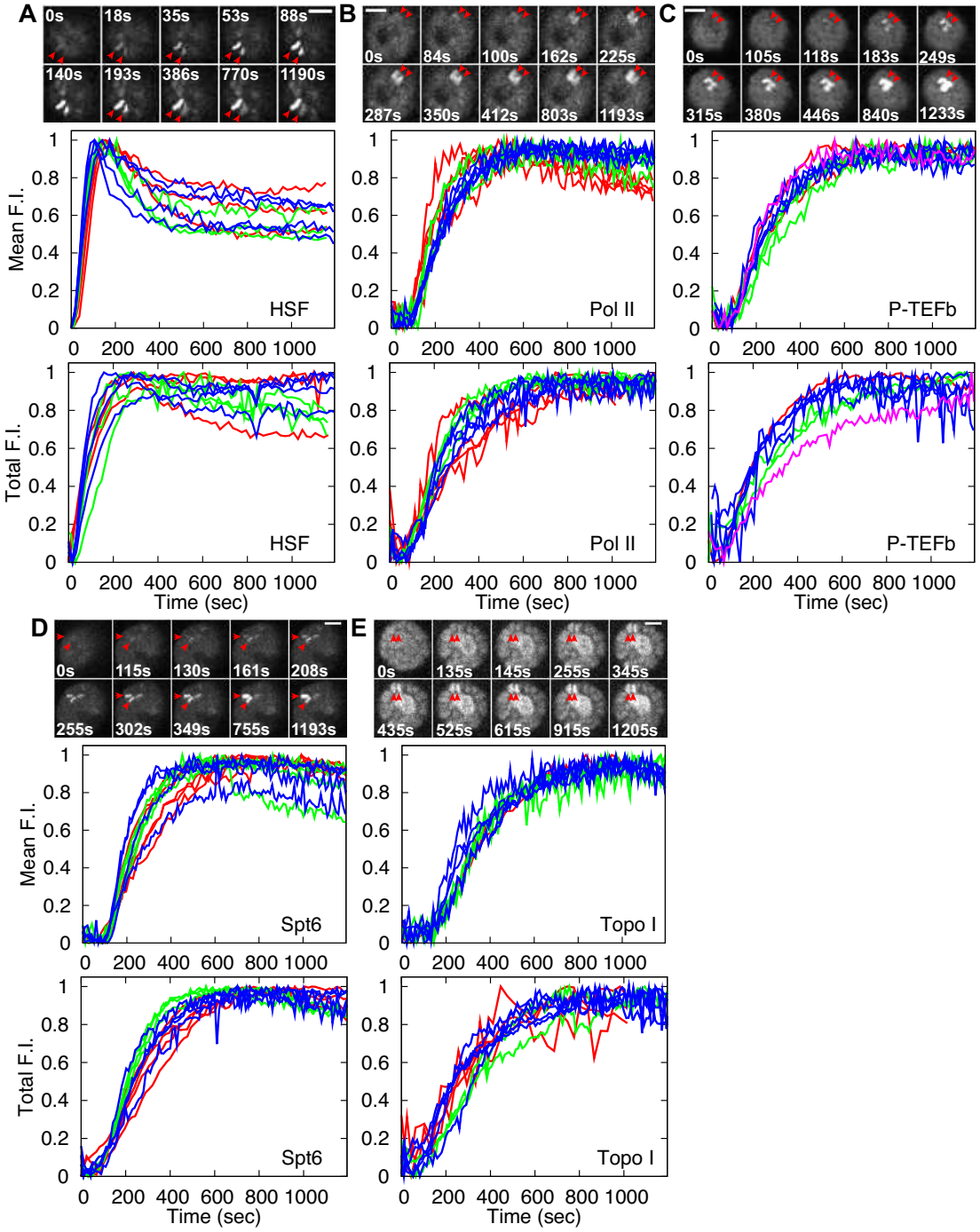
A
0s
18s
35s
53s
88s
140s
193s
386s
770s
1190s
B
0s
84s
100s
162s
225s
287s
350s
412s
803s
1193s
C
0s
105s
118s
183s
249s
315s
380s
446s
840s
1233s
Mean F.I.
Total F.I.
HSF
Pol II
P-TEFb
Time (sec)
D
0s
115s
130s
161s
208s
255s
302s
349s
755s
1193s
E
0s
135s
145s
255s
345s
435s
525s
615s
915s
1205s
Spt6
Topo I

that reflects the entry of new fluorescent Pol II onto the gene. In contrast, continued HS causes the progressive decrease in both the rate and total recovery of Pol II, even though transcription remains robust. Together, these observations indicate that there is a progressive retention of Pol II in a transcription "compartment" that allows the recycling of Pol II for continued rounds of transcription [235].

To address the possibility that this "compartment" is a more general feature of active transcription, we examined 1) whether there is an accumulation of FP-tagged factors beyond the amount needed to maximally bind the genes, and 2) if the dynamics of representative transcription factors, P-TEFb, Spt6 and Topo I, also change with the duration of HS.

First, we have compared the time for maximum recruitment to the *Hsp70* loci (Figure 3.4 Total Fluorescence Intensity Plots) and to the *Hsp70* genes (Figure 3.5). Our high-resolution recruitment assay and salivary gland ChIP of Pol II on *Hsp70* (Figures 3.4B and 3.5A) agrees with the previous report that Pol II reaches maximum intensity at the loci after maximum binding has occurred on the gene [22, 235]. We observe maximum levels at $\sim$3 minutes HS for chromatin by ChIP (Figure 3.5A) and $\sim$8 minutes HS at the locus by live cell imaging (Figure 3.4B). Salivary gland ChIP experiments for the transcription factors P-TEFb and Spt6 also show maximal gene occupancy by $\sim$3 minutes (Figure 3.5B and C), while they continue to accumulate at the *Hsp70* loci achieving maximum total intensity at 10 and 8 minutes, respectively (Figures 3.4C and D). This suggests that there is an accumulation of transcription factors at the *Hsp70* loci beyond what is required to saturate the DNA.

Second, we examined whether the dynamics of these factors change with the duration of HS using FRAP. All of the FRAP experiments were done during recruitment equilibrium, where mean and total intensities of the transcription factor are constant over

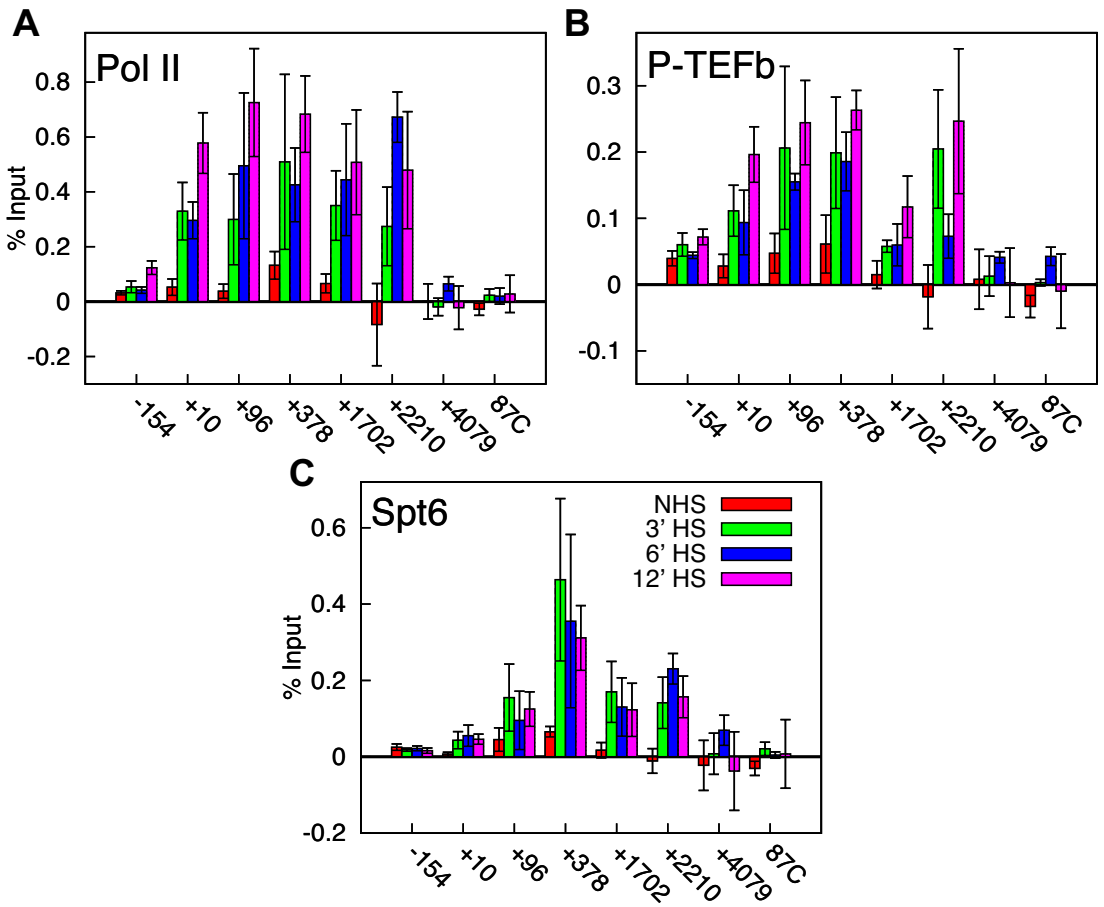

Figure 3.5: Salivary Gland ChIP shows maximum chromatin binding for Pol II, Spt6 and CycT occurs 3 minutes after HS

(A–C) Salivary gland ChIP of (A) Pol II, (B) P-TEFb and (C) Spt6. Amplicons are listed on the x-axis and were spaced throughout the *Hsp70* transcription unit and were labeled relative to the transcription start site using the center of the amplicon. Amplicons include one in the promoter region (-154), multiply primer sets in the body of the gene, one after the polyAdenylation site (+4079) and a background non-coding region (87C). Primer sequences are listed in the Supplemental Experimental Procedures. Plots show NHS in red, 3 minutes HS in green, 6 minutes HS in blue, and 12 minutes HS in pink. Error bars represent SEM where n =3 or 4.

time (Figures 3.6 and 3.7). At 10 minutes HS, shortly after reaching recruitment equilibrium, the FRAP profile provides critical information regarding the dynamics of association between the factor and the *Hsp70* loci. The $\tau_{1/2}$ can be used to identify whether recovery is limited by the dissociation of the pre-existing bleached factors from their targets of interaction, i.e. a binding event, or if recovery is limited to diffusion [202]. For mRFP-P-TEFb, eGFP-Spt6 and eGFP-Topo I, the estimated $\tau_{1/2}$ for diffusion is less than 0.030 seconds, while the observed $\tau_{1/2}$ for these factors are 30, 40, and 10 seconds, respectively (Figure 3.6B, D and F). This result indicates that these transcription factors are in fact binding at the *Hsp70* loci.

Because P-TEFb, Spt6 and Topo I are Pol II interacting proteins [154, 239, 61], we also compared their recovery curves to Pol II to see if any of these three factors were stably binding to Pol II. If a stable interaction exists, we expect the FRAP dynamics to mimic that of Pol II. At early times of HS, 10–20 minutes, Pol II recovers from photobleaching linearly for 2 minutes. This recovery corresponds to the time it takes bleached Pol II molecules to complete transcription elongation, and for new fluorescent Pol II to refill the gene [235]. The recovery curves for the three transcription factors are all exponential, indicating that these three transcription factors are not stably bound to Pol II, but instead interact transiently with Pol II and/or the *Hsp70* loci.

Prolonged HS also impacted the FRAP dynamics of the three transcription factors at the *Hsp70* loci. The most dramatic effect was seen with Spt6, which recovers to 50% initial intensity after 10 minutes HS. However after a 20 minutes HS, less recovery is observed and after 40 minutes HS no recovery is observed after FRAP (Figure 3.6C and D). Figure 3.7 confirms Spt6 is present at similar intensities at all of these time points. Together these results indicate that Spt6 becomes more stably associated with the *Hsp70* loci with increasing HS time, and these findings are consistent with this factor, which

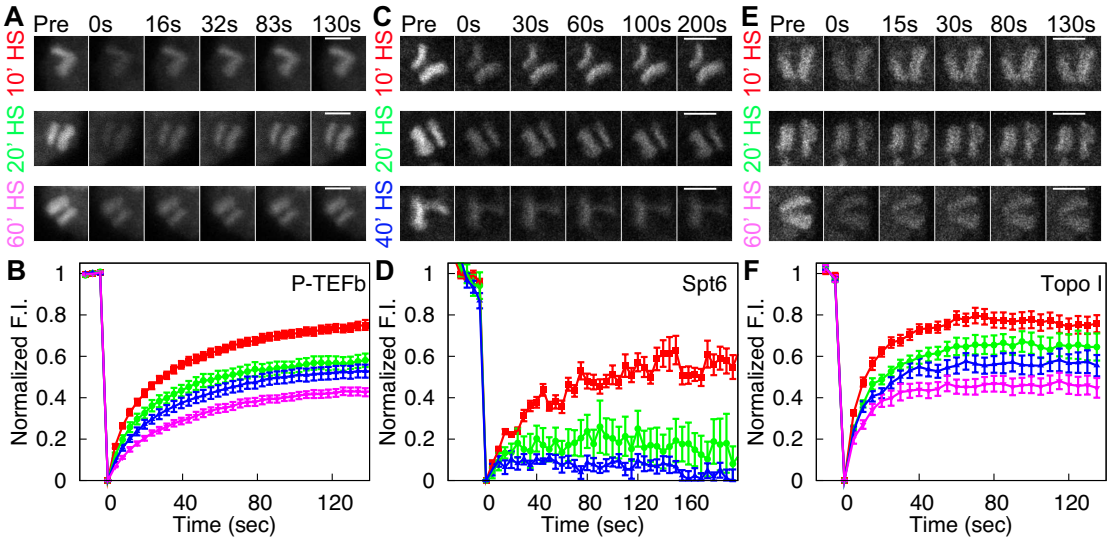

Figure 3.6: FRAP Dynamics of Transcription Factors at the *Hsp70* Loci Change After Length of HS.

(A, C, and E) FRAP of the three transcription factors after different lengths of HS: (A) mRFP-P-TEFb, (C) eGFP-Spt6 (by M. Buckley) and (E) eGFP-Topo I. Panels show representative FRAP images. The top panel was bleached after 10 minutes HS, middle panel was bleached after 20 minutes HS and lower panel was bleached after 40 minutes HS (C) or 60 minutes HS (A and E). All scale bars equal 5 μm. (B, D and F) Plots of normalized fluorescence intensity at the *Hsp70* loci. (B) mRFP-P-TEFb, (D) eGFP-Spt6 (by M. Buckley) and (F) eGFP-Topo I. Bleaching resulted in a decrease of 40-60% initial intensity, however, the plots illustrated here are normalized to the initial intensity as well as the bleach depth. Red curve, 10 minutes HS; Green curve, 20 minutes HS; Blue curve, 40 minutes HS; Purple curve, 60 minutes HS (n =11, 10, 12, 10 for P-TEFb, respectively; n =13, 6, 6 for Spt6, respectively; n =13, 20, 17, 16 for Topo I, respectively). Error bars represent the standard error.

is required for maximum transcription elongation rates [9], being reused and recycled within the “compartment”.

In contrast to Spt6, Topo I and P-TEFb remains dynamic during prolonged HS. However, increasing HS time still causes a progressive decrease in the mobile fraction of Topo I and P-TEFb, such that the immobile fraction reaches 60% of the total population in the 60 minutes HS sample (Figure 3.6E and F). P-TEFb also appears to remain dynamic after prolonged HS, and like Topo I shows a progressive decrease in the mobile fraction, such that the immobile fractions of both Topo I and P-TEFb reach 60% of the total population over 60 minutes of HS (Figure 3.6A and B). The increase in the immobile fraction observed for these two factors could be explained in a similar manner as Spt6, whereby the immobile fraction consists of an increasing number of molecules that can be recycled for use in transcription.

Together our salivary gland ChIP results and FRAP dynamic studies suggest that the transcription “compartment” is a general feature of active transcription, and is not limited to Pol II. Notably, our FRAP results emphasize that the compartmentalization process is not simply a mechanism by which transcription factors become completely retained at the loci after HS, but suggest differences in affinities with the loci, function, or size may play a role in the ability of a given transcription factor to diffuse into or out of the “compartment”.

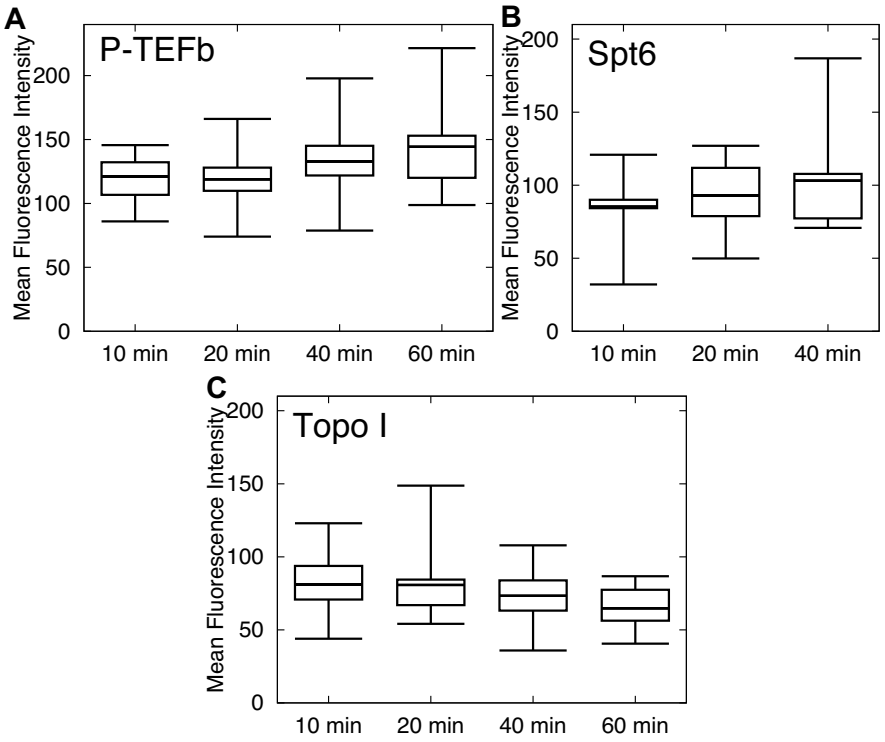

Figure 3.7: Starting Intensities of the *Hsp70* Loci for FRAP Experiments.
(A-C) Mean fluorescence intensities of the initial image before bleaching for (A) P-TEFb, (B) Spt6 and (C) Topo I. Data is plotted as a box and whisker plot to illustrate the distribution of fluorescence intensities at specified HS times. No statistical differences were seen between intensities (n =11, 10, 12, 10 for P-TEFb, respectively; n =13, 6, 6 for Spt6, respectively; n =13, 20, 17, 16 for Topo I, respectively).

3.3 Discussion

3.3.1 Recruitment Timing and Rates for Transcription Factors During HS

The *Drosophila Hsp70* genes provide a unique system with which to examine the recruitment of transcription factors to specific chromosomal loci. They are rapidly and robustly activated upon HS and are located at two cytological loci, whose appearance provides a diagnostic doublet for identifying the *Hsp70* loci in living cells. By measuring the intensity of transcription factors at the *Hsp70* loci over the course of HS, we have been able to distinguish differences in the initial timing and rates of recruitment of transcription factors.

We have previously shown, in a population of cells, that HSF appeared to be recruited to the *Hsp70* genes before Pol II [22], however our present study shows this more convincingly at high temporal resolution and also demonstrates a sequential recruitment of the other factors P-TEFb, Spt6 and Topo I to the *Hsp70* loci rather than a concerted co-recruitment of a pre-assembled transcription complex. In single cells, we observe that HSF is recruited 80 seconds before Pol II suggesting that other co-activators or modifications are required for Pol II recruitment. P-TEFb is first detected at *Hsp70* loci when Pol II also begins to increase, which is consistent with the P-TEFb kinase's role in promoting active elongation [242]. Following is the recruitment of Spt6, 10 seconds after Pol II, which is consistent with the known role of Spt6 as a chromatin remodeler and the time for Pol II to reach the first nucleosome. Then, Topo I, which interacts with the phosphorylated CTD of Pol II [31], is recruited 20 seconds after Pol II and P-TEFb. Interestingly, this raises the possibility that Pol II phosphorylation is not sufficient to recruit Topo I, but rather that Topo I recruitment may require transcription-driven accumulation of supercoiled DNA [130]. Finally, a model has been recently proposed where genes are recruited to nuclear sites called "transcription factories" that contain the tran-

scription factors required for transcription and its regulation [30]. The distinct kinetics observed here regarding the recruitment of the five transcription factors and the failure to see genes moving to new sites upon activation (here and [235]) are inconsistent with *Hsp70* genes being recruited to a preformed "transcription factory".

3.3.2 Synchronous Recruitment of Transcription Factors

This study provides a single cell analysis with the temporal resolution to address whether transcription factors are synchronously recruited to *Hsp70* loci. Our study revealed that HSF, Pol II and three transcription factors (P-TEFb, Spt6 and Topo I) are each synchronously recruited to the *Hsp70* loci. We observed a standard error for each transcription factor's recruitment timing to be less than 6 seconds. Interestingly genes that have paused Pol II may in general be synchronously activated. Boettiger and Levine examined numerous development genes in early embryos at the level of RNA accumulation in cells and observed that genes containing a paused Pol II were synchronously activated (range of 3 min), while genes without a paused Pol II were stochastically activated (range of 20 min) [23].

We propose that the paused Pol II, present on *Hsp70* genes, may facilitate the synchronous recruitment of HSF by maintaining an open chromatin state at the promoter to provide the activator, HSF, with accessible binding sites. It has been shown that HSF binding to *Hsp70* transgenes depends on an open chromatin state that in turn requires GAGA factor and paused Pol II [196]. More generally, the paused/stalled Pol II at promoters has been shown to be important in keeping nucleosomes off promoters [64]. The open chromatin state may increase the probability of activator binding its target sequence [214]. In addition, other factors may also gain more efficient access to genes that have a promoter paused Pol II. The pre-assembled general transcription factor com-

plex at these promoters should facilitate binding and initiation of newly recruited Pol II following activation [115]. Synchronous recruitment of Pol II will then promote the synchronous recruitment of the other transcription factors and synchronous transcript accumulation. Importantly, these studies provide insights into a mechanism that ensures the rapid and uniform induction of the HS response that is vital to the viability of organisms under stress conditions.

3.3.3 Transcription Compartment

The transcription "compartment" has previously been defined by Pol II's progressive retention and recycling over extended lengths of gene activation [235]. By comparing the times of maximum recruitment for the *Hsp70* loci (from live cell imaging studies) and the *Hsp70* genes (by ChIP), we were able to show there is an accumulation of molecules at the loci beyond what can bind DNA. Then, using FRAP, we showed three transcription factors, CycT, Spt6, and Topo I, are also progressively retained at the *Hsp70* loci. These findings suggest that the transcription "compartment" is not limited to Pol II, but also involves the retention, and perhaps recycling, of other components of the transcription machinery.

Moreover, our results set further limitations on the structure of the "compartment". In the case of Pol II [235] and Spt6 (Figure 3.6D), the FRAP recoveries progressively decrease until no recovery is observed. In contrast, a portion of P-TEFb and Topo I continue to exchange with the nucleoplasm even after an hour of HS, but over time, an increasing percentage of molecules remain stably associated with the locus. These different behaviors suggest that the transcription "compartment" is not a completely closed entity formed over time, but rather suggests either an affinity-based retention or the formation of a porous barrier.

Affinity-based retention and porous barrier models are not mutually exclusive. Poly(ADP) Ribose, which accumulates at the *Hsp70* and developmental loci in response to gene activation [215], could be the foundation of the porous barrier, but could also be responsible for the affinity-based retention of factors with strong nucleic acid affinity, as has been documented for histones [2].

In conclusion, our kinetic analysis of transcription factor recruitment and dynamics by live cell imaging provides insights into the overall mechanics and architecture of the transcription loci. Future development of imaging technologies should provide the ability to examine diploid cells, and thereby address the conservation of these mechanisms in different cell types and organisms.

CHAPTER 4

THE TRANSCRIPTION COMPARTMENT INVOLVES THE RETENTION H2B AND PARP AND ACCUMULATION OF POLY-ADP RIBOSE[1]

4.1 Introduction

Previously a novel structure that forms around the active *Hsp70* loci and prevents Pol II exchange with the nucleoplasm was identified [235]. Chapter 3 further characterized the transcription compartment by identifying a number of transcription factors that are similarly retained in the compartment. These results led us to the proposition that the formation of a porous barrier with nucleic-acid-like affinity may be responsible for this behavior (Chapter 3).

PAR, which accumulates at the *Hsp70* and developmental loci in response to gene activation [215], could be the foundation of the porous barrier and could also be responsible for the affinity-based retention of factors with strong nucleic acid affinity, as has been documented for histones [2]. Interestingly, PAR, either attached to protein substrates or perhaps existing as free polymers, can act as a local matrix for core histones released from destabilized nucleosomes [134, 176], suggesting that histones may also be retained within the transcription compartment.

The question of histones association or dissociation from active genes is not new. *In vivo* cross-linking of the H2A/H2B globular domains showed a decrease in association with the *Hsp70* gene after activation [150], while crosslinking of the histone tails, using a lysine specific crosslinking protocol, does not show a corresponding loss in association with *Hsp70* [150]. This result indicates that the histones are not removed from the gene loci after activation, but are instead remain associated with the gene by interac-

[1] Parts of this chapter are published in Zobeck *et al.* 2010 [244]

tions through the histone tails. However, recent studies from our lab have shown, using nucleosome protection assays and ChIP, that activation leads to a dramatic loss in nucleosome density and histone H3 at the *Hsp70* gene [164], suggesting that the histones are removed from the gene.

The PAR polymerase, PARP is involved in transcription transcription activation. In fact, the loss of nucleosome density and H3 levels on *Hsp70* is dependent on PARP act [164] and PARP activity is required for Heat Shock (HS) puff formation. When PARP activity is inhibited, decondensation of the loci does not occur [215] in *Drosophila*. Additionally, PARP has been shown to interact with nucleosomes in a manner that is mutually exclusive with linker histone H1, and preferentially associates with promoters [107]. PARP catalyzes the formation of PAR polymers from NAD^+ onto itself and various target proteins, including Histones, Pol II, Topo I, and other transcription factors [44]. Interestingly, the catalytic product of PARP activity, PAR, accumulates at the *Hsp70* loci after activation [215], and even though the average length of PAR is shorter in cells which are not suffering from DNA damage, they may be long enough to contribute to chromatin decondensation [44].

Because of the role for PARP in puff formation, it has been hypothesized that PAR polymers form the HS puff structure and may be a means to locally retain factors at the loci [215]. In this chapter, we assay the role of PAR in compartment formation by using PJ34. PJ34 is a specific inhibitor of PARP catalytic activity [199], which prevents the polymerization of NAD^+ into longer PAR chains, allowing the PAR glycohydrolase, PARG to rapidly degrade PAR [44]. In this chapter we show the dynamics of Pol II and Spt6 return to the early HS recovery dynamics upon PJ34 treatment after a 40 minute HS, suggesting that the transcription compartment is formed by the accumulation of PAR. We also assess the retention of histone H2B and PARP at the *Hsp70*

loci after activation and subsequent chromatin decondensation in order to identify additional components of the transcription compartment and address whether these factors still remain associated with the *Hsp70* loci.

4.2 Results

4.2.1 H2B is Retained at the *Hsp70* Loci after Activation

To address the localization of H2B *in vivo* we used the mRFP-tagged H2B line listed in Table 2.2. By co-expressing mRFP-tagged H2B with an eGFP-tagged Pol II we were able to identify the *Hsp70* loci in the living cells. Using spinning disk microscopy, it was possible to obtain a NHS and a 20-minute HS image of the same nucleus after an instantaneous HS. In Figure 4.1, it clear that H2B is not strongly recruited to the *Hsp70* loci, like Pol II. In fact, it appears as though it is absent from the *Hsp70* loci after activation and decondensation.

Because activation also occurs with chromatin decondensation and a concurrent increase in puff volume, it is possible that the total amount of H2B present at the locus remains constant before and after activation. To address this possibility we collected entire z-series of the nucleus for H2B and Pol II over the course of 20 minutes, as described in Subsection 2.3.3. Using Pol II as a proxy for the *Hsp70* loci, we were able to measure the mean fluorescence intensity of mRFP-H2B at the loci over the course of activation. Not surprisingly, the mean fluorescence intensity shows a dramatic decrease in H2B fluorescence intensities (Figure 4.2C). However, there is a corresponding increase in *Hsp70* volumes, as previously shown (Figure 3.3), which could be responsible for the mean fluorescence intensity decrease.

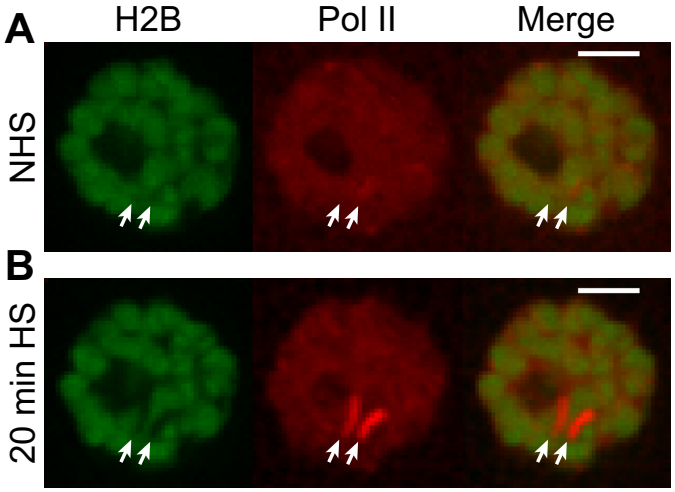

Figure 4.1: Localization of H2B and Pol II in *Drosophila* salivary glands
(A and B) LSCM images of the same polytene nuclei expressing mRFP-H2B and eGFP-Pol II (A) before HS and (B) 20 minutes after HS. For both figures the left panel is mRFP-H2B (pseudo-colored green), in the middle panel is eGFP-Pol II (psuedo-colored red) and the right panel is a merge of the two factors. Arrows point to the position of the *Hsp70* loci. Scale bars equal 10 μm.

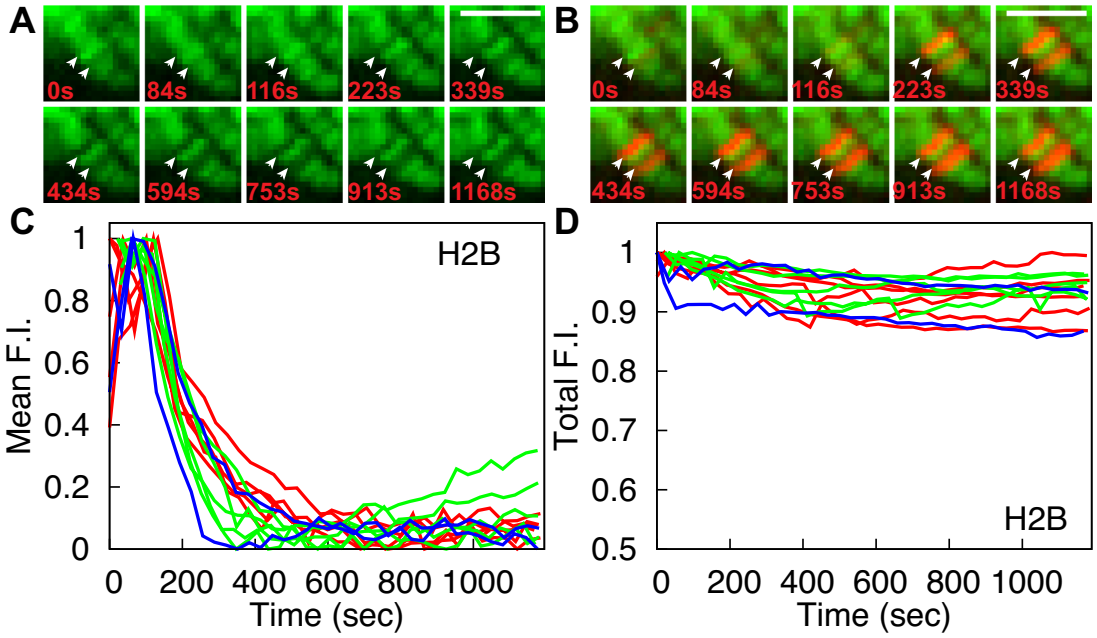

Figure 4.2: Association of H2B with *Hsp70* Loci after Decondensation.
(A and B) Representative time course images illustrating the localization of (A) mRFP-H2B (pseudocolored green) and (B) a merge between mRFP-H2B (green) and eGFP-Pol II (red) to the *Hsp70* loci after HS. The 1^{st} image (0 sec) of each panel is the NHS image, 2^{nd} image is the time point before additional Pol II recruitment and consecutive images are spaced out over the course of HS. Arrows indicate the *Hsp70* loci, and a progressive decrease in mRFP-H2B fluorescence intensity (F. I.) can be seen in these images. Scale bars are 10 μm. (C) Mean F. I. plots of mRFP-H2B using Pol II as an indicator for the volume of the *Hsp70* loci. (D) Total F. I. plots of mRFP-H2B using a constant volume. Lines of the same color are from the same gland, while different colors are from different glands. 3 glands containing 2-4 nuclei each are plotted.

To assay the total levels of H2B at the *Hsp70* loci, we needed to measure the total fluorescence intensity at the loci. However, our SDCM setup still collected some out-of-focus fluorescence, which causes a systematic increase in the total fluorescence intensity when using larger volumes. Therefore, to correct for change in volumes, we defined a constant volume encompassing the maximum volume of the *Hsp70* loci and measured total levels of fluorescence intensity in this region over time. Notably, the total fluorescence intensity remains constant, suggesting that H2B remains associated with loci after HS activation and chromatin decondensation (Figure 4.2D), even though, within two minutes of HS, the nucleosome structure is disrupted on the *Hsp70* gene [164].

4.2.2 PARP is Retained at the *Hsp70* Loci after Activation

Tulin and Spradling [215] have previously showed that PARP, an enzyme that catalyzes the polymerization of ADP ribose units from NAD^+ [106], co-localizes with the *Hsp70* loci after HS activation. By co-expressing PARP-eGFP with mRFP-Pol II we could address whether it is strongly recruited to the *Hsp70* loci. Notably, we did not observe recruitment or strong localization of PARP with the *Hsp70* loci (using Pol II to identify them) in living cells. Similar to the observation with H2B, we observed a localized reduction in fluorescence intensity at the *Hsp70* loci after 20 minutes HS compared to the surrounding chromatin and nucleoplasm (Figure 4.3).

Even though PARP is relatively excluded from the *Hsp70* loci, there are still enough fluorescence molecules present to be significantly over the level of cytoplasmic background after HS. Therefore we wanted to address, for the first time, whether the same amount of PARP was associated with the *Hsp70* loci before and after chromatin decondensation. As with H2B, the mean intensity of the *Hsp70* loci decreases over time as the volume of the loci increases (Figure 4.4C), but the total fluorescence intensity (using

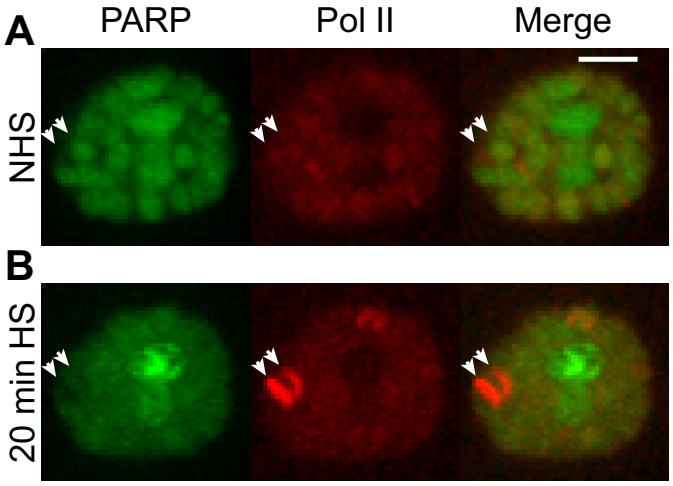

Figure 4.3: Localization of PARP and Pol II with *Drosophila* Salivary Glands.
(A and B) LSCM images of the same polytene nuclei expressing eGFP-PARP and mRFP-Pol II (A) before HS and (B) 20 minutes after HS. For both figures the left panel is eGFP-PARP (green), in the middle panel is mRFP-Pol II (red) and the right panel is a merge of the two factors. Arrows point to the position of the *Hsp70* loci. Scale bars equal 10 μm.

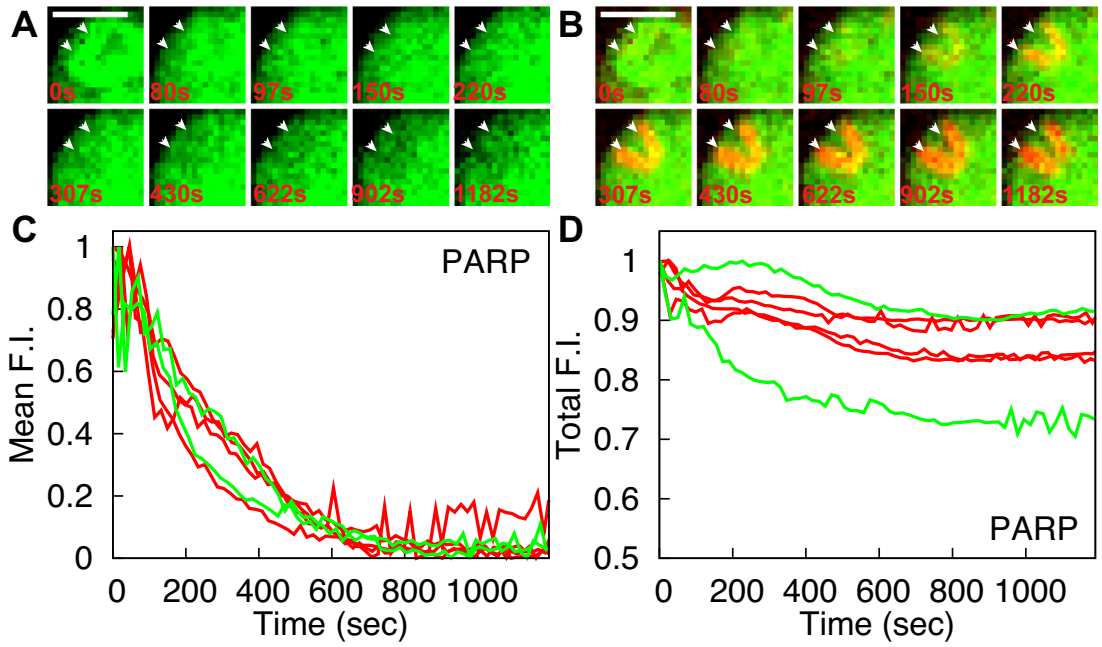

Figure 4.4: Association of PARP with *Hsp70* Loci after Decondensation.
(A and B) Representative time course images illustrating the localization of (A) eGFP-PARP (green) and (B) a merge between eGFP-PARP (green) and mRFP-Pol II (red) to the *Hsp70* loci after HS. The 1^{st} image (0 sec) of each panel is the NHS image, 2^{nd} image is the time point before additional Pol II recruitment and consecutive images are spaced out over the course of HS. Arrows indicate the *Hsp70* loci, and a progressive decrease in eGFP-PARP fluorescence intensity (F. I.) can be seen in these images. Scale bars are 10 μm. (C) Mean F. I. plots of eGFP-PARP using Pol II as an indicator for the volume of the *Hsp70* loci. (D) Total F. I. plots of eGFP-PARP using a constant volume. Lines of the same color are from the same gland, while different colors are from different glands. 2 glands containing 2-4 nuclei each are plotted.

a constant volume remain constant over the course of HS (Figure 4.4D). These results indicate that PARP, like H2B, remains associated with the *Hsp70* loci at the same level before and after chromatin decondensation.

4.2.3 PARP Activity is Responsible for the Compartmentalization of Pol II

Previous studies have shown that PAR chains accumulate at the *Hsp70* loci upon activation, and that the enzymatic activity of PARP, the enzyme that catalyzes PAR chain formation, is required for the structure of HS puff [215]. Subsection 4.2.2 extended these findings and showed that PARP continues to associate with the *Hsp70* loci upon activation. Therefore, we hypothesized that PARP catalytic activity is responsible for the retention of factors in the transcription compartment.

To address this hypothesis, we tested the effect of specifically inhibiting PARP catalytic activity, using the drug PJ34, on the compartmentalization of eGFP-Pol II, the defining factor of the transcription compartment [235], during late HS. The experimental setup is illustrated in Figure 4.5A. We heat shocked the glands for 35 minutes and then perfused 3 μM PJ34, or media only, over the glands for 5 minutes after which we acquired FRAP curves. Perfusion does not affect the compartment behavior of Pol II when compared to a 40-minute HS no-perfusion control (Figures 4.5B and D). Strikingly, PJ34 perfusion after 40 minutes HS has a drastic effect on the FRAP dynamics of Pol II, which now completely recovers over the course of 120 seconds (Figures 4.5B and C). This recovery is remarkably similar to the 10 minute HS FRAP behavior of Pol II, indicating that PARP inhibition leads to a condition resembling the pre-compartment state. This result indicates that the catalytic activity of PARP is required for retaining Pol II in a compartment.

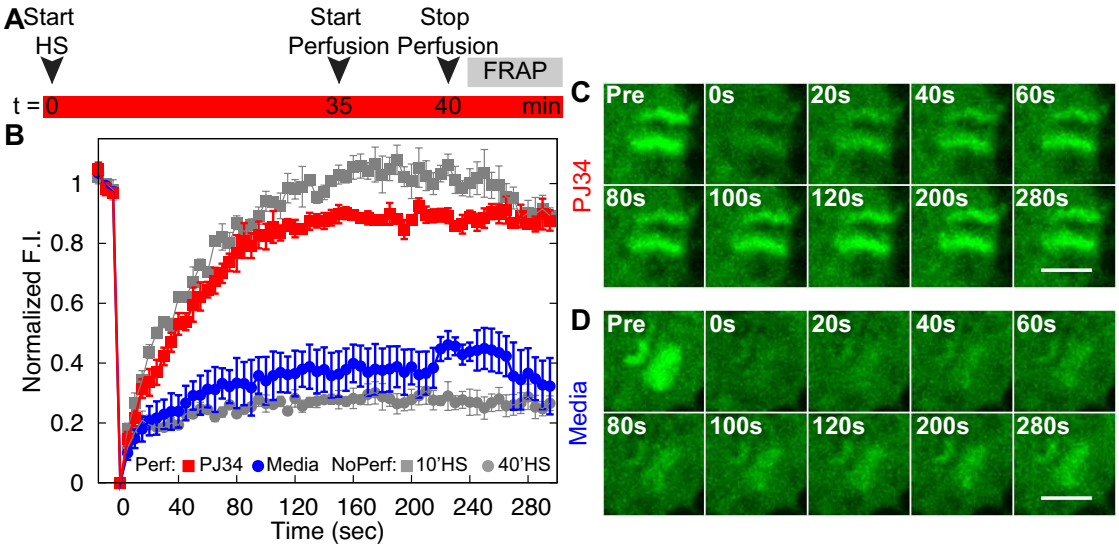

Figure 4.5: PARP Catalytic Activity is Required for the Maintenance of the Transcription Compartment.

(A) Schematic of PJ34 perfusion protocol. Media only or 3μM PJ34 was perfused over the gland for 5 minutes starting 35 minutes after HS. FRAP of eGFP-Pol II at the *Hsp70* loci was initiated as soon as perfusion stopped. (B-D) FRAP of eGFP-Pol II in PJ34 perfused glands and controls. (B) FRAP curves of eGFP-Pol II perfused with PJ34 (red, n=3) at 40 minutes HS or with Media only at 40 minutes HS (blue, n=4) and no perfusion controls at 10 minutes HS (gray squares, n=4) and 40 minutes HS (gray circles, n=3). Error bars represent the SEM. Representative images of (C) eGFP-Pol II after PJ34 perfusion and (D) after Media-only perfusion. Scale bars = 5μm.

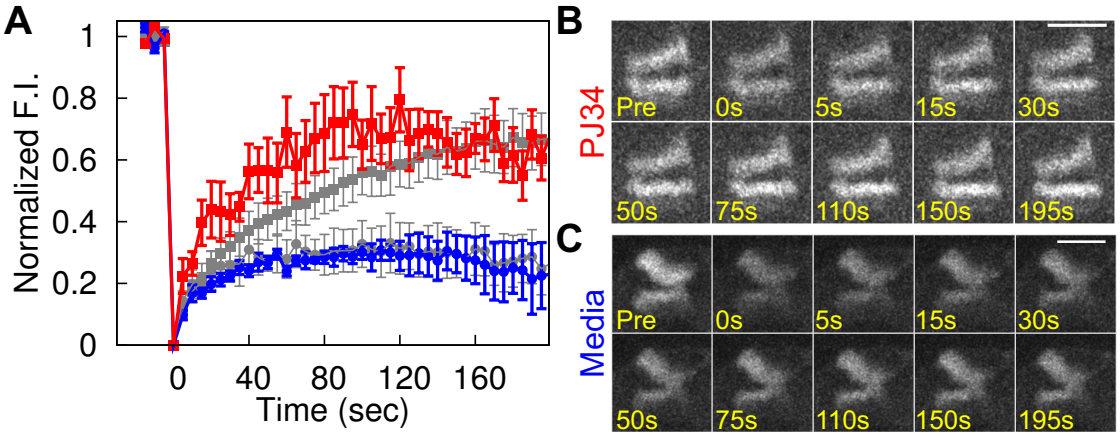

Figure 4.6: The progressive retention of Spt6 is perturbed by PJ34 treatment. Using the same perfusion protocol as Figure 4.5, we perfused Media only or 3μM PJ34 over the gland for 5 minutes starting 35 minutes after HS. FRAP of eGFP-Spt6 at the *Hsp70* loci was initiated as soon as perfusion stopped. (A-C) FRAP of eGFP-Spt6 in PJ34 perfused glands and controls. (A) FRAP curves of eGFP-Spt6 perfused with PJ34 (red, n=3) at 40 minutes HS or with Media only at 40 minutes HS (blue, n=4) and no perfusion controls at 10 minutes HS (gray squares, n=3) and 40 minutes HS (gray circles, n=3). Error bars represent the SEM. Representative images of (B) eGFP-Spt6 after PJ34 perfusion and (C) after Media-only perfusion. Scale bars = 5μm.

4.2.4 Spt6 also Requires PARP Activity for the Transcription Compartment

To confirm the role of PARP activity on the retention of other transcription factors in the transcription compartment we used the same protocol as listed in Figure 4.5A and imaged the dynamics of eGFP-Spt6. Previously, we observed an incomplete recovery, even at early HS time points followed by a complete lack of recovery, 40 minutes after HS (Figure 3.6). In this case, we saw similar effects, except the no-perfusion control at the 40-minute HS time point resulted in a very fast but small amount of recovery that is likely due to diffusion (Figure 4.6A). When we perfused in a media only at 35 minutes after HS and used FRAP at 40 minutes after HS, we saw no significant difference from the 40 minute no perfusion control(Figure 4.6A and C), however when PJ34 is perfused into the imaging chamber at the same time, unbleached eGFP-Spt6 is now able to enter the *Hsp70* loci and fully recover about 80% of initial levels (Figure 4.6A and B).

4.3 Discusion

4.3.1 Transcription Compartment

We used Pol II to test the role of PAR in compartment formation by using PJ34, a specific inhibitor of PARP catalytic activity [199] and showed that the dynamics of Pol II at the *Hsp70* loci, 40 minutes after HS, return to the early HS dynamics upon PJ34 treatment. Inhibition of PARP prevents the polymerization of more PAR, which PARG can now rapidly degrade [44]. This reduces the overall amount of PAR at the *Hsp70* loci and allows a re-mobilization of Pol II to the 10 minutes HS behavior. We hypothesized that the other factors were similarly re-mobilized, and therefore tested the PJ34 treatment with Spt6, the transcription factor that showed the strongest compartmentalization phenotype over the course of HS. As expected Spt6 dynamics were similarly perturbed,

indicating that the role of PAR plays a similar role for multiple proteins.

Based on our results, we propose a model in (Figure 4.7) in which extended HS activation leads to the accumulation of PAR chains at the *Hsp70* loci. Early on (10 minutes HS), the number or size of these chains is small enough that many proteins can easily diffuse into and out of the area. Some factors like Spt6, however, may already be partially immobilized because of their affinity for nucleic acids. Over time (20 minutes HS and then 40 minutes HS), the number of PAR chains increases at the *Hsp70* loci reducing the ability of some factors (Topo I and CycT) to freely diffuse with the nucleoplasm and fully preventing the exchange of Spt6 and Pol II with the nucleoplasm, although they can be reused for continued rounds of transcription [235].

Notably, both Pol II and Spt6 are PARylated by PARP [44, 108], which may suggest a role for the direct modification of these proteins in their progressive retention within the transcription compartment. As a large number of transcription factors are also PARylated, including Topo I, the direct PARylation of transcription could be a general mechanism for PARs involvement in compartmentalization. When PARP catalytic activity is inhibited, PARG is able to degrade existing PAR units, destroying the porous barrier that was formed over the course of HS. The destruction of the barrier now allows diffusion between the nucleoplasm and the locus, resulting in the fluorescence recovery of Pol II and Spt6 at the loci. Presumably the other factors, which are retained in the compartment, also will be remobilized and able to recover after treatment with PJ34. However, a thorough study regarding the role of PAR on the compartmentalization of transcription factors requires a future, concentrated study, and could involve a number of different interactions that restrict transcription factors in different ways.

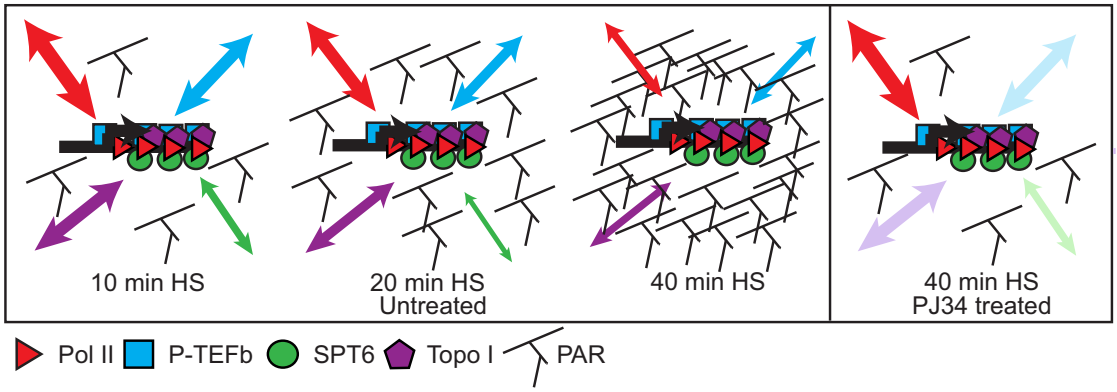

Figure 4.7: Model for the progressive formation of transcription compartment during the time course of HS.
PARylated proteins accumulate at the *Hsp70* loci over HS activation. The accumulation of PAR restricts the ability of proteins to diffuse into and out of the compartment, with individual factors behaving differently, with Spt6 and Pol II unable to exchange with the surrounding nucleoplasm by 40 minutes HS. Treatment with PJ34, a PARP inhibitor, at 40 minutes HS, reduces the amount of PAR present and restores the ability of Pol II to exchange with the nucleoplasm. Light shaded arrows represent the potential dynamics of the transcription factors after PJ34 treatment.

4.3.2 Histone and PARP retention

Finally, our study addresses whether histones remain associated with the *Hsp70* loci after activation and chromatin decondensation. This question has been debated for decades with some experiments resulting in an observed decrease of histones from the gene [164] and some experiments suggesting that they remain associated [150]. By addressing the retention of histones at the *Hsp70* loci we are able to partially reconcile these differences.

Interestingly, the results indicated that H2B remains associated with the loci even though upon activation the nucleosomes rapidly dissociate from the *Hsp70* genes [164]. Therefore, we suggest that the early transcription compartment may be involved in retaining H2B at the *Hsp70* loci. Additionally, our observation that PARP also remains associated with the *Hsp70* loci suggests that PARP might be a component of the compartment. However, further experiments are needed to test these hypotheses.

CHAPTER 5

CHARACTERIZATION OF THE RECRUITMENT AND DYNAMICS OF *DROSOPHILA* SET1[1]

5.1 Introduction

In eukaryotic organisms, the covalent modifications of histones impact the accessibility of nucleosomes [226]. Certain modifications are representative of transcriptionally active and decondensed chromatin. One of these modifications, H3K4me3, is a major mark of transcriptionally active chromatin found near the 5-end of transcriptionally-active genes in yeast and metazoans [15, 183, 188].

In metazoans, multiple enzymes (up to 10 in mammals) have been shown to be responsible for writing the H3K4 methylation mark [118, 183]. In *Drosophila*, *in vitro* and *in vivo* studies have identified three methyltransferases responsible for H3K4 methylation including: Trx6, Trr7 and Ash1 [18, 28]. To date, the widely held consensus is that these factors are responsible for deposition of the histone H3K4me3 mark in *Drosophila* [118, 55]. However, with the exception of the aforementioned studies where a limited number of genes were examined in vivo, no compelling evidence exists to show that these enzymes are responsible for writing the H3K4me3 mark at the global level.

Interestingly, in yeast, only one factor, SET1, is responsible for methylating histone H3K4. Therefore, Behfar Ardehali looked for SET1 orthologs in *Drosophila* and identified the uncharacterized CG40351 [10] and called the novel candidate gene *Drosophila* Set1 (dSet1/dKMT2, hereafter referred to as dSet1). Before its identification as a histone methlytransferase, CG40351 remained uncharacterized, except for one study where

[1] Parts of this chapter are currently being written up for publication [7]

CG40351 was knocked down (KD) by RNAi to test its involvement in dosage compensation in flies [240].

Interestingly, recent studies using RNAi knockdown of *Drosophila* H3K4 methyltransferases suggest that dSet1 is the only factor responsible for maintaining H3K4me3 levels in the cell and on transcriptionally active genes [10], suggesting that dSet1 is the principal histone H3K4 trimethyltransferase in flies. To begin to characterize its role in transcription, we addressed the localization and dynamics of an eGFP-tagged dSet1 to specific chromosomal loci in polytene nuclei. I observed that the recruitment of dSet1 precedes RNA polymerase II (Pol II), and like many transcription factors (Table 1.1), it is dynamically associated with specific chromosomal loci.

5.2 Results

5.2.1 dSet1 Co-localizes with Pol II and is Recruited to the *Hsp70* Loci upon Transcription Activation

To examine both the genomic distribution of dSet1 on polytene chromosomes as well as the kinetics of association of dSet1 with the induced *Hsp70* loci *in vivo*, we generated a GAL4-inducible transgenic fly line expressing an eGFP-dSet1 fusion protein. First we confirmed expression of eGFP-dSet1 in the salivary glands of 3^{rd} instar larvae by Western Blot (Figure 5.1A). As expected, I observed expression of a fusion protein of predicted molecular mass ($\sim$213 KDa) in eGFP-expressing glands. Furthermore, confocal reflection microscopy (CRM) produces images similar in appearance to traditional differential interference contrast microscopy (DIC), and is able to detect differences in optical densities in the sample, which allows the the nucleus (high optical density) to appear brighter in CRM and DIC images. Therefore, CRM can be used in combination

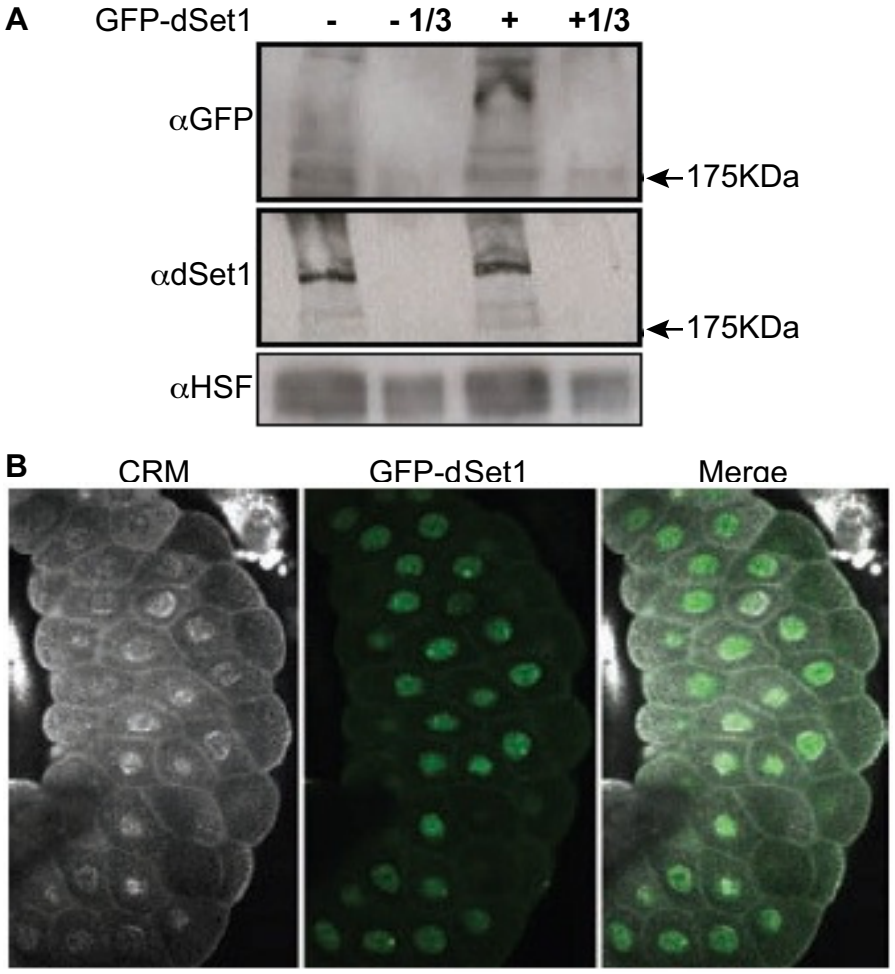

Figure 5.1: Expression of dSet1 in *Drosophila* Salivary Glands
(a)Western Blot on lysates from eGFP-dSet1 and control salivary glands showing expression of a tagged protein of the right size ($\sim$213 KDa) in the eGFP-dSet1 animals (by B. Ardehali). (b) Confocal reflection microscopy (CRM) and GFP image showing nuclear localization of eGFP-dSet1 in living salivary gland cells.

with LSCM of eGFP to reveal the nuclear association of eGFP tagged factors and has revealed that eGFP-dSet1 predominantly localizes in the nucleus (Figure 5.1B).

Nuclear localization is not the only criterium required for a factor to be involved in transcription processes. Therefore, I determined if dSet1 localizes to transcriptionally active loci, including the *Hsp70* loci, in living cells. To do this, I co-expressed eGFP-dSet1 with mRFP-Pol II and imaged nuclei before and after HS (Figure 5.2). Before HS, eGFP-dSet1 showed strong co-localization with mRFP-Pol II (Rpb3 subunit) at many developmental loci (Figure 5.2A). After HS, however, these same sites disappeared and I observed co-localization of dSet1 at the *Hsp70* loci (Figure 5.2B); supporting the notion that dSet1 is generally associated with sites of active transcription by Pol II.

We next sought to closely examine the recruitment kinetics of dSet1 to the *Hsp70* loci, 87A and 87C upon HS activation. To this end, I employed LSCM in living salivary gland cells (See Chapter 2.3.3 for Methods). Similar to what had been reported previously, Pol II was recruited to the HS loci and reached a plateau around 8 minutes after HS [235, 244]. Interestingly, and in contrast to Pol II [235, 244], eGFP-dSet1 was recruited to the *Hsp70* loci with the fluorescent intensity reaching peak intensity around 6 minutes after HS activation (Figure 5.3 C). Unlike Pol II, or any of the previously studied transcription factors at *Hsp70*, except HSF [244], dSet1 decreases in fluorescence intensity, until a steady state, above background, is reached around 8 minutes after HS (Figure 5.3 C). In Figure 5.3 A and B, this decrease in mean fluorescence intensity is apparent.

The previously observed mean fluorescence intensity decrease of HSF was attributed to chromatin decondensation and the subsequent increase if puff volume [244]. To address whether decondensation is a factor in the decrease in mean fluorescence intensity of dSet1, I measured the total fluorescence intensity of dSet1 using a constant volume

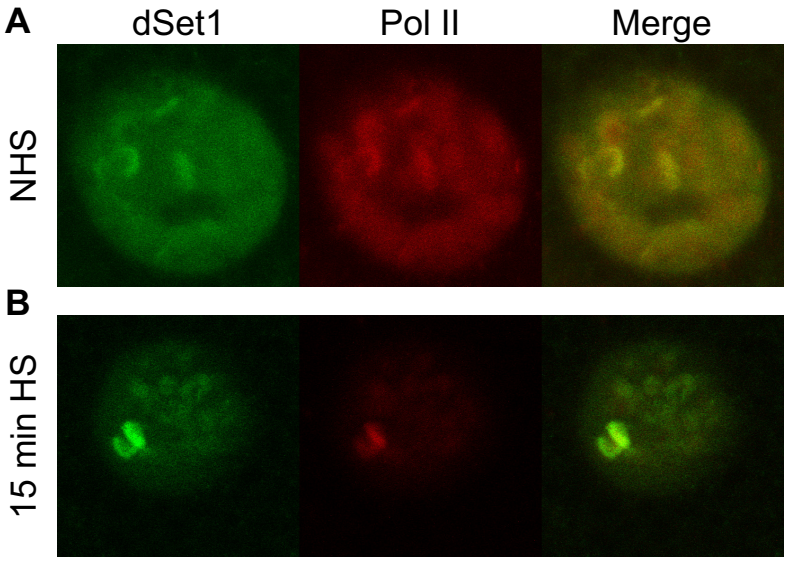

Figure 5.2: The Recruitment and Localization of Transcription Factors on the *Hsp70* gene upon HS

LSCM images of the different polytene nuclei expressing eGFP-dSet1 and mRFP-Pol II (A) before HS and (B) 20 minutes after HS. For both figures the left panel is eGFP-dSet1, in the middle panel is mRFP-Pol II and the right panel is a merge of the two factors.

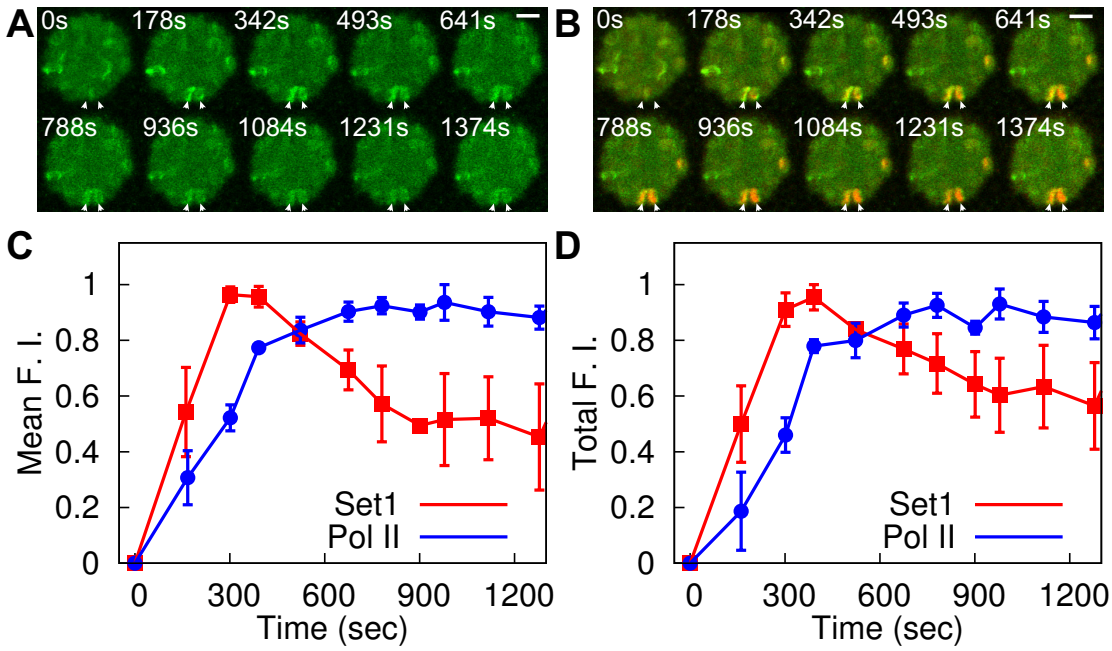

Figure 5.3: The Kinetics of dSet1 Recruitment to the *Hsp70* Loci upon HS
(A and B) Representative time course images illustrating the localization of eGFP-dSet1 over the course of HS. (A) Shows the localization of the eGFP-dSet1, while (B) a merge between the eGFP-dSet1 (green) and Pol II (red). The 1^{st} image (0 sec) of each panel is the NHS image, 2^{nd} image on represent different time points after HS. Arrows indicate the *Hsp70* loci, and a increase followed by decrease in eGFP-dSet1 intensity can be seen in these images. Scale bars are 10 μm. (C) Mean fluorescence intensity (F. I.) and (D) Total F. I. plots of eGFP-dSet1. Mean F. I. plot uses Pol II as an indicator for the volume of the *Hsp70* loci, Total F. I. plot uses a constant volume. Error bars represent the standard deviation and represent 6 nuclei.

around the *Hsp70* loci. As shown in Figure 5.3D, total dSet1 fluorescence intensity levels still drop after 6 minutes. Together with the knowledge that chromatin decondensation occurs concomitantly with Pol II recruitment, it suggests that dSet1 is in fact partially leaving the *Hsp70* loci after activation.

5.2.2 dSet1 Interacts Dynamically with Transcriptionally Active Loci

We also utilized FRAP to study the local exchange dynamics of dSet1 at the *Hsp70* loci, 87A and 87C, as well as some developmental loci that are associated with dSet1 before HS activation (Figure 5.4). I observed a fast rate of recovery ($k_{off} = 65 \pm 4 \times 10^{-3}$ seconds) for the *Hsp70* loci at 8 minutes after HS, indicating a dynamic association of dSet1 with the *Hsp70* loci. However, dSet1 only recovered to 60% of the initial levels. This lack of complete recovery can be explained by the timing of HS duration. 8 minutes after HS, dSet1 intensity at the *Hsp70* loci has already started to decrease (Figure 5.3C). Because the total amount of dSet1 is less after FRAP, it could not reach complete recovery.

The single exponential recovery profile observed with dSet1 is indicative that the majority of dSet1 participates in a dynamic interaction with the *Hsp70* loci, and is distinct from the FRAP profile of Pol II, which recovers linearly over the time course of transcription elongation [235]. Notably, the $\tau_{1/2}$ of dSet1 is $\sim$10 seconds, which is much larger than expected if dSet1 was able to freely diffuse in around the *Hsp70* loci. Therefore, like most other transcription factors (Table 1.1), dSet1 is transiently retained on the chromosome, and the recovery of dSet1 is most likely limited to the time it takes for the enzymatic reaction to occur.

In addition to photobleaching the *Hsp70* loci, we photobleached random loci in the NHS nucleus and monitored their fluorescence recovery. The sites we photobleached

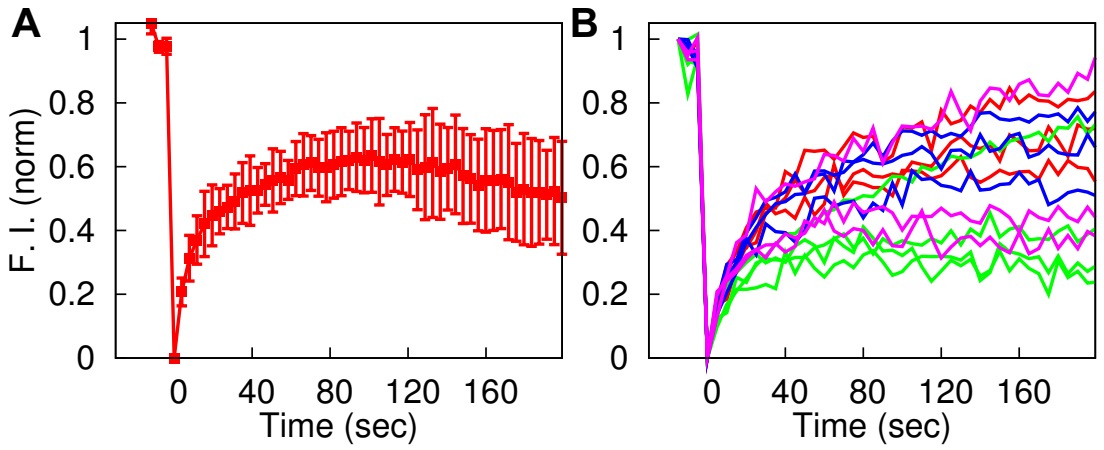

Figure 5.4: FRAP Analysis of dSet1 at the *Hsp70* Loci and Transcriptionally Active Developmental Loci

FRAP analysis of dSet1 at (A) *Hsp70* loci after 8 minutes of HS, and (B) developmental loci before HS. All sites photobleached co-localized with Pol II. FRAP curves were normalized to pre-bleach equal to 1 and first image after the bleach equals 0. Error bars in (A) represent the standard deviation and FRAP curves in (B) represent the developmental loci photobleached, with up to 4 loci being bleached in different 3 glands.

co-localized with Pol II and therefore likely represent transcriptionally active developmental loci. In all cases, FRAP of dSet1 at developmental loci showed similar rates of recovery, however there were differences in total amount of recovery with some loci recovering completely and others containing a large immobile fraction (Figure 5.4B). These differences may be due to when these genes were activated during development. Nonetheless, in all cases, these results support the dynamic association of dSet1 with active transcription loci.

5.3 Discussion

Characterization of dSet1, a previously uncharacterized gene, using live cell imaging has provided novel insights into its role in transcriptional regulation. First, co-localization between dSet1 and Pol II at specific chromosomal loci indicated dSet1 plays a role in transcriptional regulation. Furthermore the kinetic analysis of recruitment shows that dSet1 is recruited to the *Hsp70* loci either faster or earlier than Pol II, suggesting that dSet1 is trimethylating H3K4 before Pol II fully occupies the loci. Because the temporal resolution is low, this could suggest two possibilities. (1) H3K4me3 occurs as soon as Pol II begins to transcribe, therefore full recruitment of Pol II at the loci is not required for full recruitment of dSet1 at the loci or (2) H3K4me3 precedes the escape of Pol II into active elongation and addition recruitment of Pol II. A higher temporal resolution study of dSet1 recruitment to the *Hsp70* loci will distinguish between these two possibilities. However, H3K4me3 can occur on genes before they are transcriptionally active [200], indicating that H3K4me3 precedes transcription activation.

FRAP analyses have also provided insight into the association of dSet1 with the *Hsp70* loci and developmental loci. $\tau_{1/2}$ and recovery rates estimates describe a transient association between dSet1 and the transcriptionally active loci, however, like most

transcription factors, the transient association of dSet1 is retarded by an interaction between dSet1 and the loci. Kinetic modeling using a single exponential equation estimates the recovery time of dSet1 and suggests that the trimethylation of H3K4 by dSet1 lasts no longer than $65 \pm 4 \times 10^{-3}$ seconds. However, this measurement could overestimate the enzymatic rate because additional non-enzymatic interactions could occur at the loci resulting in the observed k_{off}.

Live cell imaging of transcription factors at the *Hsp70* loci in *Drosophila* polytene nuclei has previously identified the gradual accumulation and retention of all transcription factors previously studied at a transcription compartment [235, 244]. This study, has further characterized the interaction of proteins with the transcription compartment, even though it did not study the change in dSet1 dynamics over different HS durations, by FRAP, in depth. The defining results were the recruitment assays, which showed that during early HS, dSet1 is first recruited to the loci and then partially removed from it. dSet1 is the first example of a protein, imaged using live cell imaging, which actually leaves the loci during HS.

CHAPTER 6

PERSPECTIVES AND FUTURE DIRECTIONS[1]

This thesis provides a focused study of the *Hsp70* loci of *Drosophila* polytene chromosomes, which indicates that HS activation precipitates the *de novo* assembly, accumulation, and retention of transcription factors at activated regions [244] and provides a follow up to a previous study which identified a number of these features for Pol II [235]. In this thesis, I studied a number of mechanisms for the *in vivo* regulation of transcription within living cells including the recruitment of transcription factors to sites of active transcription, their accumulation and retention in a concentrated transcription compartment, and measured their binding affinity with native loci. In addition, I helped characterize a newly identified Histone H3 lysine 4 trimethyltransferase, by assaying its recruitment and dynamics to the *Hsp70* loci in living cells.

6.1 Transcription Compartment

The term "transcription compartment" has been coined to describe the changes in protein dynamics leading to the progressive, local retention of transcription factors to activated loci. In this section, I will compare our observations of a transcription compartment to the previously described transcription factories and then I will discuss the relevance and generality of the transcription compartment and future directions that can provide a beginning to this understanding.

[1] Parts of this chapter have been submitted to the 75th Cold Spring Harbor Symposium in Quantitative Biology for publication [74].

6.1.1 Comparison of the Transcription Compartment with Transcription Factories

Evidence for a transcription compartment arose from MPM, LSCM, and SDCM images of native cytological loci in living cells [235, 244]. Using FRAP at the *Hsp70* loci in polytene nuclei, it was shown that photobleached Pol II was initially replaced rapidly by unbleached Pol II 20 minutes after HS; however, recovery was not observed 60 minutes after HS [235]. This change from full exchange of Pol II at 20 minutes to undetectable exchange at 60 minutes occurs in a progressive manner [235]. Additional data indicate that transcription is still occurring after 60 minutes at these sites, suggesting that the bleached Pol II molecules are locally retained in a transcription compartment and recycled for transcription observed at late time points [235].

While the compartment was initially characterized for Pol II, this model would predict that other transcription factors would be retained in the compartment structure. Indeed, as we have shown in this thesis, the exchange of P-TEFb, Spt6, and Topo I at *Hsp70* loci, as measured by FRAP, progressively decreases after longer HS times. Interestingly, we also showed that the transcription compartment is requires PARP catalytic activity, further implicating PARP as an important player in the chromatin changes that occur following HS [164, 244]. We also showed the *de novo* recruitment and accumulation of the transcription factors at the *Hsp70* loci in *Drosophila* salivary glands, using SDCM. Interestingly, maximum recruitment of Pol II and the transcription factors occur $\sim$8-10 minutes after HS, which correlates with the time it takes for the *Hsp70* loci to reach maximum volume, but requiring more time than maximum occupancy of the *Hsp70* genes [244].

The two defining characteristic of compartments are the progressive retention of transcription factors and the *de novo* recruitment and accumulation of transcription fac-

tors at activated regions [235, 244], which have been identified through in depth studies at the *Hsp70* loci. Interestingly, compartment-like features are also found at numerous developmental loci, in *Drosophila* salivary glands, illustrating the generality of this structure [235]. However, the "transcription factory" model, proposes an alternate view, in which co-regulated genes relocate upon activation to preformed foci containing Pol II and the transcription machinery [87]. Support for the transcription factory model stems from fluorescence *in situ* hybridization (FISH) data which indicate that co-expressed genes co-localize with Pol II foci more frequently when active, compared to when they are inactive [158, 159].

However, the transcription factory model does not hold true for HS regulated genes, as FISH of *Hsp70* and *Hsp83* revealed that the frequency of interactions of these two loci and their distribution in the nucleus does not change upon gene activation in diploid cells [235]. Furthermore, live cell imaging within polytene nuclei indicates that the *Hsp70* loci are not repositioned upon gene activation. Similarly, in mouse 3134 cells it was shown that a tandem array of the MMTV promoters does not relocate within the nucleus after activation [16]. Additionally, live cell imaging of MS2-GFP binding to the nascent RNA of a β-globin gene construct harboring MS2 binding sites, revealed that transcriptional activation does not cause it to move from the nuclear membrane to the interior of the nucleoplasm [112]. These data, taken together, suggests that at minimum, the "*de novo*" accumulation of factors at active loci occurs beyond the *Hsp70* loci of *Drosophila* and is likely a general model of gene regulation.

The main features of contention between the transcription compartment and transcription factory models, as mentioned above, are the recruitment of genes to pre-formed transcription factories. To date, no live cell imaging methods have shown the recruitment of activated genes to a pre-formed transcription factory, and live cell imaging studies into

the dynamics Pol II have shown that Pol II is not stably associated with a "transcription factory" [102]. However, some features of the transcription factory model may still be compatible with the transcription compartment model, including the possibility that a local accumulation of transcription factors could occur around genes that are similarly regulated, especially if these genes already co-localize with each other [209]. In fact, it may be a way to increase the local concentration of transcription factors at these genes.

6.1.2 Retention of Transcription Factors in the Transcription Compartment

In Chapter 3, we showed that P-TEFb, Spt6 and Topo I were all progressively retained at the *Hsp70* loci over the course of transcription activation, although the degree of retention varies between the three factors. P-TEFb and Topo I are able to partially recover fluorescence even after 60 minutes of HS, while Spt6 becomes completely retained at the *Hsp70* loci by 40 minutes of HS. Together, the observations that the dynamics of these three factors are affected by the length of HS, in addition to Pol II [235], suggests that "compartmentalization", or the progressive decrease in protein dynamics over transcription activation, is a phenomenon not limited to Pol II. However, at this time, the transcription compartment and its effect on protein dynamics has only been studied at the *Hsp70* genes in *Drosophila* polytene nuclei. Therefore, in order to fully appreciate the importance of transcription compartments on the regulation of transcription, it will be important to address the presence of transcription compartments at other genes in polytene nuclei, as well as within diploid cells.

As of now, the transcription compartment has only been identified at the *Hsp70* loci in polytene nuclei; however, live cell imaging studies in diploid cells suggest that some of the characteristics of a transcription compartment are conserved [16, 112]. The following questions are critical to understand the generality of the transcription com-

partment: (1) do other genes in polytene nuclei for a transcription compartment? (2) do transcription factors compartmentalize at native loci in diploid cells? and (3) does compartmentalization occur in other organisms? To properly answer these questions, it may be necessary to develop new imaging methods, in order to improve image resolution and signal-to-noise. However, in the mean time, it may be possible to use tandem arrays in diploid cells using either *Drosophila* cells or cells from other organisms, in order to provide a first order view of this process.

6.1.3 Role of PAR in the Retention of Transcription Factors in the Transcription Compartment

Inhibition of PARP catalytic activity leads to the prevention of chromatin decondensation upon activation, which indicates that PAR plays a role in the chromatin decondensation of transcriptionally active puffs [215]. Furthermore, PAR is covalently attached as a post-translational modification onto acceptor proteins, including PARP, Histones, Pol II, Spt6 and Topo I, through the activity of PARP [44, 108]. Therefore in Chapter 4, we addressed the role of PARP catalytic activity on the retention of Pol II and Spt6 within the transcription compartment, and observed a dramatic increase in transcription factor dynamics compared to a control.

The complete remobilization of Pol II and Spt6 at the *Hsp70* loci, suggests that through the inhibition of PARP, the levels of PAR at the *Hsp70* loci are not only prevented from accumulating, but also are actively degraded during the 5 minutes inhibition of PARP. As steady state levels of PAR in the cell are regulated through the opposing activities of PARP and PARG [44], this result indicates that PARG is also present at the *Hsp70* loci and is actively regulating the levels of PAR at the *Hsp70* loci. In order to better understand the role of PAR in transcription compartment formation, we need to

address the opposing activities of PARP and PARG. Preliminary results suggest that the RNAi knockdown of PARG leads to the early formation of the transcription compartment (unpublished data). However, further studies are required to address the interplay between these PARP and PARG and their effect on the transcription compartment.

6.2 Synchronous Recruitment of Individual Transcription Factors

Previously, the synchronous transcription activation of genes in the *Drosophila* embryo has been addressed and it was observed that genes containing a paused Pol II were synchronously activated (within 3 minutes of each other) while genes without a paused Pol II were stochastically activated over the course of 20 minutes [23]. Our observation that the HSF, Pol II, P-TEFb, Spt6 and Topo I are all individually and synchronous recruitment to the *Hsp70* loci correlates with this observation, as the *Hsp70* genes contain the best studied paused Pol II, and it shows the transcriptional activation of the *Hsp70* genes, can occur synchronously, through the synchronous recruitment of transcription factors involved in both activation and elongation.

Using the *Hsp70* loci, we were not able to identify a transcription factor that is stochastically recruited, indicating either that the presence of a paused Pol II leads to the synchronous recruitment of all transcription factors or that the polytene chromosomes, and amplification of chromatids, leads to an apparent synchrony in recruitment due to the sheer number of potential interactions occurring at the loci. The ideal assay to address both of these possibilities is to measure the recruitment of transcription factors to native loci in diploid cells. However, the optical technology is not yet at the point where this measurement is possible, although currently advances are being made to provide brighter fluorophore or higher optical resolution [80, 195].

With current technology, however, it is still possible to address the role of paused Pol II in the synchronous recruitment of transcription factors using polytene chromosomes, or tandem arrays in diploid cells. Specifically, I believe that studying the inducible recruitment of transcription factors to genes either containing or lacking a paused Pol II would provide a more rigorous study of the role in pausing for the synchronous recruitment of transcription factors. Furthermore, if it were possible to see the stochastic recruitment of transcription factors in polytene chromosomes at genes lacking a paused Pol II, it would show that this observation is not a general feature of polytene chromosomes.

6.3 Retention and Dynamics of PARP and Histones

In this thesis, we addressed whether transcription factors associated with the loci before activation, such as PARP and H2B remained associated with the loci after activation and saw that these factors were retained at the *Hsp70* loci after activation. Although in both of these cases, we observed the retention of these factors, we do not yet know if it is a general mechanism of these types of transcription factors and propose that a broader understanding regarding the retention of pre-activation associated factors at the *Hsp70* loci requires the study of other factors including DSIF, NELF, and GAF. However, the results we observed indicate that the observation of a mean fluorescence intensity decrease does not correspond to the removal of PARP and H2B from the *Hsp70* loci and requires the change in volume to be considered.

6.3.1 PARP

In this thesis, we identified a new function for PARP in transcriptional regulation, its involvement in the formation of the transcription compartment after long lengths of HS (up to 60 minutes HS). However, we were not able to see the recruitment of PARP to the *Hsp70* loci upon activation, and observed the mean fluorescence intensity at the *Hsp70* loci become less intense. The Spradling lab also showed that PARP is present at the *Hsp70* after HS; however, if you look closely the levels of PARP appear to be at a lower concentration than the regions surrounding the loci [215]. Therefore, in this thesis we addressed whether there was a recruitment of PARP to the *Hsp70* loci, or the same amount of PARP was associated with the *Hsp70* loci before and after activation, or there was a decrease in total PARP levels with the *Hsp70* loci. Interestingly, we observed the total levels of PARP remained constant over the course of a 20 minute HS.

The assay looking at total fluorescence intensities does not address protein dynamics and it is possible that PARP is transiently associating with the *Hsp70* loci at these times. Therefore a complete study of the dynamics of PARP upon HS at the *Hsp70* loci would define what the mechanism of retention is for PARP upon activation. Furthermore, as the catalytic activity of PARP is responsible for the progressive retention of transcription factors at the transcription compartment, it would be interesting to determine whether the inhibition of PARP with PJ34 would lead to its dynamic association with the *Hsp70* loci or the eventual loss of PARP from the loci.

6.3.2 Histones

We also addressed the retention of the histone H2B within the loci, which was of interest because ChIP and nucleosome protection assays suggest that histones may be lost from

the *Hsp70* gene after HS [164]. However, HS requires the recruitment and activity of histone chaperones and nucleosome remodelers and previous experiment looking at the accumulation of PAR at transcriptional active loci on polytene chromosomes hypothesized a role for PAR at the loci was to keep transcription factors and histones associated with the loci [215]. This hypothesis correlates with our observation that the accumulation of PAR at the *Hsp70* loci is responsible for the progressive retention of transcription factors at the *Hsp70* loci and therefore we suggested histones would similarly be retained.

The results presented in this thesis show that the total levels of H2B remain constant before and after activation. Like the PARP studies, this result does not address dynamics of the interaction between H2B and the loci; therefore studies addressing this are required. Furthermore, we would like to address whether the initial population of H2B is reassembled on the *Hsp70* loci after recovery from a HS. A complete understanding the role of histone retention however should also include histones with known variant factors that associate with the gene after activation, such as H3 and H3.3. Together these results will identify whether histones are dynamically associated with the *Hsp70* loci and furthermore it will show whether there is a directed or indirected replacement of histones upon activation.

6.4 Characterization of Uncharacterized Transcription Factors

In Chapter 5, we applied live cell imaging methods that were applied in Chapters 3 and 4, in order to understand the recruitment and dynamics of a previously uncharacterized protein. Multiple enzymes which can trimethylate H3K4me3 have been identified in *Drosophila*, however, there is little *in vivo* evidence linking these factors to the methylation mark on a global scale. Interestingly, the only yeast H3K4 methylase, SET1, was

not previously identified in *Drosophila* until recently [7]. Therefore, we identified the localization and dynamics of dSet1 at the *Hsp70* loci and developmental loci, in order to set limits on its activity in transcription.

First, dSet1 was shown to be a nuclear localized protein that also co-localized with Pol II at developmental active loci and the active *Hsp70* loci. These results, indicate that dSet1 was involved in transcription regulation, as was suggested by its homology to the yeast SET1. Furthermore, by monitoring the recruitment of dSet1 to the *Hsp70* loci, we observed its recruitment either earlier than Pol II or at a rate that is faster than Pol II, or a combination of both, using LSCM. Using a higher temporal resolution method, such as SDCM, it would be possible to distinguish between the two different possibilities. The current results, however, suggest that dSET1 is required at a slightly earlier step than Pol II, which is consistent with the previous observation that the H3K4me3 mark can occur before Pol II recruitment [200]. Finally we measured the dynamics of dSet1 at the *Hsp70* loci and developmental loci and showed that dSet1 is transiently associated with transcriptionally active loci.

Interestingly, after dSet1 reached maximum recruitment at the loci there is a decrease in mean fluorescence intensity. Notably, this decrease does not correspond to chromatin decondensation and the total fluorescence intensity also showed a decrease. This is the first case where we saw a protein leave the *Hsp70* loci after activation and indicates that at early time points (before 20 minutes HS), factors can enter and exit the loci. Notably, dSet1 is not completely lost, but appears like it is at least partial retained at the loci. Further experiments into other proteins that have a early role in activation may help define what the transcription compartment is and how proteins are effected by its presence.

APPENDIX A

GENERATION OF TRANSGENIC *DROSOPHILA* LINES AND CROSSES

In order to generate transgenic fly lines, we used the Invitrogen Gateway® recombination cloning technology with FP-tagged *Drosophila* expression vectors. We then had the DNA injected into the *Drosophila* germline and selected flies for positive p-element integrations using the expression of the w^+ gene. Details into the specific cloning steps are listed below.

A.1 Gateway Cloning

The Invitrogen Gateway® recombination cloning technology is a convenient and flexible method for generating epitope tagged proteins for multiple uses [90]. It was first developed as a recombination cloning technology by Hartley *et. al* and is based on the site-specific recombination of bacteriophage λ [78].

Bacteriophage λ uses site-specific recombination to integrate into the bacterial host genome during the lysogenic phase and to excise from the host genome during the lytic phase [114]. Integrative recombination, during the lysogenic phase, occurs between the viral encoded *attP* site and the bacterial encoded *attB* site mediated by integrase (Int) and bacterial encoded integration host factor (IHF) to produce the hybrid sites *attL* and *attR* [114]. Excisive recombination, during the lytic phase, occurs between the *attL* and *attR* to produce *attP* and *attB* and requires the use of an additional protein excisionase (Xis) [114, 78].

Hartley *et al.* adapted this system to provide an *in vitro* recombination cloning method using two modified sets of *att* sites [78]. In this method, the gene of interest is amplified with two different *attB* sites on either end. Then, through incubation with

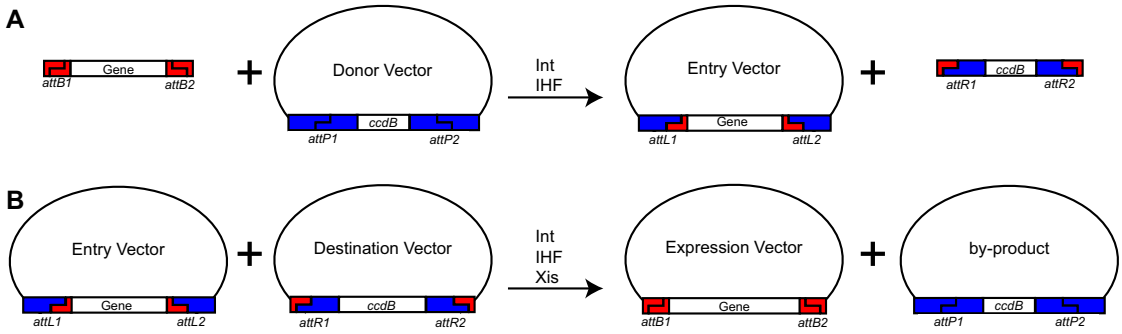

Figure A.1: Model of Gateway® Recombination Reactions.
(A) BP reaction using an *attB* flanked PCR product for the *attB* substrate. Addition of Int and IHF catalyzes the recombination of the *attB* substrate with the "Donor vector" (*attP substrate* to form an "Entry" vector containing *attL* sites and a lethal by-product. (B) LR reaction using the "Entry" vector created with the BP reaction and a "Destination" vector containing *attR* sites. Addition of Int, IHF, and Xis catalyze this reaction for form the "Expression" vector, containing *attB* sites, and a lethal by-product. The *ccdB* gene is a selection marker that inhibits the growth of specific *E. coli* strains. Modified from [90].

Int, IHF, and a "Donor" vector containing complementary *attP* sites permit recombination between the two constructs. This reaction creates an "Entry" vector containing the hybrid *attL* sites and a lethal by-product containing the *attR* sites (Figure A.1A). Further incubating the "Entry" vector with a "Destination" vector containing *attR* sites along with the enzymes Int, IHF and Xis promotes recombination between the two vectors yielding an *attB* containing "Expression" clone and a lethal by-product, due to the presence of an expressed *ccdB* gene (Figure A.1B).

"Destination" vectors have been created for a number of uses including bacterial expression [90], N- or C-terminal fusions [90] and *Drosophila* expression [148]. For our studies, we used the *Drosophila* Gateway® vectors, provided by the Murphy Lab [148], to generate epitope tagged proteins that can then be expressed in flies by integrating the plasmid into the *Drosophila* genome using P-element transformation [148]. These "Destination" vectors contain P-element binding sites which flank both the white (*w*) gene and the FP tagged Gateway® cassette under the control of the UASt promoter. The UASt promoter consist of the Upstream Activating Sequence (UAS), containing five Gal4 binding sites, followed by an *hsp70* TATA box and transcription start site.

For the Drosophila constructs generated by Gateway® Recombination (Table A.1, method: Gateway), we first amplified the cDNA with *Pfu* polymerase using the Gateway primers listed in Table A.2, which contain the necessary *attB* sites. The BP and LR reactions were done according to the manufacturers recommendation using half the volume. Briefly, 75 ng *attB* PCR product was incubated with 75 ng pDONR221 vector in the presence of BP Clonase I (or II) enzyme mixture. The reaction was allowed to proceed for 1 hour and terminated using 1 μg Proteinase K. 1 μl for reaction was transformed into *E. coli* and transformants were confirmed by sequencing [90]. Then, 75 μg of the transcription factor "Entry" vectors were incubated with an 75 μg of the appropri-

Table A.1: Drosophila Constructs Generated in the Lab
CJF–Chris J. Fecko, JY–Jie Yao, KLZ–Katie L. Zobeck, H.R.–Homologous Recombination
References (Refs) are for the source of DNA, which was amplified from w^{118} fly lines in the cases where no reference was listed. The Rpb3-eGFP and HSF-eGFP fly lines were previously published [236, 235].

Protein	Tag	Placement	Method	By	DNA Source	Refs
CycT	mRFP	N-terminus	Gateway	KLZ	pBAC-P-TEFb	[161]
H2B	mRFP	C-terminus	Gateway	CJF	dm500	[120]
H2B	paGFP	C-terminus	Gateway	CJF	dm500	[120]
HSF	eGFP	C-terminus	Gateway	JY	SD02833	[182]
Med17	mRFP	N-terminus	Gateway	KLZ	SD10038	[182]
PARP	eGFP	C-terminus	Gateway	SJP	RE04933	[205]
pRpb1	eGFP	base of CTD	H.R.	KLZ	w^{1118} DNA	
Rpb2	eGFP	C-terminus	Gateway	KLZ	LD22387	[182]
Rpb2	mRFP	C-terminus	Gateway	KLZ	LD22387	[182]
Rpb3	eGFP	N-terminus	Gateway	JY	GH07456	[182]
Rpb3	mRFP	N-terminus	Gateway	JY	GH07456	[182]
Rpb9	eGFP	C-terminus	Gateway	KLZ	w^{1118} DNA	
Rpb9	mCherry	C-terminus	Gateway	CJF	w^{1118} DNA	
Spt6	eGFP	first intron	FlyTrap	N/A	N/A	[27]
Topo I	eGFP	first intron	FlyTrap	N/A	N/A	[27]
Topo I	paGFP	N-terminus	Gateway	KLZ	RE58921	[205]

ate "Destination" vector with the LR Clonase I (or II) enzyme mixture and transformed in to *E. coli* in the same manner as the BP reaction above [90]. N-terminal eGFP, N-terminal mRFP and C-termianl eGFP tags used the Murphy Lab vectors pTGW, pTRW and pTWG, respectively. While the N-terminal paGFP and C-terminal mCherry tagged vectors were modified from the Murphy vectors by Katherine Kiekhaffer and Chris Fecko to include either photoactivatable GFP (paGFP) or mCherry a more stable RFP.

The final "Expression" vector was sent off for injection to either Best Gene Inc. or Genetic Services Inc. These companies co-inject w^{1118} flies with the DNA construct and P-element transposase in order to get a semi-random integration of the DNA construct into the *Drosophila* genome. Germline transformants can be identified by the expression

of w^+ in F1 progeny of injected embryos, and single chromosome insertions are isolated and balanced with the appropriate "balancer" chromosome.

Because a UASt promoter drives the FP-tagged gene, the resulting transformants do not express the FP-tagged transcription factor. Expression of the protein requires the expression of the yeast transcriptional activator Gal4 within the fly. Notably, there is a large collection of potential Gal4 expression lines, which express Gal4 in different tissues and stages of development using either known promoters to drive the expression of Gal4 or expression through the random p-element integration into natural enhancers. In this study we mainly used one of four Gal4 expression lines to drive the expression of the FP-tagged factors in the salivary glands. They are Sgs3-Gal4, C729-Gal4, C147-Gal4 and Fkh-Gal4. The specific crosses to express the transcription factors used in this thesis are listed in Figures 2.2 and 2.3.

A.2 Obtaining Additional Fly Lines

Not all of the transcription factors used in this thesis were generated in house, or via Gateway P-element transformation. Some of the transcription factors (Spt6 and Topo I) were obtained as a result of a large-scale protein trap screen initiated in 2001 by the Chia lab in order to endogenously tag proteins with eGFP. In this screen they used a protein trap p-element transposon, which carries an artificial exon encoding eGFP flanked by splice acceptor and donor sequences. Random integration of the P-element into the genome will generate some insertions within introns of expressed genes, which can be identified by the expression of GFP [145]. Over the years, the Chia, Cooley and Spradling labs have isolated proteins endogenously tagged with eGFP using this method, including Spt6 and Topo I (Flytrap names CC01414 and CA07692, respectively) [27], two of the major factors involved in this study. The insertion of eGFP into these two

Table A.2: Primer Sequences

Protein	Primer
Gateway *attB* Primers	
CycT fwd	5'-GGGGACAAGTTTGTACAAAAAAGCAGGCTCCATGAG TCTCCTAGC
CycT rev	5'-GGGGACCACTTTGTACAATAAAGCTGGGTTCTTGTTG TAGACGGG
Topo I fwd	5'-GGGGACAAGTTTGTACAAAAAAGCAGGCTCTGGATC CAGTGGGGATGTGGCTGCC
Topo I rev	5'-GGGGACCACTTTGTACAAGAAAGCTGGGTCACGATA ATTCTCATCGGCCATATG
Rpb2 fwd	5'-GGGGACAAGTTTGTACAAAAAAGCAGGCTTCATGAT GTACGACAACGAGGAAGAA
Rpb2 rev	5'-GGGGACCACTTTGTACAAGAAAGCTGGGTAGGTGAC CATCAGGCGTGG
Rpb9 fwd	5'-GGGGACAAGTTTGTACAAAAAAGCAGGCTTCATGAC GACTGCCTTTGATGC
Rpb9 rev	5'-GGGGACCACTTTGTACAAGAAAGCTGGGTACTCCGT CCAACGGTGGG
Homologous Recombination Primers	
Rpb1-3'-fwd	5'-TGGAATGTGCAGAAGATCTTTCAC
Rpb1-3'-rev	5'-TAACTGCTAGCGTCTTCGCTCTCCTCGAACGT
Rpb1-dwn-fwd	5'-TATATATTAGCGGCCGCTGAGGAAGGGAGGACGGG
Rpb1-dwn-rev	5'-TATATATTAGCGGCCGCTCGTACATTATTTATGGATAAC CC
GFP-NheI-fwd	5'-AAACGGCTAGCTTTGTGAGCAAGGGCGAGGAGCTGT TCA
GFP-NotI-rev	5'-AAAAGGAAAGCGGCCGCGTCACTTGTACAGCTCGTC CATGCCGAG

genes did not cause any defects in the transcription and splicing of the genes, aside from adding a eGFP exon.

We also obtained fly line through the generous contributions of individual labs, especially the Hsieh lab. The Hsieh lab provided us with a YFP-Top3α (+/+; Sco/CyO; Top3α-YFP), a YFP-Top3β (+/+; Top3β-YFP) and eGFP-Topo II (+/+; Topo II-eGFP) [232, 231]. Although, they were not used in the main thesis research, we imaged these factors and did not observe any recruitment to the *Hsp70* loci upon HS (unpub-

lished data).

A.3 Homologous Recombination Attempts for Rpb1

The transcription unit of the largest subunit of Pol II, Rpb1, consists of multiple exons and introns. A full-length cDNA of *Drosophila* Rpb1 has not been isolated nor has the Rpb1 gene endongenously tagged with eGFP intron using the FlyTrap screen. Therefore, we had three options, 1) to isolate a full-length cDNA of Rpb1, 2) to clone a full-length cDNA of Rpb1 by PCR amplifying the individual exons, or 3) to use homologous recombination to endogenously tag Rpb1 with eGFP.

Homologous recombination provides multiple benefits unavailable with the other two techniques including the expression of Rpb1 using it endogenous promoter and 100% expression of the eGFP-tagged factor. There are two methods for homologous recombination Ends In and Ends Out, which differ based on the position of double strand break position and final product. Ends In homologous recombination breaks the DNA within the homologous sequence and produces a duplication of the homologous sequence, while Ends Out homologous recombination makes a double stranded break outside of the homologous region, resulting in the replacement, not duplication, of the homologous sequence.

Because of the issue with gene duplication, we decided to used Ends Out homologous recombination and generated a homologous recombination competent plasmid based on the pP{whiteOut2} plasmid from the Sekelsky Lab [191]. This plasmid contains the necessary FRT recombination sites and I-SceI restriction sites needed for proper excision of homologous DNA and recombination events, p-element recombination sites and a *mini-white* gene for screening for p-element integration events. Between

the I-SceI sites, we added 3 kb homologous sequence to the 3' end of the gene, eGFP sequence (in the proper frame) and three kb homologous sequence to the downstream sequences using the primers listed in Table A.2. Notably, our homologous recombination competent Rpb1-eGFP vector contained an 80 bp insert after the eGFP stop codon before the down stream DNA element, but because the insert occurs after the stop codons, we do not believe it should have a large effect on the protein expression.

The final vector containing the 3' end of Rpb1, eGFP and the downstream DNA (pRpb1-eGFP) was injected into w^{1118} flies and then balanced by Best Gene Inc. To induce homologous recombination, we crossed a 2^{nd} chromosome insertion of the pRpb1-eGFP to a fly line carrying heat shock inducible Flippase (Flp) and I-SceI endonuclease (*ry*; 70-Flp v^{+23}; 70-I-SceI v^{4a} / Tm3) and heat shocked the F1 progeny twice on days 3 and 5 for an hour each at 36.5°C. F1 females were then crossed to w^{1118} males. 16–20 hour staged embryos were screened for eGFP expression using a 10x objective on wide-field epi-fluorescence microscope. However, no positive transformants were isolated, presumably because the background autofluorescence of the embryos were too high, and the positive control for GFP embryos (eGFP-Rpb3 x mTubulin) could not be distinguished from wild-type embryos, suggesting the screening protocol was flawed. Any future attempts at homologous recombination should include a detectable marker such as y^{+}. However, because the homologous recombination of eGFP onto Rpb1 failed, we plan to transgenically express a FP-tagged α-Amanitin resistant version of Rpb1. Because the inhibition of Rpb1 with α-Amanitin causes the specific degradation of Rpb1, not the α-Amanitin resistant form of Rpb1 [153], we can then increase the ratio of FP-tagged Pol II to un-tagged by treating the salivary glands with α-Amanitin, increasing the probability of observing a FRET interaction.

BIBLIOGRAPHY

[1] D. A. Agard and J. W. Sedat. Three-dimensional architecture of a polytene nucleus. *Nature*, 302(5910):676681, 1983.

[2] F. R. Althaus, L. Höfferer, H. E. Kleczkowska, M. Malanga, H. Naegeli, P. L. Panzeter, and C. A. Realini. Histone shuttling by poly ADP-ribosylation. *Mol. Cell. Biochem.*, 138(1-2):53–59, 1994.

[3] F. F. Andersen, T. Ø . Tange, T. Sinnathamby, J. R. Olesen, K. E. Andersen, O. Westergaard, J. Kjems, and B. R. Knudsen. The RNA splicing factor ASF/SF2 inhibits human topoisomerase I mediated DNA relaxation. *Journal of Molecular Biology*, 322(4):677–686, 2002.

[4] E. D. Andrulis, E. Guzmán, P. Doring, J. Werner, and J. T. Lis. High-resolution localization of Drosophila Spt5 and Spt6 at heat shock genes in vivo: roles in promoter proximal pausing and transcription elongation. *Genes Dev.*, 14(20):2635–2649, 2000.

[5] E. D. Andrulis, J. Werner, A. Nazarian, H. Erdjument-Bromage, P. Tempst, and J. T. Lis. The RNA processing exosome is linked to elongating RNA polymerase II in Drosophila. *Nature*, 420(6917):837–841, 2002.

[6] N. Aoyagi and D. A. Wassarman. Genes encoding Drosophila melanogaster RNA polymerase II general transcription factors: diversity in TFIIA and TFIID components contributes to gene-specific transcriptional regulation. *J. Cell Biol.*, 150(2):F45–50, 2000.

[7] B. Ardehali, A. Mei, K. L. Zobeck, M. Caron, J. T. Lis, and T. Kusch. The Drosophila Set1 complex regulates global histone H3 lysine 4 trimethylation and associates with transcriptionally active loci. in preparation.

[8] M. B. Ardehali and J. T. Lis. Tracking rates of transcription and splicing in vivo. *Nat. Struct. Mol. Biol.*, 16(11):1123–1124, 2009.

[9] M. B. Ardehali, J. Yao, K. Adelman, N. J. Fuda, S. J. Petesch, W. W. Webb, and J. T. Lis. DNA cloning using in vitro site-specific recombination. *Genome Res.*, 10(11):1788–1795, 2009.

[10] M. B. M. Ardehali. *Utilization of Drosophila Hsp70 Gene for Identification of Genuine Pol II Elongation Factors: Identification of Spt6 as a Factor that En-*

hances the Elongation Rate of Pol II in vivo. PhD thesis, Cornell University, 2010.

[11] K. J. Armache, H. Kettenberger, and P. Cramer. Architecture of initiation-competent 12-subunit RNA polymerase II. *Proc. Natl. Acad. Sci. U. S. A.*, 100(12):6964–6968, 2003.

[12] M. A. Balamotis, M. A. Pennella, J. L. Stevens, B. Wasylyk, A. S. Belmont, and A. J. Berk. Complexity in transcription control at the activation domain-mediator interface. *Sci. Signal.*, 2(69):ra20, 2009.

[13] A. Barberis and M. Petrascheck. Transcription Activation in Eukaryotic Cells. In *Encyclopedia of Life Sciences*. John Wiley & Sons, Ltd, Chichester, 2003.

[14] M. Barboric, T. Lenasi, H. Chen, E. B. Johansen, S. Guo, and B. M. Peterlin. 7SK snRNP/P-TEFb couples transcription elongation with alternative splicing and is essential for vertebrate development. *Proceedings of the National Academy of Sciences of the United States of America*, 106(19):7798–7803, 2009.

[15] A. Barski, S. Cuddapah, K. Cui, T. Y. Roh, D. E. Schones, Z. Wang, G. Wei, I. Chepelev, and K. Zhao. High-resolution profiling of histone methylations in the human genome. *Cell*, 129(4):823–837, 2007.

[16] M. Becker, C. Baumann, S. John, D. A. Walker, M. Vigneron, J. G. McNally, and G. L. Hager. Dynamic behavior of transcription factors on a natural promoter in living cells. *EMBO Rep.*, 3(12):1188–1194, 2002.

[17] W. Beermann. Chromomeres and genes. *Results Probl. Cell Differ.*, 4:1–33, 1972.

[18] C. Beisel, A. Imhof, J. Greene, E. Kremmer, and F. Sauer. Histone methylation by the Drosophila epigenetic transcriptional regulator Ash1. *Nature*, 419(6909):857–862, 2002.

[19] S. L. Berger and M. Meselson. Production and cleavage of Drosophila hsp70 transcripts extending beyond the polyadenylation site. *Nucleic Acids Res.*, 22(15):3218–3225, 1994.

[20] S. R. Bhaumik, T. Raha, D. P. Aiello, and M. R. Green. In vivo target of a transcriptional activator revealed by fluorescence resonance energy transfer. *Genes Dev.*, 18(3):333–343, 2004.

[21] H. Boeger, D. A. Bushnell, R. Davis, J. Griesenbeck, Y. Lorch, J. S. Strattan,

K. D. Westover, and R. D. Kornberg. Structural basis of eukaryotic gene transcription. *FEBS Lett.*, 579(4):899–903, 2005.

[22] A. K. Boehm, A. Saunders, J. Werner, and J. T. Lis. Transcription factor and polymerase recruitment, modification, and movement on dhsp70 in vivo in the minutes following heat shock. *Mol. Cell. Biol.*, 23(21):7628–7637, 2003.

[23] A. N. Boettiger and M. Levine. Synchronous and stochastic patterns of gene activation in the Drosophila embryo. *Science*, 325(5939):471–473, 2009.

[24] S. Boireau, P. Maiuri, E. Basyuk, M. de la Mata, A. Knezevich, B. Pradet-Balade, V. Backer, A. Kornblihtt, A. Marcello, and E. Bertrand. The transcriptional cycle of HIV-1 in real-time and live cells. *J. Cell Biol.*, 179(2):291–304, 2007.

[25] A. Bortvin and F. Winston. Evidence that Spt6p controls chromatin structure by a direct interaction with histones. *Science*, 272(5267):1473–1476, 1996.

[26] C. B. Bridges. SALIVARY CHROMOSOME MAPS: With a Key to the Banding of the Chromosomes of Drosophila Melanogaster. *J. Hered.*, 26(2):60–64, 1935.

[27] M. Buszczak, S. Paterno, D. Lighthouse, J. Bachman, J. Planck, S. Owen, A. D. Skora, T. G. Nystul, B. Ohlstein, A. Allen, J. E. Wilhelm, T. D. Murphy, R. W. Levis, E. Matunis, N. Srivali, R. A. Hoskins, and A. C. Spradling. The carnegie protein trap library: a versatile tool for Drosophila developmental studies. *Genetics*, 175(3):1505–1531, 2007.

[28] K. N. Byrd and A. Shearn. ASH1, a Drosophila trithorax group protein, is required for methylation of lysine 4 residues on histone H3. *Proc. Natl. Acad. Sci. U. S. A.*, 100(20):11535–11540, 2003.

[29] L. Cai and J. D. Zhu. The tumor-selective over-expression of the human Hsp70 gene is attributed to the aberrant controls at both initiation and elongation levels of transcription. *Cell Res.*, 13(2):93–109, Apr 2003.

[30] D. R. Carter, C. Eskiw, and P. R. Cook. Transcription factories. *Biochem. Soc. Trans.*, 36(Pt 4):585–589, 2008.

[31] S. M. Carty. Hyperphosphorylated C-terminal Repeat Domain-associating Proteins in the Nuclear Proteome Link Transcription to DNA/Chromatin Modification and RNA Processing. *Mol. Cell. Proteomics*, 1(8):598–610, 2002.

[32] M. Chalfie, Y. Tu, G. Euskirchen, W. W. Ward, and D. C. Prasher. Green fluorescent protein as a marker for gene expression. *Science*, 263(5148):802–805, 1994.

[33] S. H. Chao and D. H. Price. Flavopiridol inactivates P-TEFb and blocks most RNA polymerase II transcription in vivo. *J. Biol. Chem.*, 276(34):31793–31799, 2001.

[34] D. Chen, C. S. Hinkley, R. W. Henry, and S. Huang. TBP dynamics in living human cells: constitutive association of TBP with mitotic chromosomes. *Mol. Biol. Cell*, 13(1):276–284, 2002.

[35] M. O. Christensen, H. U. Barthelmes, S. Feineis, B. R. Knudsen, A. H. Andersen, F. Boege, and C. Mielke. Changes in mobility account for camptothecin-induced subnuclear relocation of topoisomerase I. *J. Biol. Chem.*, 277(18):15661–15665, 2002.

[36] M. O. Christensen, M. K. Larsen, H. U. Barthelmes, R. Hock, C. L. Andersen, E. Kjeldsen, B. R. Knudsen, O. Westergaard, F. Boege, and C. Mielke. Dynamics of human DNA topoisomerases IIalpha and IIbeta in living cells. *J. Cell Biol.*, 157(1):31–44, 2002.

[37] D. M. Chudakov, M. V. Matz, S. Lukyanov, and K. A. Lukyanov. Fluorescent proteins and their applications in imaging living cells and tissues. *Physiol. Rev.*, 90(3):1103–1163, 2010.

[38] J. A. Conchello and J. W. Lichtman. Optical sectioning microscopy. *J. Cell Biol.*, 2(12):920–931, 2005.

[39] L. J. Core, J. J. Waterfall, and J. T. Lis. Nascent RNA sequencing reveals widespread pausing and divergent initiation at human promoters. *Science*, 322(5909):1845–1848, 2008.

[40] P. Cramer, D. A. Bushnell, J. Fu, A. L. Gnatt, B. Maier-Davis, N. E. Thompson, R. R. Burgess, A. M. Edwards, P. R. David, and R. D. Kornberg. Architecture of RNA polymerase II and implications for the transcription mechanism. *Science*, 288(5466):640–649, 2000.

[41] P. Cramer, D. A. Bushnell, and R. D. Kornberg. Structural basis of transcription: RNA polymerase II at 2. 8 angstrom resolution. *Science*, 292(5523):1863–1876, 2001.

[42] A. B. Cubitt, R. Heim, S. R. Adams, A. E. Boyd, L. A. Gross, and R. Y. Tsien. Understanding, improving and using green fluorescent proteins. *Trends Biochem. Sci.*, 20(11):448–455, 1995.

[43] C. Dai, L. Whitesell, A. B. Rogers, and S. Lindquist. Heat shock factor 1 is a powerful multifaceted modifier of carcinogenesis. *Cell*, 130(6):1005–1018, 2007.

[44] D. D'Amours, S. Desnoyers, I. D'Silva, and G. G. Poirier. Poly(ADP-ribosyl)ation reactions in the regulation of nuclear functions. *Biochem. J.*, 342(2):249–268, 1999.

[45] X. Darzacq, Y. Shav-Tal, V. de Turris, Y. Brody, S. M. Shenoy, R. D. Phair, and R. H. Singer. In vivo dynamics of RNA polymerase II transcription. *Nat. Struct. Mol. Biol.*, 14(9):796–806, 2007.

[46] L. Davidovic, M. Vodenicharov, E. B. Affar, and G. G. Poirier. Importance of poly(ADP-ribose) glycohydrolase in the control of poly(ADP-ribose) metabolism. *Exp. Cell Res.*, 268(1):7–13, 2001.

[47] P. de Graaf, F. Mousson, B. Geverts, E. Scheer, L. Tora, A. B. Houtsmuller, and H. T. Timmers. Chromatin interaction of TATA-binding protein is dynamically regulated in human cells. *J. Cell Sci.*, 123(Pt 15):2663–2671, 2010.

[48] W. Denk, J. H. Strickler, and W. W. Webb. Two-photon laser scanning fluorescence microscopy. *Science*, 248(4951):73–76, Apr 1990.

[49] A. Dey, S. H. Chao, and D. P. Lane. HEXIM1 and the control of transcription elongation: from cancer and inflammation to AIDS and cardiac hypertrophy. *Cell Cycle*, 6(15):1856–1863, 2007.

[50] A. Dey, F. Chitsaz, A. Abbasi, T. Misteli, and K. Ozato. The double bromodomain protein Brd4 binds to acetylated chromatin during interphase and mitosis. *Proc. Natl. Acad. Sci. U. S. A.*, 100(15):8758–8763, 2003.

[51] A. Dey, A. Nishiyama, T. Karpova, J. McNally, and K. Ozato. Brd4 marks select genes on mitotic chromatin and directs postmitotic transcription. *Mol. Biol. Cell*, 20(23):4899–4909, 2009.

[52] J. B. Duffy. GAL4 system in Drosophila: a fly geneticist's Swiss army knife. *Genesis*, 34(1-2):1–15, 2002.

[53] M. Dundr, U. Hoffmann-Rohrer, Q. Hu, I. Grummt, L. I. Rothblum, R. D. Phair,

and T. Misteli. A kinetic framework for a mammalian RNA polymerase in vivo. *Science*, 298(5598):1623–1626, 2002.

[54] M. Durand-Dubief, J. Persson, U. Norman, E. Hartsuiker, and K. Ekwall. Topoisomerase I regulates open chromatin and controls gene expression in vivo. *EMBO J.*, 29(13):2126–2134, 2010.

[55] J. C. Eissenberg and A. Shilatifard. Histone H3 lysine 4 (H3K4) methylation in development and differentiation. *Dev. Biol.*, 339(2):240–249, 2010.

[56] M. Eitokua, L. Satoa, T. Sendab, and M. Horikoshia. Histone chaperones: 30 years from isolation to elucidation of the mechanisms of nucleosome assembly and disassembly. *Cell. Mol. Life Sci.*, 65:414–444, 2008.

[57] E. L. Elson, J. Schlessinger, D. E. Koppel, D. Axelrod, and W. W. Webb. Measurement of lateral transport on cell surfaces. *Prog. Clin. Biol. Res.*, 9:137–147, 1976.

[58] J. Elvenes, E. Sjøttem, T. Holm, G. Bjørkøy, and T. Johansen. Pax6 localizes to chromatin-rich territories and displays a slow nuclear mobility altered by disease mutations. *Cell. Mol. Life Sci.*, 2010.

[59] P. J. Farnham. Insights from genomic profiling of transcription factors. *Nat. Rev. Genet.*, 10(9):605–616, 2009.

[60] G. Ficz, R. Heintzmann, and D. J. Arndt-Jovin. Polycomb group protein complexes exchange rapidly in living Drosophila. *Development*, 132(17):3963–3976, 2005.

[61] G. Fleischmann, G. Pflugfelder, E. K. Steiner, K. Javaherian, G. C. Howard, J. C. Wang, and S. C. Elgin. Drosophila DNA topoisomerase I is associated with transcriptionally active regions of the genome. *Proc. Natl. Acad. Sci. U. S. A.*, 81(22):6958–6962, 1984.

[62] M. Fritsch and C. Wu. Phosphorylation of Drosophila heat shock transcription factor. *Cell stress chaperones*, 4(2):102–117, 1999.

[63] N. J. Fuda, M. B. Ardehali, and J. T. Lis. Defining mechanisms that regulate RNA polymerase II transcription in vivo. *Nature*, 461(7261):186–192, 2009.

[64] D. A. Gilchrist, S. Nechaev, C. Lee, S. K. Ghosh, J. B. Collins, L. Li, D. S. Gilmour, and K. Adelman. NELF-mediated stalling of Pol II can enhance gene

expression by blocking promoter-proximal nucleosome assembly. *Genes Dev.*, 22(14):1921–1933, 2008.

[65] D. S. Gilmour. Promoter proximal pausing on genes in metazoans. *Chromosoma*, 118(1):1–10, 2009.

[66] D. S. Gilmour and J. T. Lis. In vivo interactions of RNA polymerase II with genes of Drosophila melanogaster. *Molecular and cellular biology*, 5(8):2009–2018, 1985.

[67] D. S. Gilmour and J. T. Lis. RNA polymerase II interacts with the promoter region of the noninduced hsp70 gene in Drosophila melanogaster cells. *Mol. Cell. Biol.*, 6(11):3984–3989, 1986.

[68] A. L. Gnatt, P. Cramer, J. Fu, D. A. Bushnell, and R. D. Kornberg. Structural basis of transcription: an RNA polymerase II elongation complex at 3. 3 A resolution. *Science*, 292(5523):1876–1882, 2001.

[69] W. J. Gong and K. G. Golic. Loss of Hsp70 in Drosophila is pleiotropic, with effects on thermotolerance, recovery from heat shock and neurodegeneration. *Genetics*, 172(1):275–286, 2006.

[70] E. Gratton, N. P. Barry, S. Beretta, and A. Celli. Multiphoton fluorescence microscopy. *Methods*, 25(1):103–110, 2001.

[71] J. Greenblatt. RNA polymerase II holoenzyme and transcriptional regulation. *Curr. Opin. Cell Biol.*, 9(3):310–319, 1997.

[72] E. R. Griffis, N. Altan, J. Lippincott-Schwartz, and M. A. Powers. Nup98 is a mobile nucleoporin with transcription-dependent dynamics. *Mol. Biol. Cell*, 13(4):1282–1297, 2002.

[73] M. J. Guertin and J. T. Lis. Chromatin landscape dictates HSF binding to target DNA elements. *PLoS Genet.*, 6(9):e1001114, 2010.

[74] M. J. Guertin, S. J. Petesch, K. L. Zobeck, I. Min, and J. T. Lis. Drosophila Heat Shock System as a General Model to Investigate Transcriptional Regulation. *Cold Spring Harbor Symp. Quant. Biol.*, in press.

[75] B. Guillemette, A. R. Bataille, N. Gévry, M. Adam, M. Blanchette, F. Robert, and L. Gaudreau. Variant histone H2A.Z is globally localized to the promoters of in-

active yeast genes and regulates nucleosome positioning. *PLoS Biol.*, 3(12):e384, 2005.

[76] R. S. Gupta and G. B. Golding. Evolution of HSP70 gene and its implications regarding relationships between archaebacteria, eubacteria, and eukaryotes. *Journal of Molecular Evolution*, 37(6):573–582, 1993.

[77] G. L. Hager, J. G. McNally, and T. Misteli. Transcription dynamics. *Mol. Cell*, 35(6):741–753, 2009.

[78] J. L. Hartley, G. F. Temple, and M. A. Brasch. Imaging transcription dynamics at endogenous genes in living Drosophila tissues. *Methods*, 45(3):233–241, 2000.

[79] R. Heim and R. Y. Tsien. Engineering green fluorescent protein for improved brightness, longer wavelengths and fluorescence resonance energy transfer. *Curr. Biol.*, 6(2):178–182, 1996.

[80] R. Heintzmann and G. Ficz. Breaking the resolution limit in light microscopy. *Briefings Funct. Genomics Proteomics*, 5(4):289–301, 2006.

[81] J. P. Hendrick and F. U. Hartl. Molecular chaperone functions of heat-shock proteins. *Annual Review of Biochemistry*, 62:349–384, 1993.

[82] P. Hinow, C. E. Rogers, C. E. Barbieri, J. A. Pietenpol, A. K. Kenworthy, and E. DiBenedetto. The DNA binding activity of p53 displays reaction-diffusion kinetics. *Biophys. J.*, 91(1):330–342, 2006.

[83] C. K. Ho and S. Shuman. Distinct roles for CTD Ser-2 and Ser-5 phosphorylation in the recruitment and allosteric activation of mammalian mRNA capping enzyme. *Mol. Cell*, 3(3):405–411, 1999.

[84] M. Hochstrasser, D. Mathog, Y. Gruenbaum, H. Saumweber, and J. W. Sedat. Spatial organization of chromosomes in the salivary gland nuclei of Drosophila melanogaster. *J. Cell Biol.*, 102(1):112–123, 1986.

[85] M. Hochstrasser and J. W. Sedat. Three-dimensional organization of Drosophila melanogaster interphase nuclei. II. Chromosome spatial organization and gene regulation. . *J. Cell Biol.*, 104(6):14711483, 1987.

[86] A. B. Houtsmuller. Fluorescence recovery after photobleaching: application to nuclear proteins. *Adv. Biochem. Eng. /Biotechnol.*, 95:177–199, 2005.

[87] F. J. Iborra, A. Pombo, J. McManus, D. A. Jackson, and P. R. Cook. The topology of transcription by immobilized polymerases. *Exp. Cell Res.*, 229(2):167–173, 1996.

[88] A. Imhof. Histone modifications: an assembly line for active chromatin? *Curr. Biol.*, 13(1):R22–4, 2003.

[89] M. O. Imhof, P. Chatellard, and N. Mermod. Comparative study and identification of potent eukaryotic transcriptional repressors in gene switch systems. *Journal of Biotechnology*, 97(3):275–285, 2002.

[90] Invitrogen. Gateway® Technology with Clonase II. Invitrogen Product Manual, Catalog nos. 12535-029 and 12535-037, May 2009.

[91] M. Jäättelä. Over-expression of hsp70 confers tumorigenicity to mouse fibrosarcoma cells. *Int. J. Cancer*, 60(5):689–693, 1995.

[92] M. Jamrich, A. L. Greenleaf, and E. K. Bautz. Localization of RNA polymerase in polytene chromosomes of Drosophila melanogaster. *Proc. Natl. Acad. Sci. U. S. A.*, 74(5):2079–2083, May 1977.

[93] P. Jedlicka, M. A. Mortin, and C. Wu. Multiple functions of Drosophila heat shock transcription factor in vivo. *EMBO J.*, 16(9):2452–2462, 1997.

[94] T. A. Johnson, C. Elbi, B. S. Parekh, G. L. Hager, and S. John. Chromatin remodeling complexes interact dynamically with a glucocorticoid receptor-regulated promoter. *Mol. Biol. Cell*, 19(8):3308–3322, 2008.

[95] T. Juven-Gershon and J. T. Kadonaga. Regulation of gene expression via the core promoter and the basal transcriptional machinery. *Dev. Biol.*, 339(2):225–229, 2010.

[96] C. D. Kaplan, M. J. Holland, and F. Winston. Interaction between transcription elongation factors and mRNA 3'-end formation at the Saccharomyces cerevisiae GAL10-GAL7 locus. *J. Biol. Chem.*, 280(2):913–922, 2005.

[97] C. D. Kaplan, L. Laprade, and F. Winston. Transcription elongation factors repress transcription initiation from cryptic sites. *Science*, 301(5636):1096–1099, 2003.

[98] C. D. Kaplan, J. R. Morris, C. Wu, and F. Winston. Spt5 and spt6 are associated

with active transcription and have characteristics of general elongation factors in D. melanogaster. *Genes Dev.*, 14(20):2623–2634, 2000.

[99] T. S. Karpova, T. Y. Chen, B. L. Sprague, and J. G. McNally. Dynamic interactions of a transcription factor with DNA are accelerated by a chromatin remodeller. *EMBO reports*, 5(11):1064–1070, 2004.

[100] T. H. Kim, L. O. Barrera, M. Zheng, C. Qu, M. A. Singer, T. A. Richmond, Y. Wu, R. D. Green, and B. Ren. A high-resolution map of active promoters in the human genome. *Nature*, 436(7052):876–880, 2005.

[101] H. Kimura and P. R. Cook. Kinetics of core histones in living human cells: little exchange of H3 and H4 and some rapid exchange of H2B. *J. Cell Biol.*, 153(7):1341–1353, 2001.

[102] H. Kimura, K. Sugaya, and P. R. Cook. The transcription cycle of RNA polymerase II in living cells. *J. Cell Biol.*, 159(5):777–782, 2002.

[103] T. I. Klokk, P. Kurys, C. Elbi, A. K. Nagaich, A. Hendarwanto, T. Slagsvold, C. Y. Chang, G. L. Hager, and F. Saatcioglu. Ligand-specific dynamics of the androgen receptor at its response element in living cells. *Mol. Cell. Biol.*, 27(5):1823–1843, 2007.

[104] P. Komarnitsky, E. J. Cho, and S. Buratowski. Different phosphorylated forms of RNA polymerase II and associated mRNA processing factors during transcription. *Genes Dev.*, 14(19):2452–2460, 2000.

[105] T. Kouzarides. Chromatin modifications and their function. *Cell*, 128(4):693–705, 2007.

[106] W. L. Kraus and J. T. Lis. PARP goes transcription. *Cell*, 113(6):677–683, 2003.

[107] R. Krishnakumar, M. J. Gamble, K. M. Frizzell, J. G. Berrocal, M. Kininis, and W. L. Kraus. Reciprocal binding of PARP-1 and histone H1 at promoters specifies transcriptional outcomes. *Science*, 319(5864):819–821, 2008.

[108] R. Krishnakumar and W. L. Kraus. The PARP side of the nucleus: molecular actions, physiological outcomes, and clinical targets. *Mol. Cell*, 39(1):8–24, 2010.

[109] P. E. Kroeger and T. C. Rowe. Analysis of topoisomerase I and II cleavage sites on the Drosophila actin and Hsp70 heat shock genes. *Biochemistry*, 31(9):2492–2501, Mar 10 1992.

[110] N. J. Krogan, M. Kim, S. H. Ahn, G. Zhong, M. S. Kobor, G. Cagney, A. Emili, A. Shilatifard, S. Buratowski, and J. F. Greenblatt. RNA polymerase II elongation factors of Saccharomyces cerevisiae: a targeted proteomics approach. *Mol. Cell. Biol.*, 22(20):6979–6992, 2002.

[111] M. J. Kruhlak, M. A. Lever, W. Fischle, E. Verdin, D. P. Bazett-Jones, and M. J. Hendzel. Reduced mobility of the alternate splicing factor (ASF) through the nucleoplasm and steady state speckle compartments. *J. Cell Biol.*, 150(1):41–51, 2000.

[112] R. I. Kumaran and D. L. Spector. A genetic locus targeted to the nuclear periphery in living cells maintains its transcriptional competence. *J. Cell Biol.*, 180(1):51–65, 2008.

[113] P. D. Kurth, E. N. Moudrianakis, and M. Bustin. Histone localization in polytene chromosomes by immunofluorescence. *J. Cell Biol.*, 78(3):910–918, 1978.

[114] A. Landy. Dynamic, structural, and regulatory aspects of lambda site-specific recombination. *Annu. Rev. Biochem.*, 58:913–949, 1989.

[115] L. A. Lebedeva, E. N. Nabirochkina, M. M. Kurshakova, F. Robert, A. N. Krasnov, M. B. Evgen'ev, J. T. Kadonaga, S. G. Georgieva, and L. Tora. Occupancy of the Drosophila hsp70 promoter by a subset of basal transcription factors diminishes upon transcriptional activation. *Proc. Natl. Acad. Sci. U. S. A.*, 102(50):18087–18092, 2005.

[116] C. Lee, X. Li, A. Hechmer, M. Eisen, M. D. Biggin, B. J. Venters, C. Jiang, J. Li, B. F. Pugh, and D. S. Gilmour. NELF and GAGA factor are linked to promoter-proximal pausing at many genes in Drosophila. *Molecular and cellular biology*, 28(10):3290–3300, 2008.

[117] M. A. Lever, J. P. Th'ng, X. Sun, and M. J. Hendzel. Rapid exchange of histone H1. 1 on chromatin in living human cells. *Nature*, 408(6814):873–876, 2000.

[118] B. Li, M. Carey, and J. L. Workman. The role of chromatin during transcription. *Cell*, 128(4):707–719, 2007.

[119] Q. Li, J. J. Cooper, G. H. Altwerger, M. D. Feldkamp, M. A. Shea, and D. H. Price. HEXIM1 is a promiscuous double-stranded RNA-binding protein and interacts with RNAs in addition to 7SK in cultured cells. *Nucleic Acids Res.*, 35(8):2503–2512, 2007.

[120] R. P. Lifton, M. L. Goldberg, R. W. Karp, and D. S. Hogness. The organization of the histone genes in Drosophila melanogaster: functional and evolutionary implications. *Cold Spring Harbor Symp. Quant. Biol*, 42(2):1047–1051, 1978.

[121] S. Lindquist. The heat-shock response. *Annu. Rev. Biochem.*, 55:1151–1191, 1986.

[122] J. R. Lipford, G. T. Smith, Y. Chi, and R. J. Deshaies. A putative stimulatory role for activator turnover in gene expression. *Nature*, 438(7064):113–116, 2005.

[123] J. Lippincott-Schwartz and G. H. Patterson. Development and use of fluorescent protein markers in living cells. *Science*, 300(5616):87–91, 2003.

[124] J. Lis and C. Wu. Protein traffic on the heat shock promoter: parking, stalling, and trucking along. *Cell*, 74(1):1–4, 1993.

[125] J. T. Lis. Promoter-associated pausing in promoter architecture and postinitiation transcriptional regulation. *Cold Spring Harbor Symp. Quant. Biol.*, 63:347–356, 1998.

[126] J. T. Lis. Imaging Drosophila gene activation and polymerase pausing in vivo. *Nature*, 450(7167):198–202, 2007.

[127] J. T. Lis, P. Mason, J. Peng, D. H. Price, and J. Werner. P-TEFb kinase recruitment and function at heat shock loci. *Genes Dev.*, 14(7):792–803, Apr 2000.

[128] Y. Lorch, J. W. LaPointe, and R. D. Kornberg. Nucleosomes inhibit the initiation of transcription but allow chain elongation with the displacement of histones. *Cell*, 49(2):203–210, 1987.

[129] W. Luo and D. Bentley. A ribonucleolytic rat torpedoes RNA polymerase II. *Cell*, 119(7):911–914, 2004.

[130] K. R. Madden, L. Stewart, and J. J. Champoux. Preferential binding of human topoisomerase I to superhelical DNA. *EMBO J.*, 14(21):5399–5409, 1995.

[131] T. Maniatis and R. Reed. An extensive network of coupling among gene expression machines. *Nature*, 416(6880):499–506, 2002.

[132] N. F. Marshall, J. Peng, Z. Xie, and D. H. Price. Control of RNA polymerase II elongation potential by a novel carboxyl-terminal domain kinase. *J. Biol. Chem.*, 271(43):27176–27183, 1996.

[133] P. Maruvada, C. T. Baumann, G. L. Hager, and P. M. Yen. Dynamic shuttling and intranuclear mobility of nuclear hormone receptors. *J. Biol. Chem.*, 278(14):12425–12432, 2003.

[134] G. Mathis and F. R. Althaus. Release of core DNA from nucleosomal core particles following (ADP-ribose)n-modification in vitro. *Biochem. Biophys. Res. Commun.*, 143(3):1049–1054, 1987.

[135] D. Mathog, M. Hochstrasser, Y. Gruenbaum, H. Saumweber, and J. Sedat. Characteristic folding pattern of polytene chromosomes in Drosophila salivary gland nuclei. *Nature*, 308(5958):414421, 1984.

[136] J. G. McNally, W. G. Muller, D. Walker, R. Wolford, and G. L. Hager. The glucocorticoid receptor: rapid exchange with regulatory sites in living cells. *Science*, 287(5456):1262–1265, 2000.

[137] S. H. Meijsing, C. Elbi, H. F. Luecke, G. L. Hager, and K. R. Yamamoto. The ligand binding domain controls glucocorticoid receptor dynamics independent of ligand release. *Mol. Cell. Biol.*, 27(7):2442–2451, 2007.

[138] A. Meinhart, T. Kamenski, S. Hoeppner, S. Baumli, and P. Cramer. A structural perspective of CTD function. *Genes Dev.*, 19(12):1401–1415, 2005.

[139] T. Misteli, J. F. Cáceres, and D. L. Spector. The dynamics of a pre-mRNA splicing factor in living cells. *Nature*, 387(6632):523–527, 1997.

[140] T. Misteli, A. Gunjan, R. Hock, M. Bustin, and D. T. Brown. Dynamic binding of histone H1 to chromatin in living cells. *Nature*, 408(6814):877–881, 2000.

[141] T. Miyamoto, T. Kakizawa, and K. Hashizume. Inhibition of nuclear receptor signalling by poly(ADP-ribose) polymerase. *Mol. Cell. Biol.*, 19(4):2644–2649, 1999.

[142] D. Molle, P. Maiuri, S. Boireau, E. Bertrand, A. Knezevich, A. Marcello, and E. Basyuk. A real-time view of the TAR:Tat:P-TEFb complex at HIV-1 transcription sites. *Retrovirology*, 4:36–40, 2007.

[143] N. Mondal, Y. Zhang, Z. Jonsson, S. K. Dhar, M. Kannapiran, and J. D. Parvin. Elongation by RNA polymerase II on chromatin templates requires topoisomerase activity. *Nucleic Acids Res.*, 31(17):5016–5024, 2003.

[144] R. I. Morimoto. Cells in stress: transcriptional activation of heat shock genes. *Science*, 259(5100):1409–1410, 1993.

[145] X. Morin, R. Daneman, M. Zavortink, and W. Chia. A protein trap strategy to detect GFP-tagged proteins expressed from their endogenous loci in *Drosophila*. *Proc. Natl. Acad. Sci. U. S. A.*, 98(26):15050–15055, 2001.

[146] F. Mueller, P. Wach, and J. G. McNally. Evidence for a common mode of transcription factor interaction with chromatin as revealed by improved quantitative fluorescence recovery after photobleaching. *Biophys. J.*, 94(8):3323–39, 2008.

[147] M. T. Muller, M. P. Pfund, V. B. Mehta, and D. K. Trask. Eukaryotic type I topoisomerase is enriched in the nucleolus and catalytically active on ribosomal DNA. *EMBO J.*, 4(5):1237–1243, May 1985.

[148] T. D. Murphy. The Drosophila Gateway® Vector Collection. `http://www.ciwemb.edu/labs/murphy/Gateway%20vectors.html`, 2003.

[149] G. W. Muse, D. A. Gilchrist, S. Nechaev, R. Shah, J. S. Parker, S. F. Grissom, J. Zeitlinger, and K. Adelman. RNA polymerase is poised for activation across the genome. *Nat. Genet.*, 39(12):1507–1511, 2007.

[150] G. A. Nacheva, D. Y. Guschin, O. V. Preobrazhenskaya, V. L. Karpov, K. K. Ebralidse, and A. D. Mirzabekov. Change in the pattern of histone binding to DNA upon transcriptional activation. *Cell*, 58(1):27–36, 1989.

[151] G. J. Narlikar, H. Y. Fan, and R. E. Kingston. Cooperation between complexes that regulate chromatin structure and transcription. *Cell*, 108(4):475–487, 2002.

[152] A. W. Nguyen, X. You, A. M. Jabaiah, and P. S. Daughterty. Fluorescent Protein FRET Applications Protein Engineering, Inracellular Sensing and Interaction Screening. In *Rev. Fluoresc. 2008*, pages 321–335. Springer, 2010.

[153] V. T. Nguyen, F. Giannoni, M. F. Dubois, S. J. Seo, M. Vigneron, C. Kedinger, and O. Bensaude. In vivo degradation of RNA polymerase II largest subunit triggered by alpha-amanitin. *Nucleic Acids Res.*, 24(15):2924–2929, 1996.

[154] Z. Ni, A. Saunders, N. J. Fuda, J. Yao, J. R. Suarez, W. W. Webb, and J. T. Lis. P-TEFb is critical for the maturation of RNA polymerase II into productive elongation in vivo. *Mol. Cell. Biol.*, 28(3):1161–1170, 2008.

[155] Z. Ni, B. E. Schwartz, J. Werner, J. R. Suarez, and J. T. Lis. Coordination of

transcription, RNA processing, and surveillance by P-TEFb kinase on heat shock genes. *Mol. Cell*, 13(1):55–65, 2004.

[156] T. O'Brien and J. T. Lis. Rapid changes in Drosophila transcription after an instantaneous heat shock. *Mol. Cell. Biol.*, 13(6):3456–3463, 1993.

[157] G. Orphanides, W. H. Wu, W. S. Lane, M. Hampsey, and D. Reinberg. The chromatin-specific transcription elongation factor FACT comprises human SPT16 and SSRP1 proteins. *Nature*, 400(6741):284–288, 1999.

[158] C. S. Osborne, L. Chakalova, K. E. Brown, D. Carter, A. Horton, E. Debrand, B. Goyenechea, J. A. Mitchell, S. Lopes, W. Reik, and P. Fraser. Active genes dynamically colocalize to shared sites of ongoing transcription. *Nat. Genet.*, 36(10):1065–1071, 2004.

[159] C. S. Osborne, L. Chakalova, J. A. Mitchell, A. Horton, A. L. Wood, D. J. Bolland, A. E. Corcoran, and P. Fraser. Myc dynamically and preferentially relocates to a transcription factory occupied by Igh. *PLoS Biol.*, 5(8):e192, 2007.

[160] T. Owen-Hughes and J. L. Workman. Experimental analysis of chromatin function in transcription control. *Crit. Rev. Euk. Gene Exp.*, 4(4):403–441, 1994.

[161] J. Peng, N. F. Marshall, and D. H. Price. Identification of a Cyclin Subunit Required for the Function of Drosophila P-TEFb. *J. Biol. Chem.*, 273:13855–13860, May 1998.

[162] O. Perisic, H. Xiao, and J. T. Lis. Stable binding of Drosophila heat shock factor to head-to-head and tail-to-tail repeats of a conserved 5 bp recognition unit. *Cell*, 59(5):797–806, 1989.

[163] B. M. Peterlin and D. H. Price. Controlling the elongation phase of transcription with P-TEFb. *Mol. Cell*, 23(3):297–305, 2006.

[164] S. J. Petesch and J. T. Lis. Rapid, transcription-independent loss of nucleosomes over a large chromatin domain at Hsp70 loci. *Cell*, 134(1):74–84, 2008.

[165] R. D. Phair, P. Scaffidi, C. Elbi, J. Vecerová, A. Dey, K. Ozato, D. T. Brown, G. Hager, M. Bustin, and T. Misteli. Global nature of dynamic protein-chromatin interactions in vivo: three-dimensional genome scanning and dynamic interaction networks of chromatin proteins. *Mol. Cell. Biol.*, 24(14):6393–6402, 2004.

[166] H. P. Phatnani and A. L. Greenleaf. Phosphorylation and functions of the RNA polymerase II CTD. *Genes Dev.*, 20(21):2922–2936, 2006.

[167] H. P. Phatnani, J. C. Jones, and A. L. Greenleaf. Expanding the functional repertoire of CTD kinase I and RNA polymerase II: novel phosphoCTD-associating proteins in the yeast proteome. *Biochemistry*, 43(50):15702–15719, 2004.

[168] A. Pinnola, N. Naumova, M. Shah, and A. V. Tulin. Nucleosomal core histones mediate dynamic regulation of poly(ADP-ribose) polymerase 1 protein binding to chromatin and induction of its enzymatic activity. *J. Biol. Chem.*, 282(44):32511–32519, 2007.

[169] D. H. Price. P-TEFb, a cyclin-dependent kinase controlling elongation by RNA polymerase II. *Mol. Cell. Biol.*, 20(8):2629–2634, 2000.

[170] N. J. Proudfoot. How RNA polymerase II terminates transcription in higher eukaryotes. *Trends in biochemical sciences*, 14(3):105–110, 1989.

[171] B. A. Purnell, P. A. Emanuel, and D. S. Gilmour. TFIID sequence recognition of the initiator and sequences farther downstream in Drosophila class II genes. *Genes Dev.*, 8(7):830–842, 1994.

[172] S. K. Rabindran, R. I. Haroun, J. Clos, J. Wisniewski, and C. Wu. Regulation of heat shock factor trimer formation: role of a conserved leucine zipper. *Science*, 259(5092):230–234, 1993.

[173] W. S. Rasband, P. J. Magelhaes, and S. J. Ram. Image Processing with ImageJ. *Biophotonics International*, 11(7):36–42, 2004.

[174] E. B. Rasmussen and J. T. Lis. In vivo transcriptional pausing and cap formation on three Drosophila heat shock genes. *Proc. Natl. Acad. Sci. U. S. A.*, 90(17):7923–7927, 1993.

[175] G. V. Rayasam, C. Elbi, D. A. Walker, R. Wolford, T. M. Fletcher, D. P. Edwards, and G. L. Hager. Ligand-specific dynamics of the progesterone receptor in living cells and during chromatin remodeling in vitro. *Mol. Cell. Biol.*, 25(6):2406–2418, 2005.

[176] C. A. Realini and F. R. Althaus. Histone shuttling by poly(ADP-ribosylation). *J. Biol. Chem.*, 267(26):18858–18865, 1992.

[177] F. A. Ritossa. A new puffing pattern induced by temperature shock and DNP in Drosophila. *Experientia*, 18:571–573, 1962.

[178] C. C. Robinett, A. Straight, G. Li, C. Willhelm, G. Sudlow, A. Murray, and A. S. Belmont. In vivo localization of DNA sequences and visualization of large-scale chromatin organization using lac operator/repressor recognition. *J. Cell Biol.*, 135(6 Pt 2):1685–1700, 1996.

[179] R. G. Roeder. The role of general initiation factors in transcription by RNA polymerase II. *Trends Biochem. Sci.*, 21(9):327–335, 1996.

[180] F. Rossi, E. Labourier, T. Forné, G. Divita, J. Derancourt, J. F. Riou, E. Antoine, G. Cathala, C. Brunel, and J. Tazi. Specific phosphorylation of SR proteins by mammalian DNA topoisomerase I. *Nature*, 381(6577):80–82, 1996.

[181] A. E. Rougvie and J. T. Lis. The RNA polymerase II molecule at the 5' end of the uninduced hsp70 gene of D. melanogaster is transcriptionally engaged. *Cell*, 54(6):795–804, 1988.

[182] G. M. Rubin, L. Hong, P. Brokstein, M. Evans-Holm, E. Frise, M. Stapleton, and D. A. Harvey. A Drosophila complementary DNA resource. *Science*, 287(5461):2222–2224, 2000.

[183] A. J. Ruthenburg, C. D. Allis, and J. Wysocka. Methylation of lysine 4 on histone H3: intricacy of writing and reading a single epigenetic mark. *Mol. Cell*, 25(1):15–30, 2007.

[184] A. Saunders, L. J. Core, and J. T. Lis. Breaking barriers to transcription elongation. *Nat. Rev. Mol. Cell Biol.*, 7(8):557–567, 2006.

[185] A. Saunders, J. Werner, E. D. Andrulis, T. Nakayama, S. Hirose, D. Reinberg, and J. T. Lis. Tracking FACT and the RNA polymerase II elongation complex through chromatin in vivo. *Science*, 301(5636):1094–1096, 2003.

[186] M. J. Schaaf, L. J. Lewis-Tuffin, and J. A. Cidlowski. Ligand-selective targeting of the glucocorticoid receptor to nuclear subdomains is associated with decreased receptor mobility. *Mol. Endocrinol.*, 19(6):1501–1515, 2005.

[187] M. J. Schaaf, L. Willetts, B. P. Hayes, B. Maschera, E. Stylianou, and S. N. Farrow. The relationship between intranuclear mobility of the NF-kappaB subunit p65 and its DNA binding affinity. *J. Biol. Chem.*, 281(31):22409–22420, 2006.

[188] D. Schübeler, D. M. MacAlpine, D. Scalzo, C. Wirbelauer, C. Kooperberg, F. van Leeuwen, D. E. Gottschling, L. P. O'Neill, B. M. Turner, J. Delrow, S. P. Bell, and M. Groudine. The histone modification pattern of active genes revealed through genome-wide chromatin analysis of a higher eukaryote. *Genes Dev.*, 18(11):1263–1271, 2004.

[189] B. E. Schwartz and K. Ahmad. Transcriptional activation triggers deposition and removal of the histone variant H3.3. *Genes Dev.*, 19(7):804–814, 2005.

[190] R. B. Sekar and A. Periasamy. Fluorescence resonance energy transfer (FRET) microscopy imaging of live cell protein localizations. *J. Cell Biol.*, 160(5):629–633, 2003.

[191] J. Sekelsky. Targeted Gene Replacement. `http://sekelsky.bio.unc.edu/Research/Targeting/Targeting.html`, 2008.

[192] V. F. Semeshin, E. S. Belyaeva, V. V. Shloma, and I. F. Zhimulev. Electron Microscopy of Polytene Chromosomes. *Methods Mol. Biol.*, 247:305324, 2004.

[193] W. L. Shaiu and T. S. Hsieh. Targeting to transcriptionally active loci by the hydrophilic N-terminal domain of Drosophila DNA topoisomerase I. *Mol. Cell. Biol.*, 18(7):4358–4367, 1998.

[194] N. C. Shaner, R. E. Campbell, P. A. Steinbach, B. N. Giepmans, A. E. Palmer, and R. Y. Tsien. Improved monomeric red, orange and yellow fluorescent proteins derived from Discosoma sp. red fluorescent protein. *Nat. Biotechnol.*, 22(12):1567–1572, 2004.

[195] N. C. Shaner, M. Z. Lin, M. R. McKeown, P. A. Steinbach, K. L. Hazelwood, M. W. Davidson, and R. Y. Tsien. Improving the photostability of bright monomeric orange and red fluorescent proteins. *Nat. Methods*, 5(6):545–551, 2008.

[196] L. S. Shopland, K. Hirayoshi, M. Fernandes, and J. T. Lis. HSF access to heat shock elements in vivo depends critically on promoter architecture defined by GAGA factor, TFIID, and RNA polymerase II binding sites. *Genes Dev.*, 9(22):2756–2769, 1995.

[197] L. S. Shopland and J. T. Lis. HSF recruitment and loss at most Drosophila heat shock loci is coordinated and depends on proximal promoter sequences. *Chromosoma*, 105(3):158–171, 1996.

[198] J. S. Siino, I. B. Nazarov, M. P. Svetlova, L. V. Solovjeva, R. H. Adamson, I. A. Zalenskaya, P. M. Yau, E. M. Bradbury, and N. V. Tomilin. Photobleaching of GFP-labeled H2AX in chromatin: H2AX has low diffusional mobility in the nucleus. *Biochem. Biophys. Res. Commun.*, 297(5):1318–1323, 2002.

[199] F. Garcia Soriano, L. Virág, P. Jagtap, E. Szabó, J. G. Mabley, L. Liaudet, A. Marton, D. G. Hoyt, K. G. Murthy, A. L. Salzman, G. J. Southan, and C. Szabó. Diabetic endothelial dysfunction: the role of poly(ADP-ribose) polymerase activation. *Nat. Med.*, 7(1):108–113, 2001.

[200] N. Soshnikova and D. Duboule. Epigenetic temporal control of mouse Hox genes in vivo. *Science*, 324(5932):1320–1323, 2009.

[201] E. Soutoglou, M. A. Demény, E. Scheer, G. Fienga, P. Sassone-Corsi, and L. Tora. The nuclear import of TAF10 is regulated by one of its three histone fold domain-containing interaction partners. *Mol. Cell. Biol.*, 25(10):4092–4104, 2005.

[202] B. L. Sprague and J. G. McNally. FRAP analysis of binding: proper and fitting. *Trends Cell Biol.*, 15(2):84–91, 2005.

[203] B. L. Sprague, R. L. Pego, D. A. Stavreva, and J. G. McNally. Analysis of binding reactions by fluorescence recovery after photobleaching. *Biophys. J.*, 86(6):3473–3495, 2004.

[204] R. O. Sprouse, M. N. Wells, and D. T. Auble. TATA-binding protein variants that bypass the requirement for Mot1 in vivo. *J. Biol. Chem.*, 284(7):4525–35, 2009.

[205] M. Stapleton, G. Liao, P. Brokstein, L. Hong, P. Carninci, T. Shiraki, Y. Hayashizaki, M. Champe, J. Pacleb, K. Wan, C. Yu, J. Carlson, R. George, S. Celniker, and G. M. Rubin. The Drosophila gene collection: identification of putative full-length cDNAs for 70% of D. melanogaster genes. *Genome Res.*, 12(8):1294–1300, 2002.

[206] D. L. Stenoien, A. C. Nye, M. G. Mancini, K. Patel, M. Dutertre, B. W. O'Malley, C. L. Smith, A. S. Belmont, and M. A. Mancini. Ligand-mediated assembly and real-time cellular dynamics of estrogen receptor alpha-coactivator complexes in living cells. *Mol. Cell. Biol.*, 21(13):4404–4412, 2001.

[207] D. L. Stenoien, K. Patel, M. G. Mancini, M. Dutertre, C. L. Smith, B. W. O'Malley, and M. A. Mancini. FRAP reveals that mobility of oestrogen receptor-alpha is ligand- and proteasome-dependent. *Nat. Cell Biol.*, 3(1):15–23, 2001.

[208] M. H. Sung, L. Salvatore, R. De Lorenzi, A. Indrawan, M. Pasparakis, G. L. Hager, M. E. Bianchi, and A. Agresti. Sustained oscillations of NF-kappaB produce distinct genome scanning and gene expression profiles. *PloS one*, 4(9):e7163, 2009.

[209] H. Sutherland and W. A. Bickmore. Transcription factories: gene expression in unions? *Nat. Rev. Genet.*, 10(7):457–466, 2009.

[210] R. Swaminathan, C. P. Hoang, and A. S. Verkman. Photobleaching recovery and anisotropy decay of green fluorescent protein GFP-S65T in solution and cells: cytoplasmic viscosity probed by green fluorescent protein translational and rotational diffusion. *Biophys. J.*, 72(4):1900–1907, 1997.

[211] S. Tanuma, T. Yagi, and G. S. Johnson. Endogenous ADP ribosylation of high mobility group proteins 1 and 2 and histone H1 following DNA damage in intact cells. *Arch. Biochem. Biophys*, 237(1):38–42, 1985.

[212] M. C. Thomas and C. M. Chiang. The general transcription machinery and general cofactors. *Crit. Rev. Biochem. Mol. Biol.*, 41(3):105–178, 2006.

[213] Y. P. Tsao, H. Y. Wu, and L. F. Liu. Transcription-driven supercoiling of DNA: direct biochemical evidence from in vitro studies. *Cell*, 56(1):111–118, 1989.

[214] T. Tsukiyama, P. B. Becker, and C. Wu. ATP-dependent nucleosome disruption at a heat-shock promoter mediated by binding of GAGA transcription factor. *Nature*, 367(6463):525–532, 1994.

[215] A. Tulin and A. Spradling. Chromatin loosening by poly(ADP)-ribose polymerase (PARP) at Drosophila puff loci. *Science*, 299(5606):560–562, 2003.

[216] J. Vazquez, A. S. Belmont, and J. W. Sedat. Multiple regimes of constrained chromosome motion are regulated in the interphase Drosophila nucleus. *Curr. Biol.*, 11(16):1227–1239, 2001.

[217] T. C. Voss and G. L. Hager. Visualizing chromatin dynamics in intact cells. *Biochim. Biophys. Acta*, 1783(11):2044–2051, 2008.

[218] J. C. Wang. DNA topoisomerases. *Annu. Rev. Biochem.*, 65:635–692, 1996.

[219] J. C. Wang. Cellular roles of DNA topoisomerases: a molecular perspective. *Nat. Rev. Mol. Cell Biol.*, 3(6):430–440, 2002.

[220] J. T. Westwood, J. Clos, and C. Wu. Stress-induced oligomerization and chromosomal relocalization of heat-shock factor. *Nature*, 353(6347):822–827, 1991.

[221] R. C. Wilkins and J. T. Lis. Dynamics of potentiation and activation: GAGA factor and its role in heat shock gene regulation. *Nucleic Acids Res.*, 25(20):3963–3968, 1997.

[222] R. M. Williams, W. R. Zipfel, and W. W. Webb. Multiphoton microscopy in biological research. *Curr. Opin. Chem. Biol.*, 5(5):603–608, 2001.

[223] N. A. Winegarden, K. S. Wong, M. Sopta, and J. T. Westwood. Sodium salicylate decreases intracellular ATP, induces both heat shock factor binding and chromosomal puffing, but does not induce hsp 70 gene transcription in Drosophila. *J. Biol. Chem.*, 271(43):26971–26980, 1996.

[224] C. Wirbelauer, O. Bell, and D. Schübeler. Variant histone H3.3 is deposited at sites of nucleosomal displacement throughout transcribed genes while active histone modifications show a promoter-proximal bias. *Genes Dev.*, 19(15):1761–1766, 2005.

[225] J. Wisniewski, A. Orosz, R. Allada, and C. Wu. The C-terminal region of Drosophila heat shock factor (HSF) contains a constitutively functional transactivation domain. *Nucleic Acids Res.*, 24(2):367–374, 1996.

[226] J. L. Workman. Nucleosome displacement in transcription. *Genes Dev.*, 20, 2006.

[227] C. Wotzlaw, T. Otto, U. Berchner-Pfannschmidt, E. Metzen, H. Acker, and J. Fandrey. Optical analysis of the HIF-1 complex in living cells by FRET and FRAP. *FASEB J.*, 21(3):700–707, 2007.

[228] C. Wu. Heat shock transcription factors: structure and regulation. *Annu. Rev. Cell Dev. Biol.*, 11:441–469, 1995.

[229] C. H. Wu, L. Madabusi, H. Nishioka, P. Emanuel, M. Sypes, I. Arkhipova, and D. S. Gilmour. Analysis of core promoter sequences located downstream from the TATA element in the hsp70 promoter from Drosophila melanogaster. *Mol. Cell. Biol.*, 21(5):1593–1602, 2001.

[230] C. H. Wu, Y. Yamaguchi, L. R. Benjamin, M. Horvat-Gordon, J. Washinsky, E. Enerly, J. Larsson, A. Lambertsson, H. Handa, and D. Gilmour. NELF and DSIF cause promoter proximal pausing on the hsp70 promoter in Drosophila. *Genes Dev.*, 17(11):1402–1414, 2003.

[231] J. Wu, L. Feng, and T. S. Hsieh. Drosophila topo IIIalpha is required for the maintenance of mitochondrial genome and male germ-line stem cells. *Proc. Natl. Acad. Sci. U. S. A.*, 107(14):6228–6233, 2010.

[232] J. Wu, J. H. Hou, and T. S. Hsieh. A new Drosophila gene wh (wuho) with WD40 repeats is essential for spermatogenesis and has maximal expression in hub cells. *Dev. Biol.*, 296(1):219–230, 2006.

[233] H. Xiao and J. T. Lis. Germline transformation used to define key features of heat-shock response elements. *Science*, 239(4844):1139–1142, 1988.

[234] N. Xiao and D. B. DeFranco. Overexpression of unliganded steroid receptors activates endogenous heat shock factor. *Mol. Endocrinol.*, 11(9):1365–1374, 1997.

[235] J. Yao, M. B. Ardehali, C. J. Fecko, W. W. Webb, and J. T. Lis. Intranuclear distribution and local dynamics of RNA polymerase II during transcription activation. *Mol. Cell*, 28(6):978–990, 2007.

[236] J. Yao, K. M. Munson, W. W. Webb, and J. T. Lis. Dynamics of heat shock factor association with native gene loci in living cells. *Nature*, 442(7106):1050–1053, 2006.

[237] J. Yao, K. L. Zobeck, J. T. Lis, and W. W. Webb. Imaging transcription dynamics at endogenous genes in living Drosophila tissues. *Methods*, 45(3):233–241, 2008.

[238] J. H. Yik, R. Chen, R. Nishimura, J. L. Jennings, A. J. Link, and Q. Zhou. Inhibition of P-TEFb (CDK9/Cyclin T) kinase and RNA polymerase II transcription by the coordinated actions of HEXIM1 and 7SK snRNA. *Mol. Cell*, 12(4):971–982, 2003.

[239] S. M. Yoh, H. Cho, L. Pickle, R. M. Evans, and K. A. Jones. The Spt6 SH2 domain binds Ser2-P RNAPII to direct Iws1-dependent mRNA splicing and export. *Genes Dev.*, 21(2):160–174, 2007.

[240] R. Yokoyama, A. Pannuti, H. Ling, E. R. Smith, and J. C. Lucchesi. A plasmid model system shows that Drosophila dosage compensation depends on the global acetylation of histone H4 at lysine 16 and is not affected by depletion of common transcription elongation chromatin marks. *Mol. Cell Biol.*, 27(22):7865–7870, 2007.

[241] N. Yudkovsky, J. A. Ranish, and S. Hahn. A transcription reinitiation intermediate that is stabilized by activator. *Nature*, 408(6809):225–229, 2000.

[242] M. Zhou, M. A. Halanski, M. F. Radonovich, F. Kashanchi, J. Peng, D. H. Price, and J. N. Brady. Tat modifies the activity of CDK9 to phosphorylate serine 5 of the RNA polymerase II carboxyl-terminal domain during human immunodeficiency virus type 1 transcription. *Mol. Cell. Biol.*, 20(14):5077–5086, 2000.

[243] W. R. Zipfel, R. M. Williams, and W. W. Webb. Nonlinear magic: Multiphoton microscopy in the biosciences. *Nat. Biotechnol.*, 21(11):1369–1377, 2003.

[244] K. L. Zobeck, M. S. Buckley, W. R. Zipfel, and J. T. Lis. Recruitment Timing and Dynamics of Transcription Factors at the Hsp70 Loci in Living Cells. *Mol. Cell*, in press.